

RARE EARTH ELEMENTS (REE) IN CRUDE OIL IN THE LANSING-KANSAS CITY  
FORMATIONS IN CENTRAL KANSAS; POTENTIAL INDICATIONS ABOUT THEIR  
SOURCES, LOCALLY DERIVED OR LONG-DISTANCE DERIVED

by

MICHAEL CHRISTOPHER MCINTIRE

B.S., Kansas State University, 2012

A THESIS

submitted in partial fulfillment of the requirements for the degree

MASTER OF SCIENCE

Department of Geology  
College of Arts and Sciences

KANSAS STATE UNIVERSITY  
Manhattan, Kansas

2014

Approved by:

Major Professor  
Dr. Matthew Totten

# **Copyright**

MICHAEL CHRISTOPHER MCINTIRE

2014

## Abstract

There are some who hold the view that liquid hydrocarbons in the upper Paleozoic formations in Kansas are being locally derived. It has been the long held belief that the liquid hydrocarbons found in Kansas have come from distant sources in Oklahoma. To shed further light on this issue about the origin of hydrocarbons in the upper Paleozoic formations in Kansas, a study was conducted to analyze the geochemical characteristics of REE in Lansing-Kansas City oils that were collected from several locations in a small area within Rooks County, Kansas. The total REE contents in these oils ranges from about 3.1 ng (or 10-12 gram) per Liter of oil to about 131 ng per Liter of oil. The pattern of relative distribution of the REEs for each oil sample has been constructed from values that were obtained by dividing the individual REE concentrations of a given oil sample by the respective concentrations of the REEs in a standard or a reference sample (such as PAAS, a representation of average argillaceous sediments in the crust that is commonly used for the analyses of a variety of crust originated sedimentary products). A standard-normalized relative distribution pattern of an oil sample can reveal an important history of chemical evolution of the oil of interest. The PAAS-normalized patterns of relative distribution of the REEs in the Lansing-Kansas City oils from Rooks County, Kansas are significantly diverse. Although nearly all oil samples investigated in this study have varied degrees of light REE-enrichment across the REE series from La to Sm, they differed in their relative Ce abundances. Some samples have positive Ce anomalies; some have negative Ce anomalies, and some others with the absence of any Ce anomaly. The oils also differed in their PAAS-normalized relative distribution of the middle rare earth elements (MREEs), ranging from Sm to Tb. All oil samples were relatively enriched in the MREEs, but with varied degrees of enrichment from a prominent one to almost a barely noticeable one. The oils differed in their relative distributions of Eu, as some were with a positive Eu anomaly, some with a negative Eu anomaly, and some with the absence of any Eu anomaly. The trends of the heavy rare earth elements (HREEs) from Tb to Lu among the oils ranged from nearly flat for the most oils to a progressive depletion across the series for few samples. Furthermore, the oils were varied in having prominently anomalous relative distributions, in some cases with a positive anomaly and in others with negative anomaly, for such elements as Tb, Ho, and Tm (MM-JS-04, MM-MC-3A, and MM-MC-01). The anomalies for Tb, Ho, Tm are reflections of enzyme activity of

source material during its primary (growth) environment. The metals are known to be preferentially located at the active sites of the enzymes. The oils not only differed significantly in their REE-geochemical characteristics, they also had a wide range of K/Rb weight ratios from about 877 to about 2000. These high values are typically the ones that can be assigned to organic materials, well exceeding the range of values that are associated with common silicate minerals and rocks, having an average value of 250-350ppm. Different zones in the Lansing-Kansas City formations also show distinct REE distribution patterns. There are four broadly classified distribution patterns. MREE enrichment can be observed in samples with production from the middle Lansing-Kansas City zones (G-I). In samples with comingling Lansing-Kansas City zones, amplification of anomalies from differing source materials can be observed. The diversity in the REE distribution patterns and K/Rb ratios in oils collected from central Kansas makes a strong argument against long distance transportation from a distant source in Oklahoma.

# Table of Contents

List of Figures .....	vii
List of Tables .....	ix
Acknowledgements.....	x
Chapter 1 - Introduction.....	1
1.1 Rare Earth Elements .....	5
1.2 Crude Oil Composition.....	10
1.3- Gas Chromatography.....	14
1.3.1 n-Alkanes and Isoprenoids.....	14
1.3.2 Biodegradation of Crude Oil.....	15
1.4 Geological Setting.....	18
1.4.1 Lansing Kansas City Group .....	19
1.4.2 Lansing-Kansas City Production in Central Kansas .....	21
Chapter 2 - Methodology .....	23
2.1 Study Area and Sample Locations.....	23
2.2 Sample Well Logs.....	26
2.3 Methodology for Oil Analysis .....	32
2.3.1 Potential Sources for Analytical Error .....	34
Chapter 3 - Results.....	35
3.1 Crude Oil REE Concentrations.....	35
3.2 REE Distribution Patterns of Crude Oil .....	38
3.3 K/Rb Ratios.....	41
3.4 Crude Oil Gas Chromatograph Analysis .....	42
Chapter 4 – Discussion .....	45
4.1 REE Relative Distribution Signatures in Crude Oil .....	45
4.1.1 Light Rare Earth Elements (LREE) .....	46
Cerium Anomalies .....	46
4.1.2 Middle Rare Earth Elements (MREE) .....	47
MREE Enrichment.....	47

Europium Anomalies .....	47
4.1.3 Heavy Rare Earth Elements (HREE) .....	48
Terbium, Holmium, and Tm Enrichments .....	48
4.2- Lansing-Kansas City Zone Correlation .....	49
4.3-K/Rb Ratios in Crude Oil .....	50
4.3 Biomarkers .....	51
Chapter 5 – Conclusions .....	54
5.1 Future Work .....	54
Bibliography .....	56
Appendix A - REE Distribution Patterns in Crude Oil .....	65
Appendix B - Gas Chromatograph Analysis of Crude Oil .....	70

## List of Figures

Figure 1 Map showing potential oil migration from Anadarko basin (Modified from Gerhard, 2004). .....	2
Figure 2 Rare Earth Elements or Lanthanides in the Periodic Table.....	5
Figure 3 Lanthanide Contraction (Ramirez, 2013). .....	7
Figure 4 REE values for Post Archean Australian Shale (PAAS).....	9
Figure 5 Compounds found in oil containing Oxygen molecules .....	11
Figure 6 Schematic Asphaltene Molecule (Hunt, 1995).....	12
Figure 7 Gas chromatograms showing the effects of biodegradation with decreasing amounts of alteration (top to bottom). (Peters et al. 2005) .....	16
Figure 8 Structure map of Kansas with study area location (Watney, 1980). .....	18
Figure 9 Type well log of Lansing-Kansas City group. Taken from Conoco Adell L-KC Unit 406 from section 2-T6S-R27W (Watney, 1980).....	20
Figure 10 Distribution of Kansas oil production by geologic formation.....	21
Figure 11 Lansing-Kansas City total oil production by county (MMBO). .....	22
Figure 12 Structure map at top of Lansing-Kansas City group with Lansing-Kansas City oil production. ....	22
Figure 13 Regional map showing study area and sample locations. ....	24
Figure 14 Lansing-Kansas City zone breakdowns. (Modified from Brown, 1984). ....	25
Figure 15 Gamma ray log of McElhaney #1 with perforations marked. ....	26
Figure 16 Gamma ray log of McElhaney #1A with perforations marked. ....	27
Figure 17 Gamma ray log of McElhaney #3A with perforations marked. ....	27
Figure 18 Gamma ray log of McElhaney #4 with perforations marked. ....	28
Figure 19 Gamma ray log of Jones #2 with perforations marked.....	28
Figure 20 Gamma ray log of Jones #3 with perforations marked.....	29
Figure 21 Gamma ray log of Jones #4 with perforations marked.....	30
Figure 22 Gamma ray log of Jackson #1 with perforations marked.....	31
Figure 23 Gamma ray log of Williams #11A with perforations marked.....	31
Figure 24 Oil sample preparation flow chart (Modified from Ramirez, 2013). ....	33
Figure 25 Distribution of total REE concentration in Lansing-Kansas City oil samples. ....	37

Figure 26 Relative distribution patterns of REE concentrations in three Lansing-Kansas City oil samples (MM-WM-11A, MM-MC-1A, MM-MC-4A). Normalized to PAAS. Samples are grouped with similar distribution patterns. Zones of production are highlighted with correlating colors. ....	38
Figure 27 Relative distribution patterns of REE concentrations in three Lansing-Kansas City oil samples (MM-JS-02, MM-JS-03, MM-JK-01). Normalized to PAAS. Samples are grouped with similar distribution patterns. Zones of production are highlighted with correlating colors.....	39
Figure 28 Relative distribution patterns of REE concentrations in two Lansing-Kansas City oil samples (MM-JS-04 and MM-MC-3A). Normalized to PAAS. Samples are grouped with similar distribution patterns. Zones of production are highlighted with correlating colors.....	39
Figure 29 Relative distribution patterns of REE concentrations in one Lansing-Kansas City oil samples (MM-MC-01). Normalized to PAAS. Zone of production is highlighted with a correlating color.....	40
Figure 30 K/Rb ratios of Lansing-Kansas City crude oil samples. Average of silicate minerals (clays) included for reference (Chaudhuri et al., 2007). ....	41
Figure 31 n-Alkanes in Lansing-Kansas City oils. ....	42
Figure 32 Isoprenoids of Lansing-Kansas City oil samples. ....	43
Figure 33 Gas Chromatograms of Lansing-Kansas City crude oil. (1) MM-DJ-02 (2) MM-MC-3A (3) MM-MC-4A (4) MM-JK-01 (5) MM-WM-11A (6) MM-JS-04 (7) MM-JS-02 (8) MM-MC-01 (9) MM-JS-03 (10) MM-MC-1A (11) MM-JS-03.....	44
Figure 34 Relative distribution patterns of Lansing-Kansas City oils. MM-JS-04 showing positive Tb and Ho anomalies. MM-MC-3A showing a positive Ho anomaly. MM-MC-01 showing positive Ho and Tm anomalies. ....	48



## List of Tables

Table 1 Atomic number and Ionic Radii for the REE. ....	6
Table 2 Elemental Composition of Natural Materials (Hunt, 1995) .....	10
Table 3 Composition of a 35 ° API Gravity Crude Oil (Hunt, 1995) .....	11
Table 4 Resins and Asphaltenes in Crude Oils (Erdman and Saraceno, 1962) .....	13
Table 5 Table with well identification, sample names, and Lansing-Kansas City zones. ....	26
Table 6 REE and trace element analytical results for Lansing-Kansas City oil samples .....	35
Table 7 Lanthanum to Lutetium ratio showing LREE enrichment.....	45
Table 8 Cerium anomalies in Lansing-Kansas City oil samples. ....	46
Table 9 Europium anomalies in Lansing-Kansas City oil samples. ....	47
Table 10 Pristane/Phytane ratios for Lansing-Kansas City oil samples. ....	52
Table 11 Carbon Preference Index (CPI) of Lansing-Kansas City oil samples. ....	52

## **Acknowledgements**

I'd like to first thank Dr. Matthew Totten and Dr. Sambhudas Chaudhuri for their dedication and passion to build the Kansas State University petroleum geology program. I appreciate the both of you taking me on as a graduate student and mentoring me during my time at K-State. A big thank you to Gary Sandlin and Steve Kirkwood for mentoring and teaching me what it takes to be a successful petroleum geologist. I will forever be in your debt for the valuable knowledge and experience you have provided me. Also, thank you to the Strunk's and the Sandlin's for providing me with the financial aid needed to attend K-State. Thank you to Roland Nyp, Mike Jones, and Gary Wagner for taking time out of you busy days to take me around to different LKC wells in Rooks County. Thank you to Dr. R.P. Philp and all of the people at OU for running my samples on such short notice. I would like to the people of UNISTRA. Thank you Norbert Clauer, Rene Boutin, and K. Semhi for analyzing my samples and contributing your time and effort to make this study possible. Finally, I would like to thank my family and friends for always supporting and pushing me to finish my thesis.

## Chapter 1 - Introduction

The purpose of this study is to use Rare Earth Elements (REE) as a means of geochemically analyzing oil produced from the Lansing-Kansas City Group in central Kansas. REE have proven to be useful tracers in many geological and geochemical investigations and demonstrate important applications in igneous, metamorphic, and sedimentary petrology (Rollinson, 1993). To date, studies by Abanda and Hannigan (2006), Dao-Hui et al. (2013), and Ramirez (2013) are the only investigations to examine the REE content in the organic matter. Of these three, Ramirez (2013) is the only study to address REE geochemical potential for organic source bed and crude oil correlations. In Ramirez (2013), REE geochemical investigations were targeted on oils generated in the Woodford shale and overlying Mississippian formation located in the Anadarko Basin, in north-central Oklahoma. This is the first study that takes a holistic approach to gain additional insight about oil generation using REE composition in crude oils. This study takes the same approach as Ramirez (2013), but as a means to identify organic source bed and crude oil correlation in the Lansing-Kansas City group in Rooks County, Kansas. It is believed by most of geologists that crude oil in the mid-continent is sourced primarily from the Woodford Shale in central Oklahoma. By placing the source of the midcontinent petroleum system in central Oklahoma, oil in northwestern Kansas would have to be transported approximately two hundred miles. This study hypothesizes that oil in the Lansing-Kansas City group in central Kansas is being locally sourced rather than originating from the Woodford Shale and migrating north.

In order to understand this study, it is first important to understand the concept of a petroleum system. Petroleum systems are broken into several key components. The most important part of a petroleum system is the source rock. The source rock is considered the “kitchen” of the entire petroleum system. It is where the hydrocarbons are generated from compacted organic materials. When buried to a certain depth and given the right amount of heat, these organics undergo a process known as catagenesis that transforms them into hydrocarbons. Once the source rock has undergone catagenesis, the hydrocarbons are expelled and migrate through carrier beds into a porous rock unit known as a reservoir rock. The reservoir rock needs to be stratigraphically or structurally trapped beneath an impermeable rock layer called the seal.

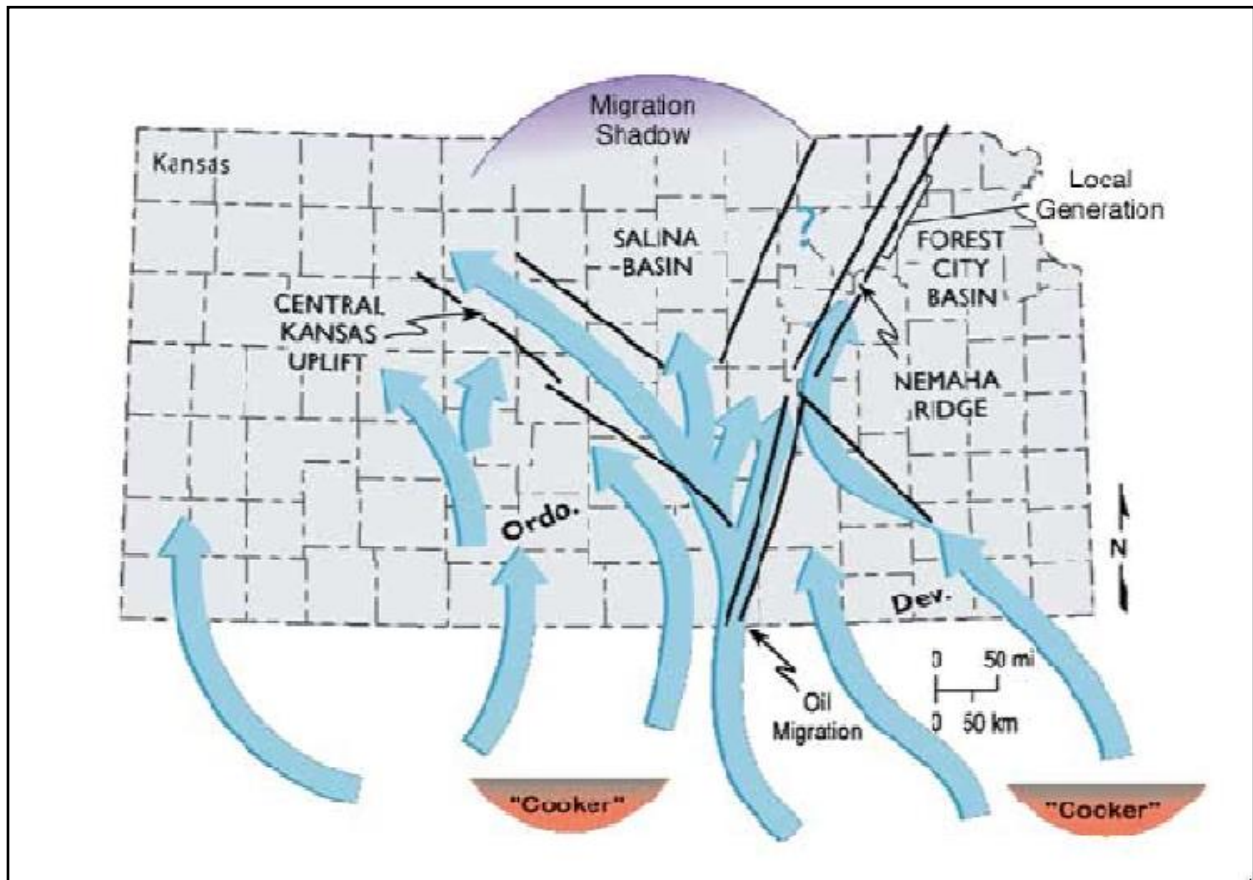


**Figure 1 Map showing potential oil migration from Anadarko basin (Modified from Gerhard, 2004).**

This project focuses on determining whether the source of the upper Pennsylvanian Lansing-Kansas City group in central Kansas has migrated a long distance (Woodford Shale), or if the hydrocarbons are originating from a local source in Kansas by analysis of REE data and gas chromatograph data collected on ten crude oil samples from Rooks County, Kansas. The Lansing-Kansas City group is the second largest producing unit in Kansas, with over one billion barrels recovered to date. This prolific rock unit accounts for 19% of Kansas' total oil produced each year. The majority of Lansing-Kansas City production has come from conventional production due to the nature of the rock unit (thin interbedded limestone and shale), but there could be the possibility for unconventional production in the future. The unique property of the Lansing-Kansas City group is that it has the ability to produce from multiple zones in one well. In Rooks County, Kansas the Lansing-Kansas City consists of 14 zones of alternating limestone units (zones A-L) separated by shales. Of these 14 zones, the Lansing-Kansas City produces

from 7-8 different limestone zones. Several of the wells sampled in this study are producing from multiple zones within the Lansing-Kansas City.

Traditional methods of oil-oil correlation have employed the organic constituents identified by GC and GC-MS of crude oils for correlation. This study takes a relatively new approach to oil-oil correlation. The premise takes consideration of the traditional organic data-based means of liquid hydrocarbon correlation. The new approach used in this study goes beyond examining the organic compositions of the crude oils, relying on information about their inorganic metal constituents. This study, however, is not the first one to use inorganic constituents as a means of correlating crude oils. There have been several attempts in the past to use trace elements as potential tools for correlating crude oils. Early reports on presence of metals include the works of Corbett (1967), Filby (1975), Shirey (1931), Witherspoon (1957), and Yen (1975). Many of these early studies looked specifically into the concentrations of vanadium and nickel. Corbett (1967) found that vanadium, nickel, and iron are commonly present but in minor amounts. The work showed that almost 70% of the total vanadium are present in the asphaltene fraction with about 30% in the non-volatile raffinate, pointing to the fact that the metals are associated more with the highest molecular weight components.

Studies by Lewan and Maynard (1982) and others have claimed that vanadium and nickel are acquired by sediments, especially those on the ocean floor, at the sediment-water interface during the deposition of sediments. Their distributions in the sediments are influenced by the pH and Eh conditions of the environment at the interface. Lewan and Maynard (1982) concluded that the vanadium nickel ratios remain unchanged during migration of the liquid hydrocarbons from source bed to the reservoir rocks, implying that the ratios of the liquids would be a good indicator of the sources from which the liquids are derived. Studies have sought variation trends of both vanadium and nickel in crude oil. It is not too common to find good correlations in the variations between the two. A case in point may be the study of Kansas oils by Schumacher and Chaudhuri (2014). The failure to see the good correlations between the two goes beyond the source rock variation. The two elements are influenced differently by the Eh and pH conditions. The nickel concentrations will be influenced by pH considering it exists as a divalent ion. On the other hand, the V concentration will be impacted by the oxidation states. This study has considered using REEs as tracers for the origin of crude oils at their source area. These elements as a group behave similarly, with the exception of two among them. The group, in general, has

3+ oxidation states in natural environments. The two exceptions referred here have one lower oxidation state ( $\text{Eu}^{2+}$ ) for one and the other with a higher oxidation state ( $\text{Ce}^{4+}$ ). A low pH environment promotes the mobility of the group, in particular under the influence of complexation with a variety of organic and inorganic ligands. This general geochemical behavior makes them potentially a useful tracer for the sources of oils in which these elements can be found. The geochemical discussions of this group that follows are important toward an understanding of how these elements can be used for oil correlation or source differentiation.

## 1.1 Rare Earth Elements

The REEs or lanthanides (Ln) are a group of 14 elements from lanthanum (La) to lutetium (Lu) (atomic numbers 57-71). They are located in block 5d of the periodic table (Figure 2). Rare earth elements have completely filled  $5s^2$ ,  $4d^{10}$ ,  $5p^6$ , and  $6s^2$  orbitals. The elements differ from each other in their electronic configurations based on electron filling at the next higher energy orbitals beyond  $6s^2$ . The differences occur at the 4f orbitals or a higher-energy 5d orbital. All the lanthanides are present as trivalent ions ( $Ln^{+3}$ ), with the exceptions of europium (Eu) and cerium. Europium also occurs as a divalent ( $Eu^{2+}$ ) and cerium (Ce) can also have a valence of 4 ( $Ce^{4+}$ ).

**Periodic Table of the Elements**

1A 1 H 1.00794																	2 He 4.002602
3 Li 6.941	4 Be 9.012182											5 B 10.811	6 C 12.0107	7 N 14.0067	8 O 15.9994	9 F 18.9984032	10 Ne 20.1797
11 Na 22.989769	12 Mg 24.3050	3B	4B	5B	6B	7B	8B		1B	2B	13 Al 26.9815386	14 Si 28.0855	15 P 30.973762	16 S 32.065	17 Cl 35.453	18 Ar 39.948	
19 K 39.0983	20 Ca 40.078	21 Sc 44.955912	22 Ti 47.867	23 V 50.9415	24 Cr 51.9961	25 Mn 54.938045	26 Fe 55.845	27 Co 58.933195	28 Ni 58.6934	29 Cu 63.546	30 Zn 65.38	31 Ga 69.723	32 Ge 72.64	33 As 74.92160	34 Se 78.96	35 Br 79.904	36 Kr 83.798
37 Rb 85.4678	38 Sr 87.62	39 Y 88.90585	40 Zr 91.224	41 Nb 92.90638	42 Mo 95.96	43 Tc [98]	44 Ru 101.07	45 Rh 102.90550	46 Pd 106.42	47 Ag 107.8682	48 Cd 112.411	49 In 114.818	50 Sn 118.710	51 Sb 121.760	52 Te 127.60	53 I 126.90447	54 Xe 131.293
55 Cs 132.9054519	56 Ba 137.327	57-71 Lanthanides	72 Hf 178.49	73 Ta 180.94788	74 W 183.84	75 Re 186.207	76 Os 190.23	77 Ir 192.217	78 Pt 195.084	79 Au 196.966569	80 Hg 200.59	81 Tl 204.3833	82 Pb 207.2	83 Bi 208.98040	84 Po [209]	85 At [210]	86 Rn [222]
87 Fr [223]	88 Ra [226]	89-103 Actinides	104 Rf [261]	105 Db [269]	106 Sg [271]	107 Bh [272]	108 Hs [270]	109 Mt [276]	110 Ds [281]	111 Rg [280]	112 Cn [285]	113 Uut [284]	114 Uuq [289]	115 Uup [288]	116 Uuh [293]	117 Uus [294]	118 Uuo [294]
Lanthanides		57 La 138.90547	58 Ce 140.116	59 Pr 140.90765	60 Nd 144.242	61 Pm [145]	62 Sm 150.36	63 Eu 151.964	64 Gd 157.25	65 Tb 158.92535	66 Dy 162.500	67 Ho 164.93032	68 Er 167.259	69 Tm 168.93421	70 Yb 173.054	71 Lu 174.9668	
Actinides		89 Ac [227]	90 Th 232.03806	91 Pa 231.03588	92 U 238.02891	93 Np [237]	94 Pu [244]	95 Am [243]	96 Cm [247]	97 Bk [247]	98 Cf [251]	99 Es [252]	100 Fm [257]	101 Md [258]	102 No [259]	103 Lr [262]	

**Figure 2 Rare Earth Elements or Lanthanides in the Periodic Table**

There are several well-known coherent chemical properties of Ln ions and their interactions with compounds. In Table 1, the atomic number and ionic radii's values are shown for each individual REE. A major property of the Ln is the "lanthanide contraction". This is the progressive decrease in the size of the atom, or decrease in the ionic radius, with increasing atomic number (Smith, 1963; Evans, 1990). This property makes REEs great tracers for defining many different natural inorganic and organic geological processes.

**Table 1 Atomic number and Ionic Radii for the REE.**

Element	La	Ce	Pr	Nd	Pm	Sm	Eu	Gd	Tb	Dy	Ho	Er	Tm	Yb	Lu
Atomic electron configuration (all begin with [Xe])	5d <sup>1</sup> 6s <sup>2</sup>	4f <sup>1</sup> 5d <sup>1</sup> 6s <sup>2</sup>	4f <sup>3</sup> 6s <sup>2</sup>	4f <sup>4</sup> 6s <sup>2</sup>	4f <sup>5</sup> 6s <sup>2</sup>	4f <sup>6</sup> 6s <sup>2</sup>	4f <sup>7</sup> 6s <sup>2</sup>	4f <sup>7</sup> 5d <sup>1</sup> 6s <sup>2</sup>	4f <sup>9</sup> 6s <sup>2</sup>	4f <sup>10</sup> 6s <sup>2</sup>	4f <sup>11</sup> 6s <sup>2</sup>	4f <sup>12</sup> 6s <sup>2</sup>	4f <sup>13</sup> 6s <sup>2</sup>	4f <sup>14</sup> 6s <sup>2</sup>	4f <sup>14</sup> 5d <sup>1</sup> 6s <sup>2</sup>
Atomic number	57	58	59	60	61	62	63	64	65	66	67	68	69	70	71
Ln <sup>3+</sup> radius (pm) (6coordinate)	103.2	101	99	98.3	97	95.8	94.7	93.5	92.3	91.2	90.1	89	88	86.8	86.1

+3,+4

+2,+3

The lanthanide contraction arises from insufficient shielding of the increasing nuclear attractive force with each additional proton at the nucleus and accompanying additional electron that fills the 4f orbital, as the atomic number increases. The imperfect shielding thus causes a reduction in size of the entire 4f sub shell and a steady contraction in the ionic radii (Cotton and Wilkinson, 1962). Lanthanides vary primarily in the number of 4f electrons, causing these elements to have very similar chemical properties. This property also allows the REEs to exist in many materials together as a group. However, their occurrence together in natural materials does not imply that they respond equally to chemical changes of natural systems. In fact, the Ln ions separate to some degree when the correct size accommodation in mineral structures is available. REEs can also become involved in complex ligands that have different stabilities, specifically in the formation of chelates (the same ligand offering two donor atoms to form bonds with the REEs). In some mineral structures, such as those in amphiboles and garnets, REEs with smaller ionic radii (heavy REE) are accommodated, whereas in some other mineral structures, such as in the feldspars, REE with larger ionic radii (light REE) are favored. In solutions, some degree of separation among REE occurs because the stability constants of many different REE-ligand complexes are typically varied in a gradual or steady fashion, but not necessarily in a smooth pattern, across the REE series.

The observed trends in REE distribution patterns among samples of interest may cast light on similarities or dissimilarities of their chemical evolutionary processes. The REE relative distribution patterns of natural materials fall into a small number of broad categories. The



variations that have been observed in natural materials have led studies on REE to subdivide the elements into three groups (Figure 2):

- Light REEs (La, Ce, Pr, Nd, Sm, and Eu – from atomic number 57 to 63)
- Middle REEs (Sm, Eu, Gd, Tb, Dy, and Ho – from atomic number 62 to 67)
- Heavy REEs (Gd, Tb, Dy, Ho, Er, Tm, Yb, and Lu – from atomic number 64 to 71).

The middle REE group includes the two end-members (Sm and Eu) of the light REE group and the first four members (Gd, Tb, Dy, and Ho) of the heavy REE group (Topp, 1965).

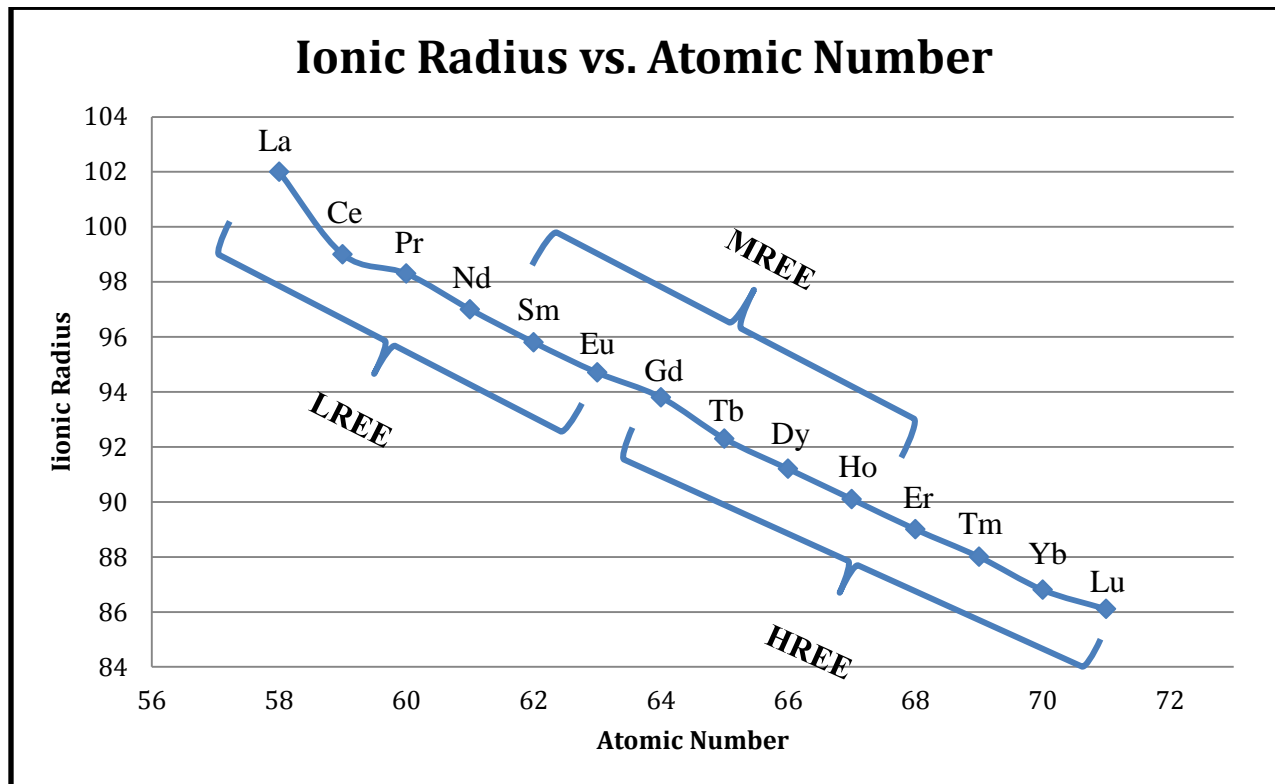


**Figure 3 Lanthanide Contraction (Ramirez, 2013).**

In Pearson’s (1963) terminology, the  $\text{Ln}^{3+}$  ions are classified as “hard” ions, which causes them to bond preferentially with “hard” base ligands such as  $\text{H}_2\text{O}$ ,  $\text{OH}^-$ ,  $\text{CO}_3^{2-}$ ,  $\text{NO}_3^-$ ,  $\text{SO}_4^{2-}$ ,  $\text{PO}_4^{3-}$ ,  $\text{O}^{2-}$ ,  $\text{F}^-$ ,  $\text{CH}_3\text{COO}^-$ , and  $\text{R-OH}$  (alcohols). Lanthanides, like many other “hard” acid ions, have a strong preference for O donor atoms. Bonding to  $\text{Cl}^-$  ions has been known, but it is relatively weak compared to bonds created with  $\text{O}^{2-}$  and  $\text{F}^-$  anions. Complexes solely with  $\text{NH}_3$ ,  $\text{R-NH}_2$  (amines),  $\text{HS}^-$  and  $\text{CN}^-$  are extremely weak (Evans, 1990, Wood, 1990). In general, the Ln ions preference for donor atoms is  $\text{O} > \text{N} > \text{S}$  (Thompson, 1979).

Wood (1990) gave a comprehensive review of the stability constants of Ln-complexes with many common inorganic ligands. Thompson (1979) and Evans (1990) provided data on stability constants of Ln-complexes with a number of different organic ligands. The sulfate ligands cause very little fractionation between the light Ln<sup>3+</sup> ions (LREE) and the heavy Ln<sup>3+</sup> ions (HREE). Fluoride complexation can cause fractionation of the Ln ions in dilute fluoride solutions. Similar to fluoride complexations, the stability of Ln-CO<sub>3</sub><sup>+</sup> complexes also progressively increases with increasing atomic number of the Ln. The stability of chloro-complexes decreases with increasing atomic number. This trend is opposite of the behavior of the fluoro-complexes (Wood, 1990). Several studies have noted the precipitation of phosphate minerals from solution. The phosphate precipitation causes the minerals to have a relative enrichment of the middle Ln across the series, displaying a convex relative distribution pattern. This pattern is often marked by the highest enrichment in Sm and the corresponding equilibrium solutions to have a relative depletion for the middle Ln, displaying a concave upward relative distribution pattern with the most depletion of Sm (Byrne et al., 1996).

Variations in the ionic size of the Ln the stability of the complexes impose some distinctive geochemical characteristics on the Ln compositions of natural materials. As stated earlier in the chapter two Ln ions have a valence other than 3, Eu<sup>2+</sup> and Ce<sup>4+</sup>. These two REE may be fractionated, if reducing (Eu<sup>2+</sup>) or oxidizing (Ce<sup>4+</sup>) conditions are present. When analyzing relative distribution patterns of REEs, increased values above the expected trivalent abundance are considered positive anomalies, while lower values are negative. Crystallographic controls on these elements are fairly well known, for example the affinity of feldspars for Eu<sup>2+</sup>. Enzymatic effects are not as well known.

Variations within the coherent chemical properties make the Ln group a good tracer for the differentiation of inorganic and organic processes. Subtle differences in the chemical history of a group of solids, solutions, or solid-solution reactions may be best revealed through an examination of the relative distribution of the REEs for each substance of interest when compared with a known standard or reference material.

Moving across the rare-earth series with increasing atomic number, a distribution pattern of the REEs for a given substance is shown as the ratio of the concentration of each individual REE of the substance to the concentration of the same element of a chosen standard or reference material. REE studies in igneous petrology use chondrite as reference material. Sedimentary

studies with REE use the Post Archean Australian Shale (PAAS) or the North American Shale Composite (NASC). When analyzing a specific sample, the reference material used should be appropriate to the material analyzed. Using chondrite as a reference material for the REE study in oil might not be appropriate. The PAAS is the reference material used throughout this study. When normalizing REE concentrations to a reference material, a smooth distribution pattern within the LREEs may be interrupted at Ce and Eu. Europium positive or negative anomalies may be linked to a crystallo-chemical or solution-chemistry effect. An example of this is feldspars that accommodate  $\text{Eu}^{2+}$  over  $\text{Eu}^{3+}$ . This effect might not be applicable in all materials, particularly when studying organic matter. Europium can be biochemically controlled by enzymatic effect in a living system. Cerium anomalies can also be attributed to crystallographic effects, in the case of Manganese oxide precipitation. Ce has also been found with anomalies in plants. Positive anomalies are identified in these elements if their observed relative concentrations are in excess of relative concentrations that could be predicted from the relative distribution trend defined by their two immediate respective neighbors. Negative anomalies are identified if the observed relative distribution values are depleted relative to the predicted values determined by the trend line that connects their two respective immediate neighbor REEs.

<b>Element</b>	<b>PAAS</b>
<b>La</b>	38.2
<b>Ce</b>	79.6
<b>Pr</b>	8.83
<b>Nd</b>	33.9
<b>Sm</b>	5.55
<b>Eu</b>	1.08
<b>Gd</b>	4.66
<b>Tb</b>	0.774
<b>Dy</b>	4.68
<b>Ho</b>	0.991
<b>Er</b>	2.85
<b>Tm</b>	0.405
<b>Yb</b>	2.82
<b>Lu</b>	0.43

**Figure 4 REE values for Post Archean Australian Shale (PAAS).**

## 1.2 Crude Oil Composition

Petroleum is composed almost completely of hydrogen and carbon, with 1.85 times more hydrogen atoms than carbon. Sulfur, nitrogen and oxygen constitute less than 3 percent of petroleum. From kerogen to the asphalt to the oil, an increase can be observed in hydrogen and a decrease in sulfur, nitrogen and oxygen relative to carbon.

**Table 2 Elemental Composition of Natural Materials (Hunt, 1995)**

ELEMENT	VOLUME PERCENT		
	Oil	Asphalt	Kerogen
<b>Carbon</b>	84.5	84	79
<b>Hydrogen</b>	13	10	6
<b>Sulfur</b>	1.5	3	5
<b>Nitrogen</b>	0.5	1	2
<b>Oxygen</b>	0.5	2	8
<b>Total</b>	100	100	100

Table 2 shows average composition levels for oils worldwide. Hydrocarbons vary in their structural forms comprising different molecular arrangements. Paraffins are alkanes (open-chain molecules with single bonds between the carbon atoms). They are the second most common constituents of crude oil, and comprise most of the gasoline fraction of crude oil. Naphthenes are cycloalkanes (alkane rings). They are the most common molecular structures in petroleum. These rings usually contain 5 or 6 carbon atoms. The average crude oil contains approximately 50% naphthenes, with higher amounts in the heavier fraction and less in the lighter fraction. Aromatic hydrocarbons contain at least one benzene ring (a ring with 6 carbons and 6 hydrogens attached to each carbon). Aromatics rarely make up more than 15% of total crude oil, and are concentrated mostly in the heavy fractions of petroleum. Crude oil also contains molecules other than hydrogen and carbon. These molecules include nitrogen, sulfur and oxygen. These are present through the entire boiling range of crude oil. The compounds that contain oxygen are of particular interest due to the REEs affinity to oxygen.

Since REE may be found bound to oxygen bearing sites, it is important to note some compounds that contain oxygen molecules (Figure 3). Oxygen compounds are made of chain or ring acids. Phenols and Carboxylic acids encompass these compounds, which consist of chains or ring acids.

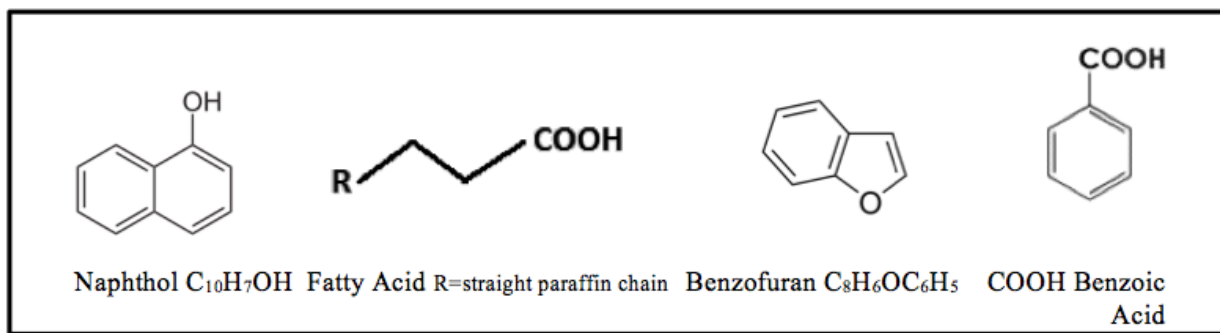


**Figure 5 Compounds found in oil containing Oxygen molecules**

Compounds containing Nitrogen, Sulfur and Oxygen and Aromatics represent about 75% of the residuum portion of crude oil. Residuum entails approximately 18% of the total volume of an average 35° API gravity crude oil (Table 3). Residuum is the most complex fraction of petroleum and also the least understood. The main components of residuum are heavy oils, resins, asphaltenes, and high molecular weight waxes.

**Table 3 Composition of a 35 ° API Gravity Crude Oil (Hunt, 1995)**

Molecular Size	Volume Percent
Gasoline (C <sub>5</sub> to C <sub>10</sub> )	27
Kerosine (C <sub>11</sub> to C <sub>13</sub> )	13
Diesel Fuel (C <sub>14</sub> to C <sub>18</sub> )	12
Heavy Gas Oil (C <sub>19</sub> to C <sub>25</sub> )	10
Lubricating Oil (C <sub>26</sub> to C <sub>40</sub> )	20
Residuum (>C <sub>40</sub> )	18
<b>Total</b>	<b>100</b>

Asphaltenes are dark brown to black amorphous solids. Moving from oils to resins to asphaltenes, the molecular weight, the aromaticity, nitrogen, oxygen and sulfur content increases. Asphaltenes exist in petroleum as colloidal particles dispersed in an oily medium. As the oily medium is removed by distillation, the particles become more concentrated to form asphalt,

which at room temperatures is highly viscous, resembling a hard solid. According to Hunt (1995) an asphaltene molecule consists of 10 to 20 condensed aromatic and naphthenic rings with paraffin and naphthenic side chains. These condensed aromatic structures also contain space for free radicals, where highly reactive unpaired electrons are employed. Some of these sites are capable of complexing metals.

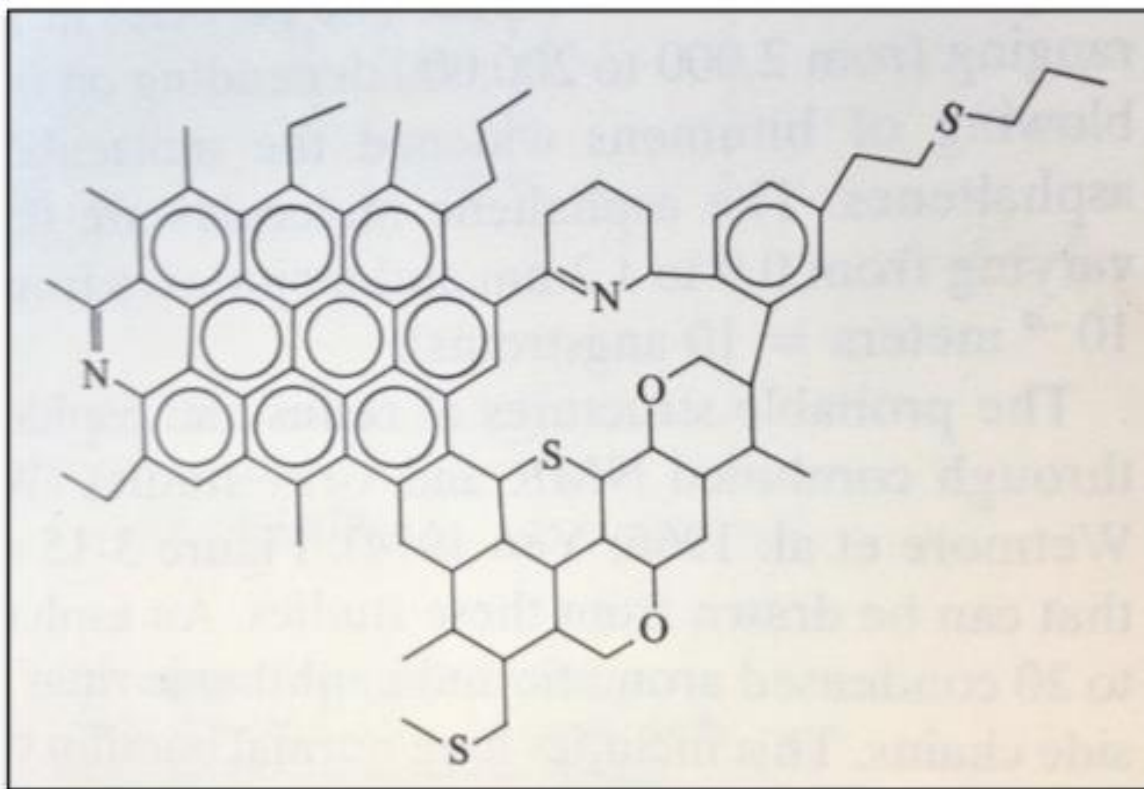


**Figure 6 Schematic Asphaltene Molecule (Hunt, 1995).**

The following table displays the percent of resins and asphaltenes in various crude oils.

**Table 4 Resins and Asphaltenes in Crude Oils (Erdman and Saraceno, 1962)**

Crude Oil	Source	Weight percent	
		Resins	Asphaltenes
<b>Ellenburger</b>	W. Texas	4.2	0.24
<b>Ragusa</b>	Sicily	9	0.28
<b>Grozni</b>	USSR	8	1.5
<b>Karami</b>	China	14	1.8
<b>Wilmington</b>	California	14	5
<b>N. Beldridge</b>	California	18	5
<b>Khaudag</b>	USSR	33	8
<b>Belaim</b>	Egypt	20	13
<b>Boscan</b>	Venezuela	29	18
<b>Athabasca</b>	Canada	24	19

Heavy crude oils have more oxygen with residue comprising over 5 % oxygen most of the times (Hunt 1995). It is important to note that Oxygen is present in the composition of crude oil. Analysis of REE is possible due to the previously mentioned characteristic of REE, the affinity REE have to create ligands with oxygen.

### **1.3- Gas Chromatography**

The basis for this study is the analyses of REEs in crude oils. Gas chromatograph data was also used, to help constrain the REE results. Dr. R.P. Philp and his colleagues conducted the gas chromatograph data at the University of Oklahoma.

Samples were run through an Agilent Technologies 5957c GC analyzer that was set to a sampling time of 100 minutes where initial temperature was set at 40 degrees Celsius and reached a maximum temperature of 300 degrees Celsius. Oil samples were injected from a syringe with oil volumes at 10 milliliter in to a capillary column having a constant flow rate of 1.4 mL per minute at 21.725 psi, having a velocity through machine averaging 30.339 cm/sec. The mass spectrometry analyzer was running the same volume as the GC, where the electro-magnet was running on 2435 volts. The analysis took place between 10 minutes and 80 minutes.

#### ***1.3.1 n-Alkanes and Isoprenoids***

There are numerous types of petroleum hydrocarbon chains. Chains as simple as a n-alkane to as complicated as saturated cyclical hydrocarbons. A more useful and easier series to understand are the normal (n) alkanes and the isoprenoids. These organic carbons can provide a lot of useful information to determine crude oil's formation history. Alkanes are the combination of carbons and a number of hydrogen atoms needed to satisfy carbon's valence charge of 4. This commonly gives rise to a chemical compound having  $C_nH_{2n+2}$ . The number of carbon atoms can greatly increase, reaching even  $C_{40}$  amounts, indicating alkane complexity. The most useful n-alkane range used in oil biomarker evaluation is the  $C_{11}$ - $C_{25}$ , with special emphasis on the  $C_{18}$  and  $C_{19}$ , plus the carbon preference index between  $C_{11}$ - $C_{22}$  biomarkers.

Isoprenes contain a series of five-carbons, and are commonly found in all oil biomarkers. These complex hydrocarbons come from the biosynthesis by polymerizing the appropriate 5-carbons isoprenes (Peters et al., 2005). The two commonly used isoprenoids used in biomarker analysis are pristane and phytane. Both fall into the acyclic, diterpane series where pristane is created by the degradation of phytane by losing a methyl group. In conjunction with n- $C_{17-18}$  chains, much can be interpreted about the source rock and the post-accumulation alterations of oil. Pristane and phytane are commonly looked at together as a ratio (Pr/Ph). The Pr/Ph ratio of a crude oil is a reflection of the source of the original organic matter and the paleoenvironmental



conditions during decomposition and early burial. Higher Pr/Ph values (3 to 15) indicate a source from mostly land derived organic matter that has passed through a highly oxygenated state in its decomposition. Low Pr/Ph values (1.1 to 2) indicate oil that has been generated from marine organic source materials.

### ***1.3.2 Biodegradation of Crude Oil***

Petroleum commonly encounters many alterations following the expulsion from its source, with the most usual forms being biodegradation. This process occurs in the subsurface, and can only occur in areas where life can be sustained; environments containing food, water, correct salinities and pHs.

Moldowan and Peters (2005) discussed that for an organism to break down oils as a food source it can be done in more than one way. Some microorganisms have been known to secrete biosurfactants for cellular breakdown, the creation and use of enzymes and biopolymers, which can transform oils into water-soluble compounds. Some microorganisms may convert the oil in carbon dioxide, water and nutrients via oxidation, while another may use nitrates, sulfates and ferric ions to break down the hydrocarbon.

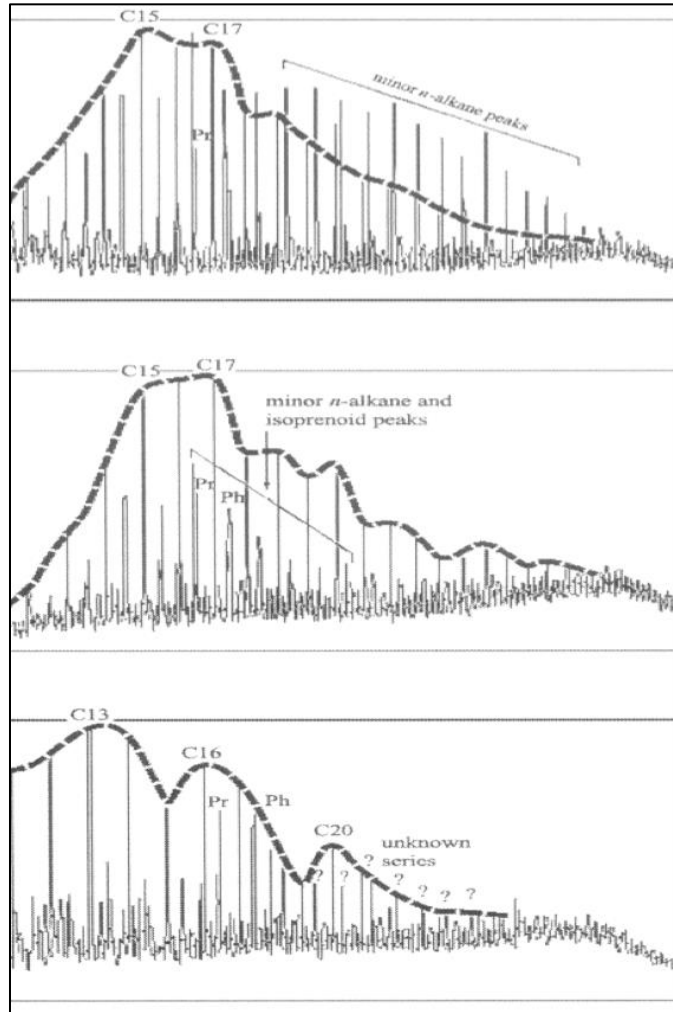


**Figure 7 Gas chromatograms showing the effects of biodegradation with decreasing amounts of alteration (top to bottom). (Peters et al. 2005)**

Under prolonged exposure to microbes and the effects that they bring about, an overall understanding should be discussed. As stated in the previous parts of the chapter, microbes will consume the hydrocarbon chains, changing the oils composition, but will also change the physical make-up. As the consumption continues, the oil will become heavier and heavier in density and more enriched with nickel, sulfur and vanadium, indicating alterations. Also, when considering an oils alteration and characteristics gas-to-oil ratio (GOR) values are important in understanding what effects are influencing and controlling these values. Arouri et al (2010) stated that thermal maturity and type of source rock, the charge history and the regional distribution of the carrier, reservoir and seal bed influence GOR distribution in a field. However, this only controls initial characteristics of the GOR, when obviously alterations will occur post

accumulation. Sited by Arouri et al (2010) are water-washing, oil cracking, biodegradation, segregation, and phase separation caused by pressure drop or gas influx. When gas migrates into a laterally extensive reservoir, it has the habit of displacing oils into shallower areas (Gussow, 1954). According to Gussow's principle, API gravity and GOR increases towards the basin's center. In addition, preference by microbes and water for the lighter end n-alkanes tends to decrease oils GOR, where the lighter end alkanes tend to compose natural gas.

## 1.4 Geological Setting

The study area is located in northwestern Kansas in Rooks County. The major structural features that affect the study area are the Cambridge Arch and the Central Kansas Uplift. Together these two structures are referred to as the Central Kansas Uplift. These anticlinal structures are ridges of Precambrian granite running northwest-southeast that formed during major periods of tectonic movement during pre-Mississippian and Middle Pennsylvanian times. Movement of the Cambridge Arch also occurred during Mesozoic time (Newell et. al. 1987). Above the basement granite lays the Cambro-Ordovician Arbuckle Dolomite, which is the primary oil producing rock unit in Kansas (Figure 4). As the Central Kansas Uplift is approached the formations below the Pennsylvanian and above the Arbuckle tend to pinch out until the Lansing-Kansas City rests upon the Arbuckle. At points on the Central Kansas Uplift the Arbuckle is completely eroded away. The Central Kansas Uplift and Cambridge Arch are bound on each side by similar basin areas: the Salina Basin to the northeast, the Hugoton Embayment to the west, and the Anadarko Basin to the south. The study area, Rooks County, is located on the eastern flank of the Central Kansas Uplift (Figure 6). The majority of Lansing-Kansas City oil production in Kansas occurs on the Central Kansas Uplift.

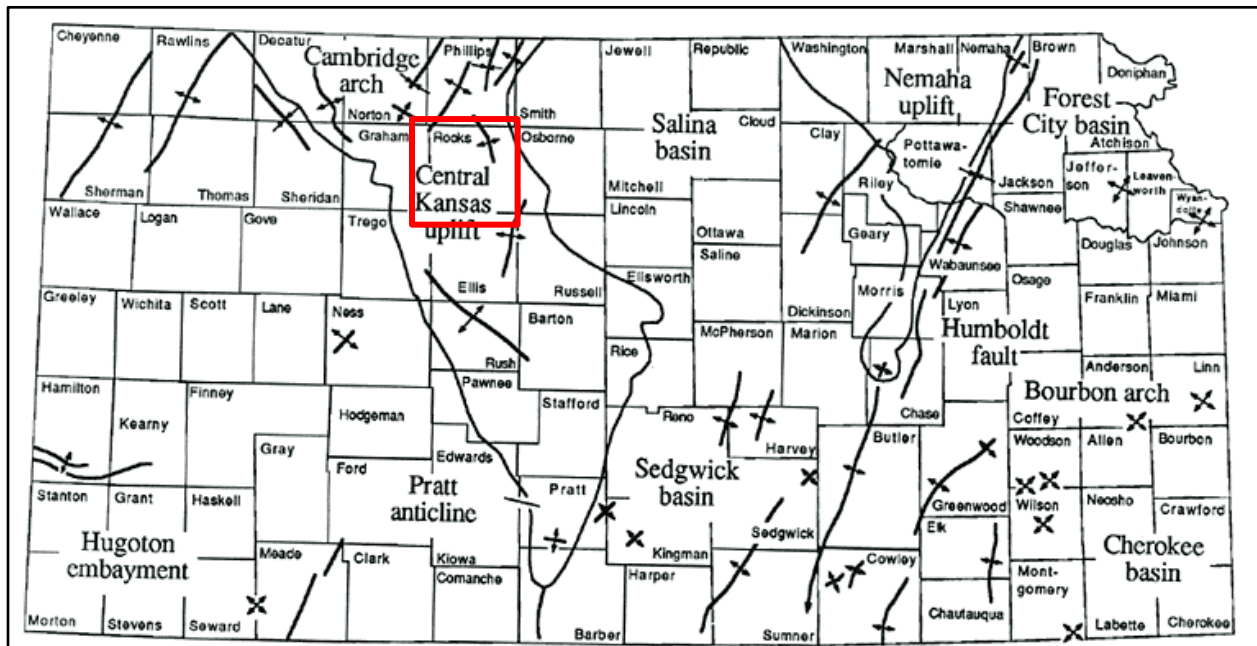


Figure 8 Structure map of Kansas with study area location (Watney, 1980).

### ***1.4.1 Lansing Kansas City Group***

The Lansing-Kansas City formations are part of the Missourian Stage of the Upper Pennsylvanian series. Most Pennsylvanian rocks in Central Kansas were deposited in shallow seas that alternately covered, then retreated from the land. The reoccurrence of the rising and falling sea levels caused the Pennsylvanian rocks in Kansas to occur as interbedded limestone and shales with occasional coal deposits and sandstones. In northwestern Kansas carbonate facies in the Lansing-Kansas City are highly variable (Watney, 1980). The Lansing-Kansas City ranges from 200-400ft in thickness over the Central Kansas Uplift. Moving south from the Cambridge Arch towards the Anadarko Basin, the Lansing-Kansas City groups become more massive. This indicates the Anadarko Basin was subsiding and expanding northward from Morrowan through Missourian time, after which subsidence decreased, resulting in shoreline regression and basin filling during Virgilian and later time. The act of subsidence and expansion created the alternating cyclic terrigenous clastic and carbonate strata. Individual cycles less than 30 meters in thickness were deposited in northwestern Kansas as a response to fluctuations of sea level and progradation of sediments. Each cycle in this area is characterized by four basic components: a thin but distinctive basal transgressive unit, overlain by marine shale, followed by the regressive carbonate and regressive shale (Merriam 1963).

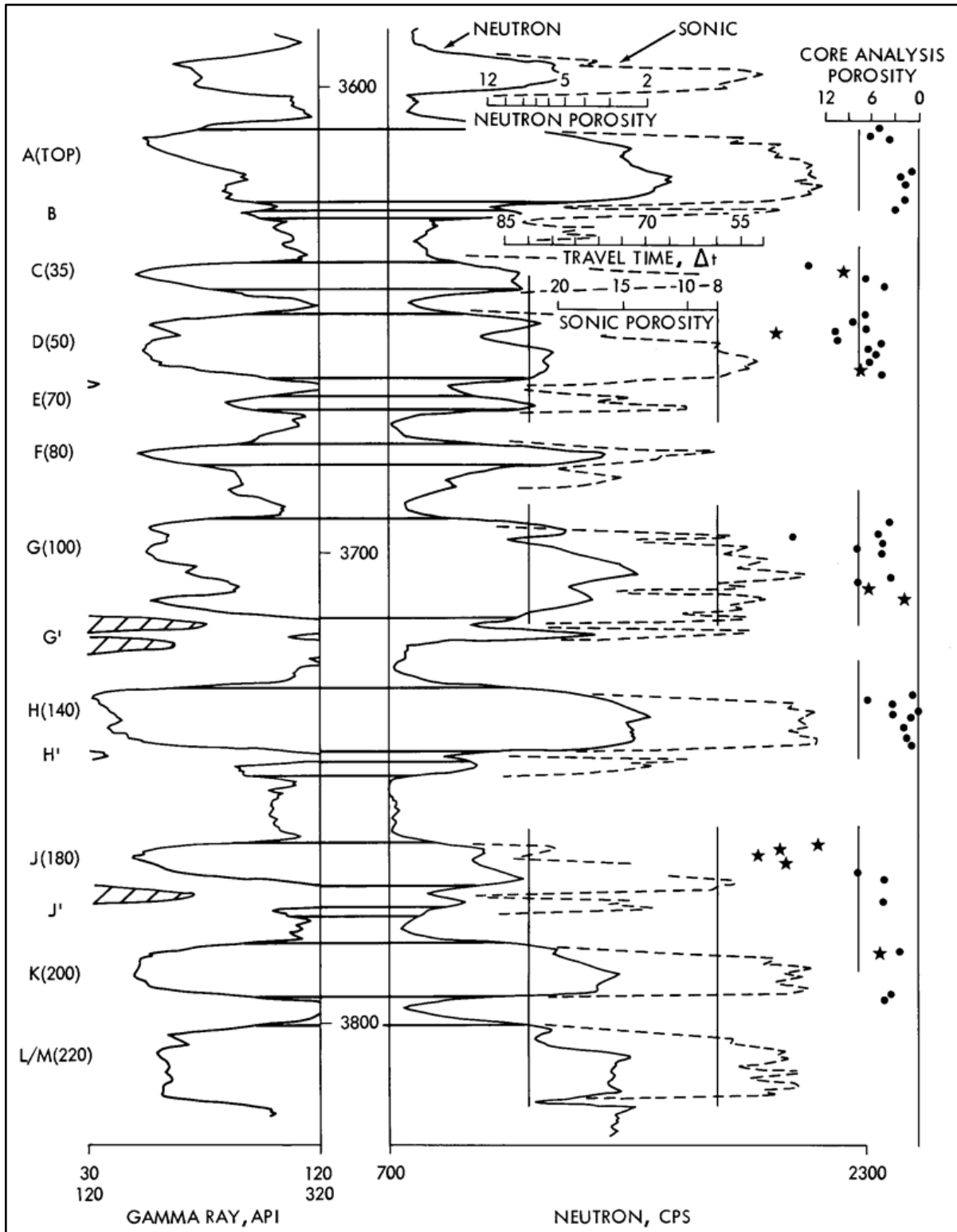
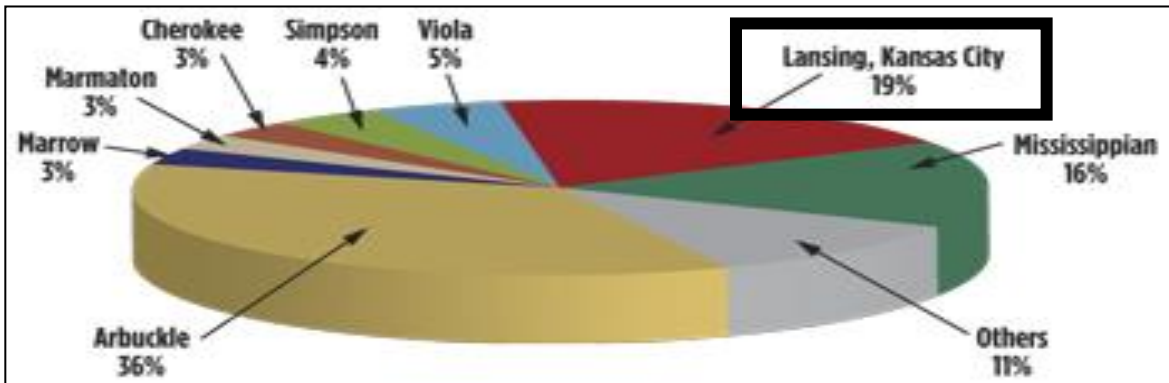


Figure 9 Type well log of Lansing-Kansas City group. Taken from Conoco Adell L-KC Unit 406 from section 2-T6S-R27W (Watney, 1980).

### 1.4.2 Lansing-Kansas City Production in Central Kansas

Oil and gas production has been a crucial element of the Kansas economy since the beginning of the twentieth century. The state currently ranks eighth among all states in annual oil production and fifth in annual gas production (Newell et al., 1989). Kansas's reservoirs have produced nearly 6 billion barrels of oil to date, with a significant majority of the past production coming from reservoirs in proximity to the Central Kansas Uplift (CKU). The Lansing-Kansas City group is the second largest producer of hydrocarbons in Kansas (Figure 2), accounting for 19% of Kansas's annual oil production. The mature, well-developed areas of production of oil and gas from Lansing-Kansas City rocks are located principally on the Central Kansas Uplift. Rooks County is one of the largest producers of oil from the Lansing-Kansas City group in the state of Kansas, accounting for more than 68.9 MMBO. Russell County, southeast of Rooks County, is the largest Lansing-Kansas City oil producer with more than 183.2 MMBO (Figure 5).



**Figure 10 Distribution of Kansas oil production by geologic formation.**

The majority of Kansas's Lansing-Kansas City production comes from central and north central Kansas, in areas on the Central Kansas Uplift. The largest producing county from the Lansing-Kansas City formation is Russell County, Kansas in the central portion of the state. According to Figure 10, Rooks County has produced approximately 68.9 MMBO from the Lansing-Kansas-City formation. The 68.9 MMBO of Lansing-Kansas City oil produced from Rooks County ranks 6<sup>th</sup> among all counties in Kansas.

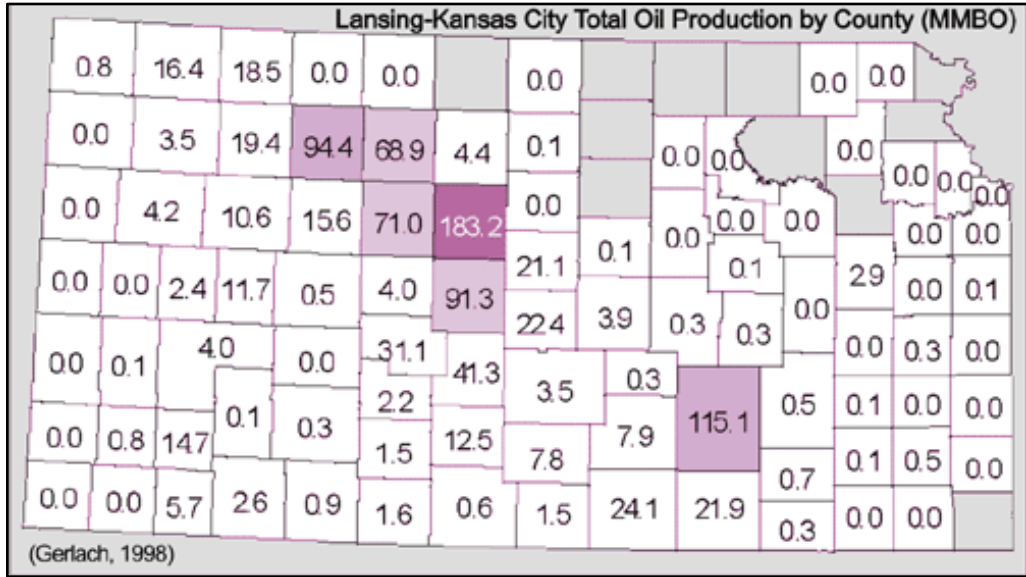


**Figure 11 Lansing-Kansas City total oil production by county (MMBO).**

The Lansing-Kansas City formations extend over the majority of the state of Kansas, except for the eastern portion of the state, where it outcrops. The Lansing-Kansas City received its name for outcropping in the Kansas City area. The Lansing-Kansas City is deepest in the south-central portion of the state, where it begins to enter the Anadarko Basin. Along the Central Kansas Uplift, where Lansing-Kansas City production is most prolific, the top of the Lansing formations can be found between 1500-2000 feet below sea level.

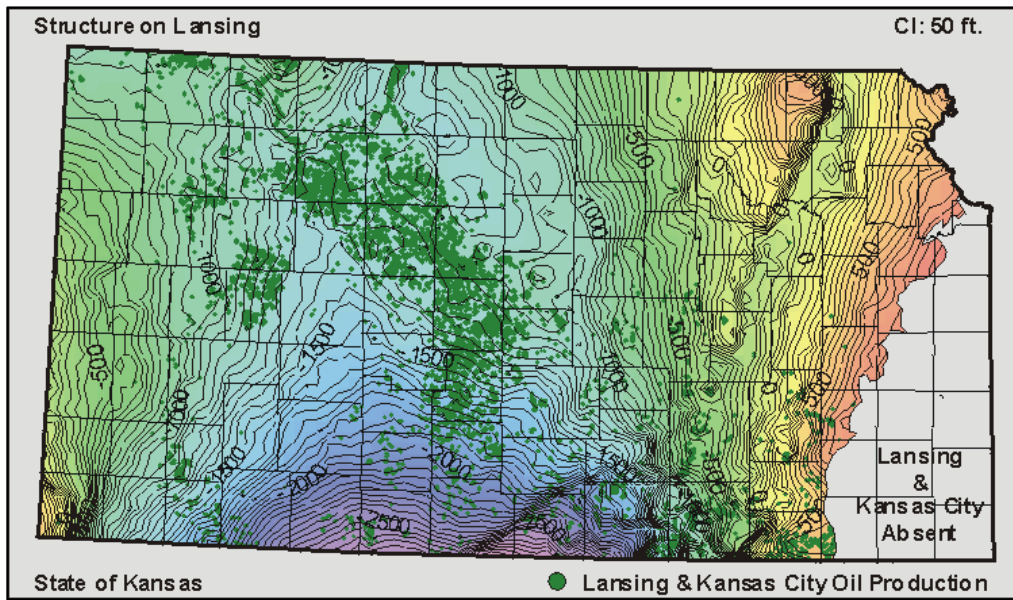


**Figure 12 Structure map at top of Lansing-Kansas City group with Lansing-Kansas City oil production.**



## **Chapter 2 - Methodology**

### **2.1 Study Area and Sample Locations**

The study area is comprised of Rooks County, Kansas, which sits on the eastern flank of the Central Kansas Uplift in northwest Kansas. Ten oil and nine brine samples were collected from various oil well pumps in Rooks County for this study. The wells that were sampled are all conventionally producing oil wells, meaning that they do not employ horizontal drilling or hydraulic fracturing. Each well is producing from the Lansing-Kansas City at depths ranging from 3000-5000 feet below sea level. Initial oil sampling began in May 2013, with McElhaney 1, 1A, 3A, and 4. The Petty John #1 and Dopita J #2 were also sampled, but produced more water than oil. These wells were used for brine analysis, which will be discussed later. Oil samples were collected in 1000ml narrow mouth clean Nalgene bottles. Lansing-Kansas City oil is generally very lightweight and wells produce an adequate amount of water as well as oil. Four liters of oil/brine were collected from each well to insure enough oil would be obtained for analyses. The remaining oil samples were collected in October 2013 using the same sample techniques. All wells sampled were found within Rooks County, Kansas and locations are given in Table 2. Seven of the ten oil samples were taken from two different Lansing-Kansas City fields: the McElhaney and Jones fields. Locating wells with Lansing-Kansas City production to sample was a time consuming process. The Kansas Geological Survey Oil and Gas well database was the main tool used to locate LKC wells. Originally, my goal was to locate LKC wells that were producing from only one zone, and collect oil from each zone for correlation. I soon found out that this was nearly impossible. In Rooks County it is more common to find wells producing from multiple zones in the LKC. I decided to break down the LKC into upper, middle, and lower sections and locate oil for each section (Figure 13). The lower section consists of zones J-L/M. The middle section consists of zones G-I. The upper section consists of zones A-F. This method proved to be much easier and I found that production in multiple zones generally matches the division of the Lansing-Kansas City in three sections.

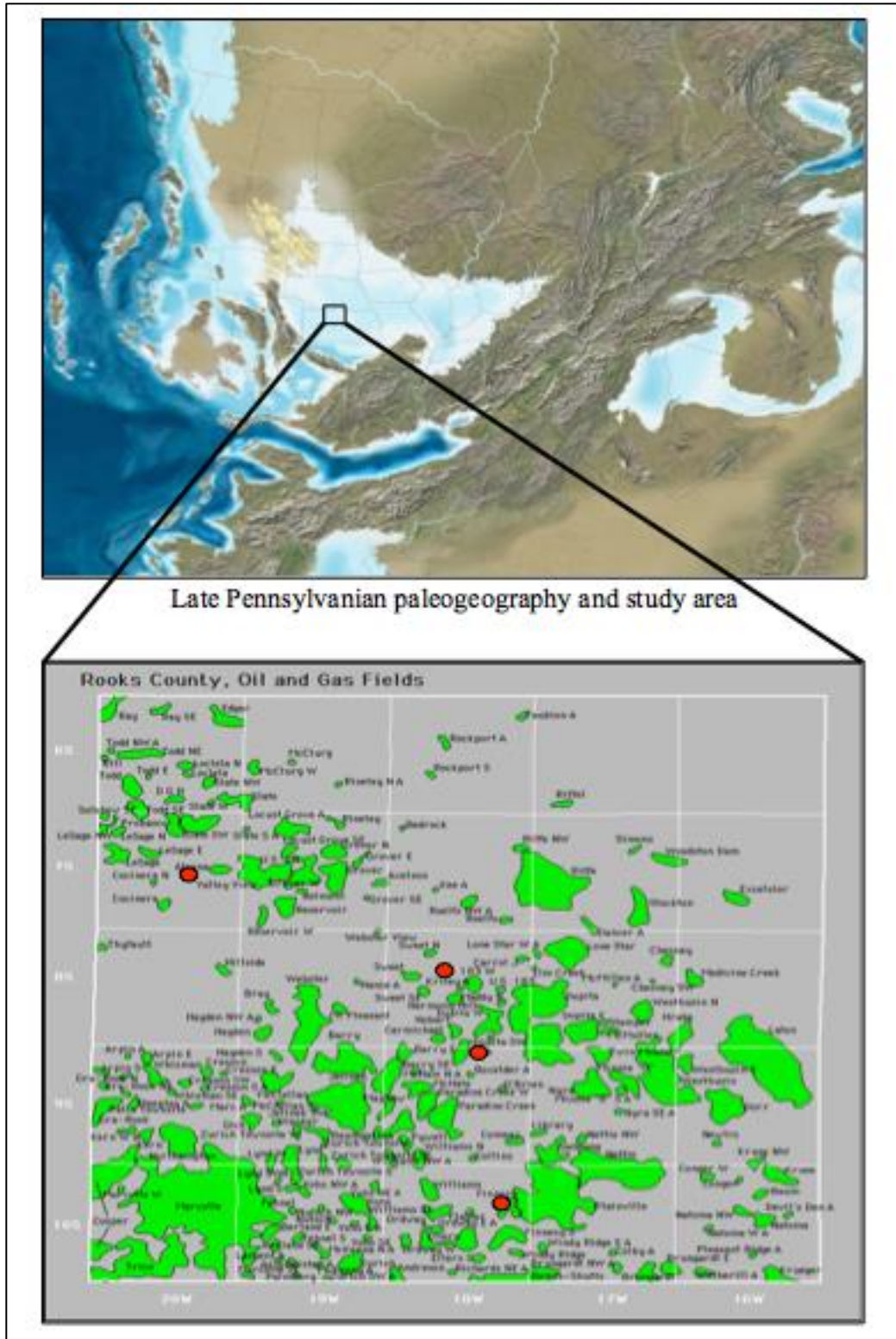


**Figure 13 Regional map showing study area and sample locations.**

Figure 13 is a gamma ray log taken modified from Brown (1984) showing a zone breakdown of the Lansing-Kansas City group in Haskell County, Kansas. The log has been broken down into upper, middle, and lower sections according to the sea level depth at the time of deposition.

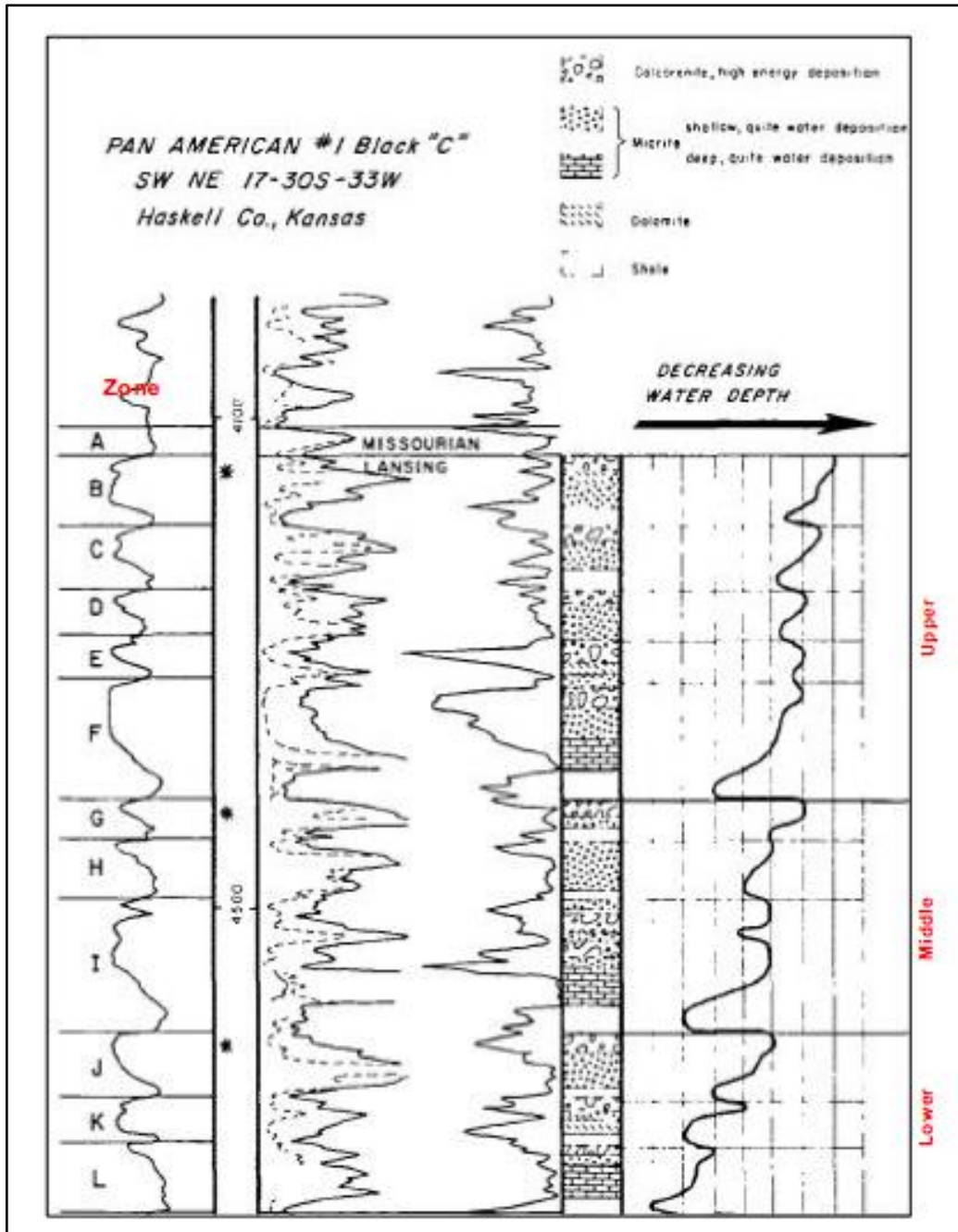


Figure 14 Lansing-Kansas City zone breakdowns. (Modified from Brown, 1984).

## 2.2 Sample Well Logs

The following logs correspond to wells sampled in this study. Each log is marked by which zone/zones within the Lansing-Kansas City it is producing from. This information was gathered from the Kansas Geological Survey Oil and Gas well database. Perforation depths are marked according corresponding scout cards for each well. Lansing-Kansas City zones were determined by referencing Figure 13.

**Table 5 Table with well identification, sample names, and Lansing-Kansas City zones.**

Sample Name	Sample Number	Analyses	Latitude	Longitude	Section	TWP	RNG	County	LKC Zone
McElhaney #1	MM-MC-01	REE & GC	39.3034811	-99.311033	3	9S	18W	Rooks	A
McElhaney #1A	MM-MC-1A	REE & GC	39.3034735	-99.3086999	3	9S	18W	Rooks	G
McElhaney #3A	MM-MC-3A	REE & GC	39.3052951	-99.3114419	3	9S	18W	Rooks	F
McElhaney #4	MM-MC-04	REE & GC	39.3034887	-99.3133662	3	9S	18W	Rooks	F
Jones #2	MM-JS-02	REE & GC	39.1879317	-99.2801643	13	10S	18W	Rooks	H,I
Jones #3	MM-JS-03	REE & GC	39.1860931	-99.2848029	13	10S	18W	Rooks	C,H,J,K,L
Jones #4	MM-JS-04	REE & GC	39.1898119	-99.2850068	13	10S	18W	Rooks	C,G,H,J,K,L
Jackson #1	MM-JK-01	REE & GC	39.4338917	-99.5360287	22	7S	20W	Rooks	A,J,K
Williams 11A-16-818	MM-WM-11A	REE & GC	39.3565945	-99.3352661	16	8S	18W	Rooks	J,K
Petty John #1	MM-PJ-01	GC	39.35561	-99.312945	15	8S	18W	Rooks	F,I,H,J,K
Dopita J #2	MM-DJ-02	GC	39.311155	-99.267061	31	8S	17W	Rooks	Lower LKC

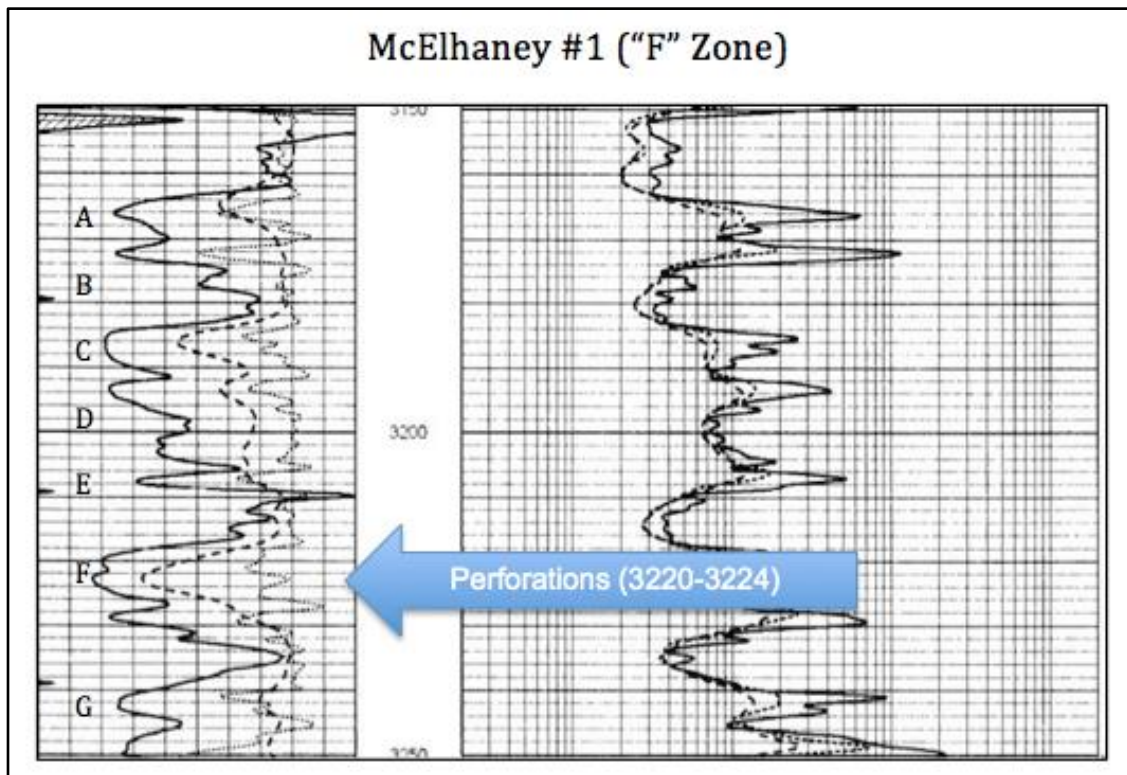


**Figure 15 Gamma ray log of McElhaney #1 with perforations marked.**

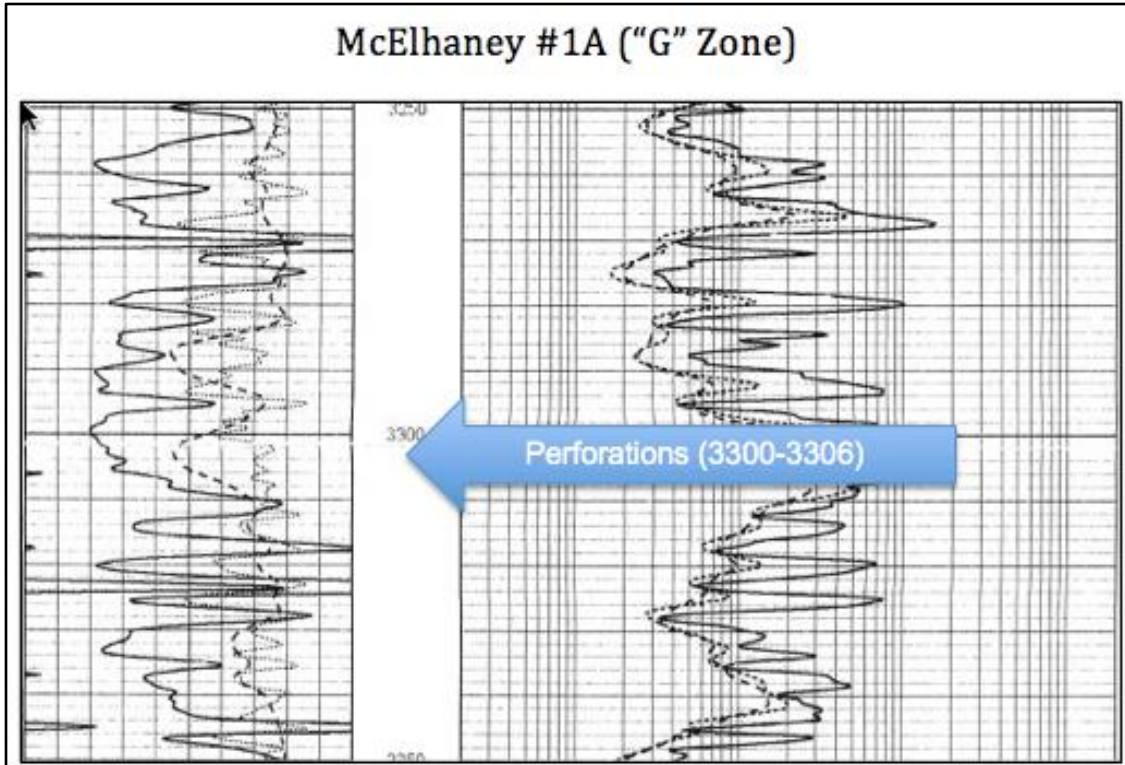


**Figure 16 Gamma ray log of McElhaney #1A with perforations marked.**

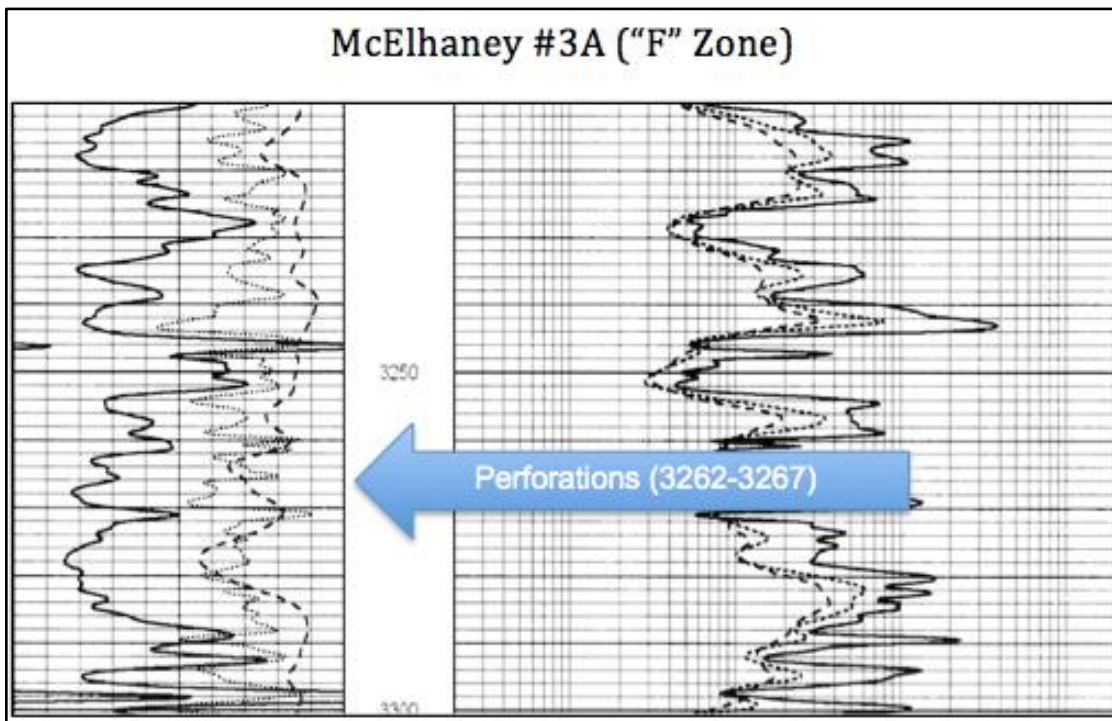


**Figure 17 Gamma ray log of McElhaney #3A with perforations marked.**

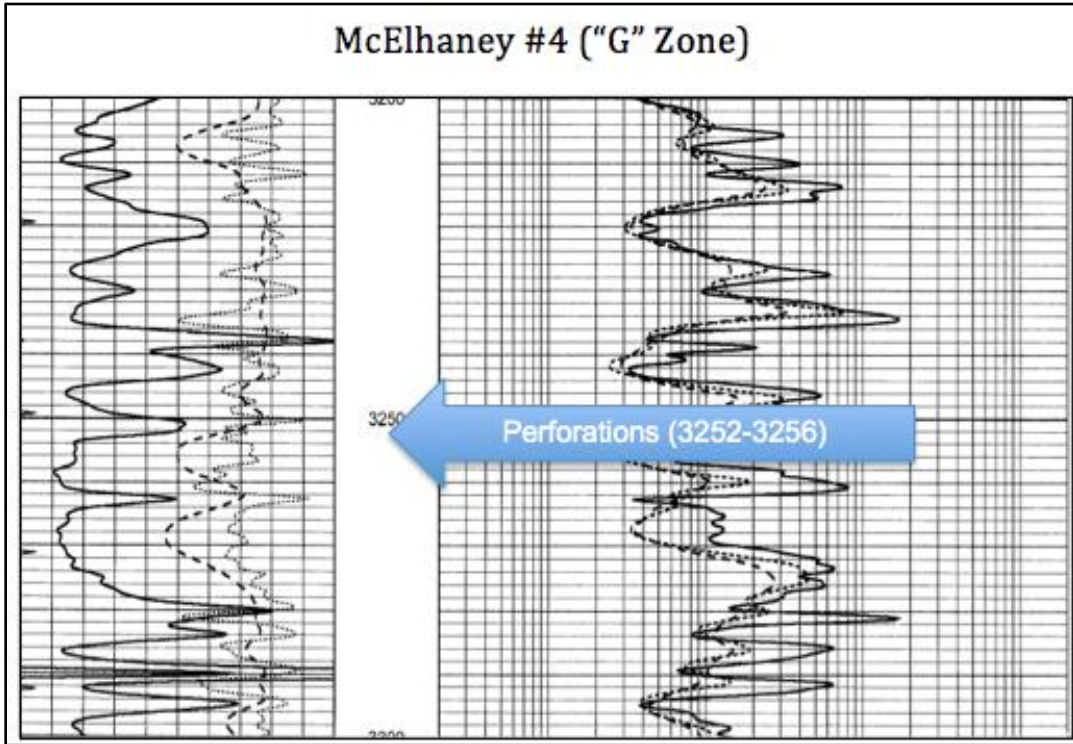


Figure 18 Gamma ray log of McElhaney #4 with perforations marked.

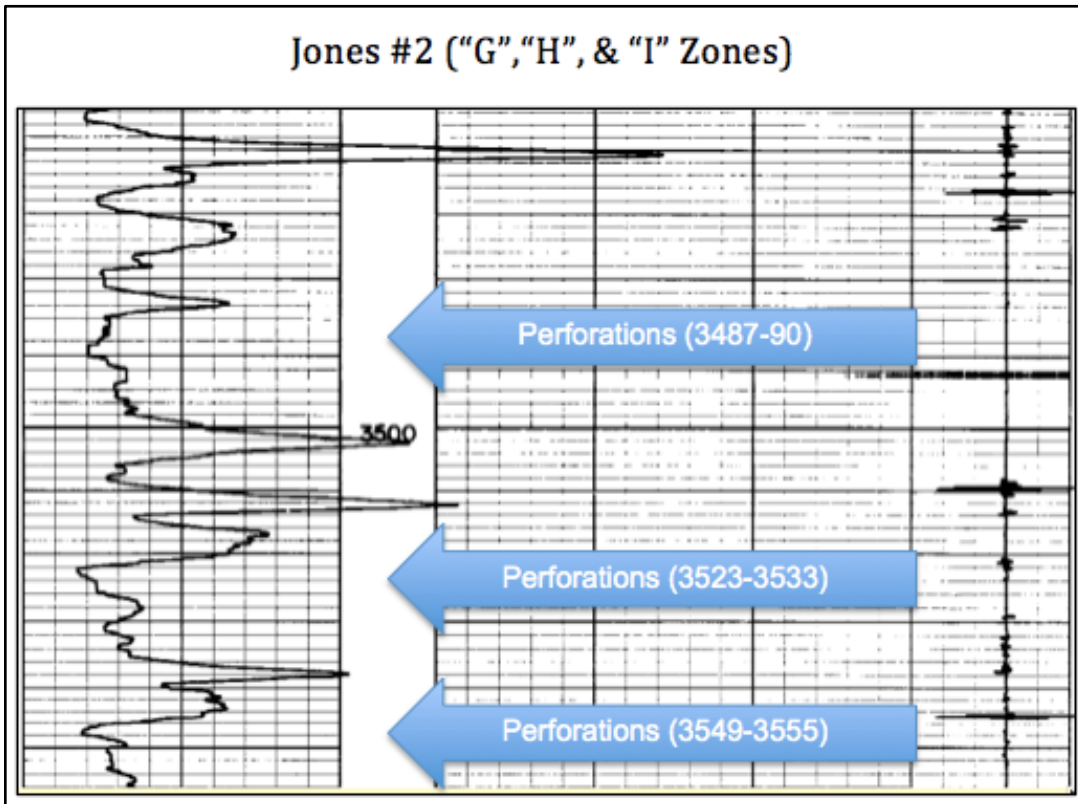
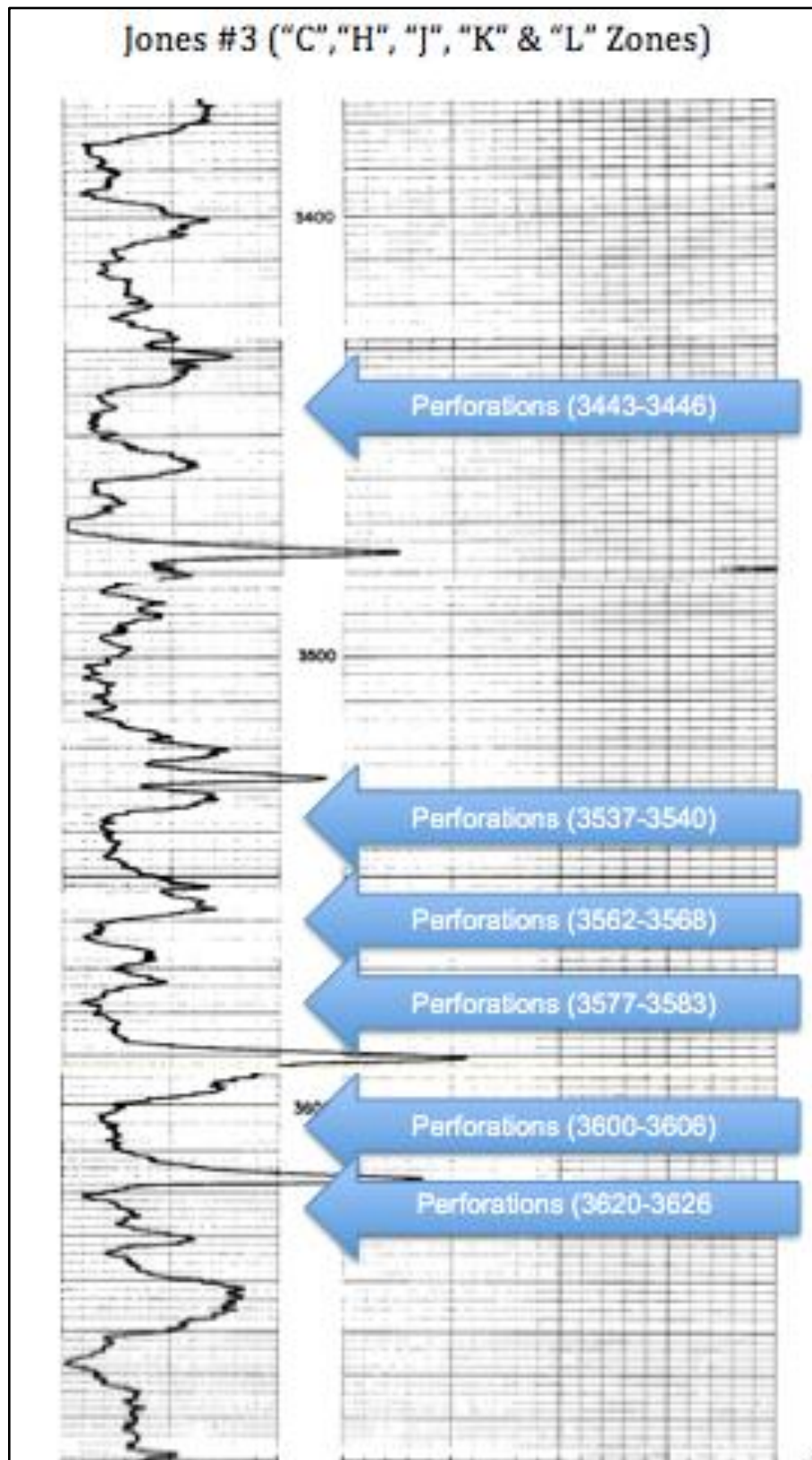


Figure 19 Gamma ray log of Jones #2 with perforations marked.



**Figure 20 Gamma ray log of Jones #3 with perforations marked.**

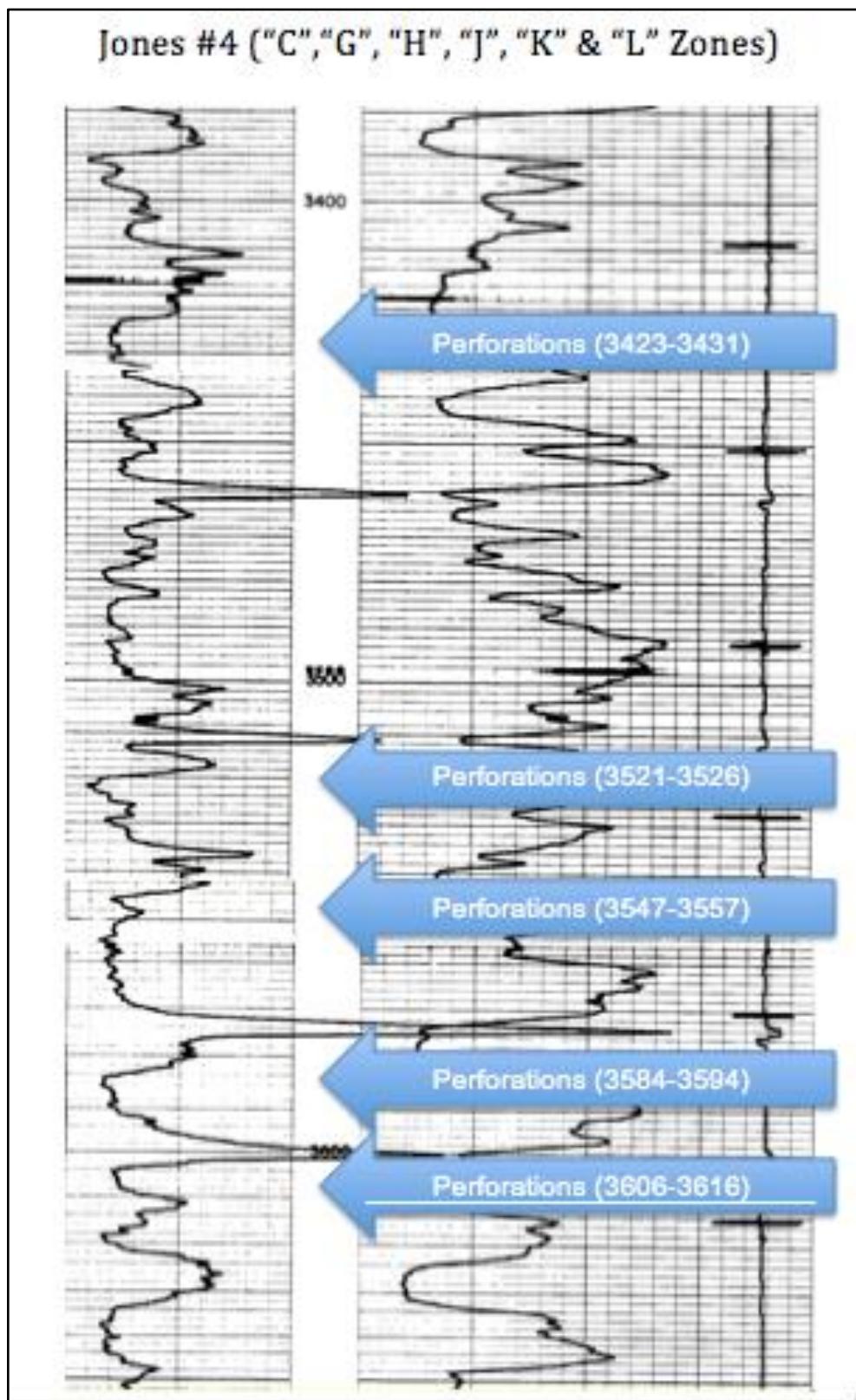


Figure 21 Gamma ray log of Jones #4 with perforations marked.



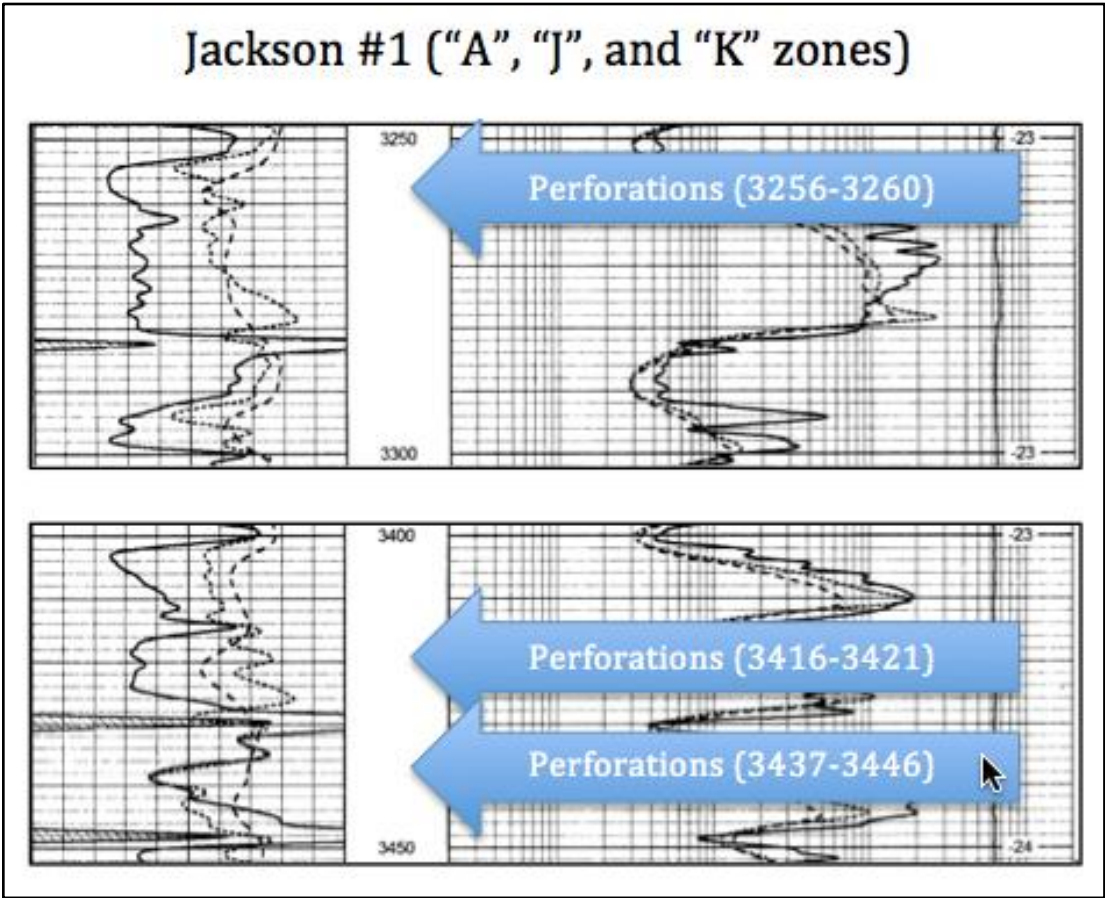


Figure 22 Gamma ray log of Jackson #1 with perforations marked.

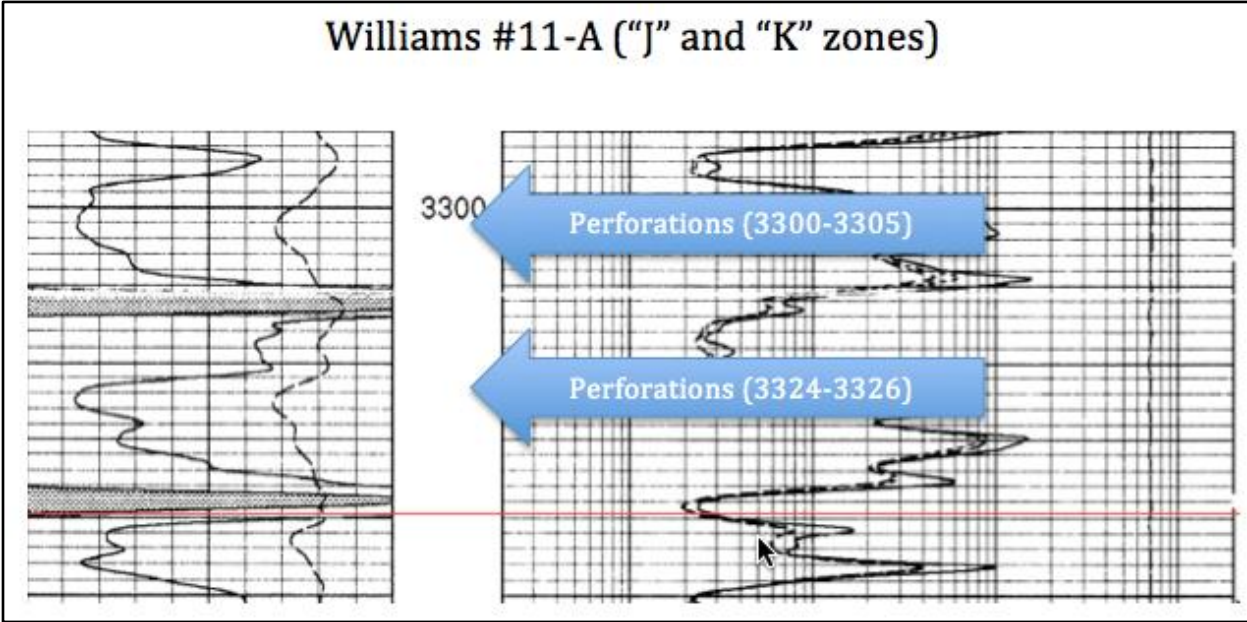


Figure 23 Gamma ray log of Williams #11A with perforations marked.

### **2.3 Methodology for Oil Analysis**

The nine oil samples in this study were processed at a designated lab in the Chemistry and Biochemistry Department at Kansas State University and then sent for ICP-MS and ICP-AES analysis at the University of Strasbourg in Strasbourg, France.

Initially, 100ml of oil was taken and treated with 30ml of vacuum sealed doubly distilled purified nitric acid. The acid was diluted 3 times of the original concentration. This showed no detectable amount of REEs by ICP-MS analysis. Next we used 200ml of oil treated with the same volume of 3 times diluted concentrated nitric acid. Again, no REE could be detected by ICP-MS analysis. Then we used 500ml of oil, and this time only La, Ce, and Nd were detectable. Sm to Lu was not detectable at all. Finally, 1000ml of oil was used with the same amount of reagent added to it as before. All elements were detectable by ICP-MS analysis.

The sample processing began by extracting crude oil from sample bottles. The sample bottles contained a mixture of crude oil and brine that is associated with oil. The oil was extracted by carefully pipetting out of the sample bottle, avoiding contact with the brine. The pipetted oil sample was placed into 22 cleaned 50ml centrifuge tubes. Each sample was then centrifuged for 4 hours to ensure separation of oil and brine. It was observed that centrifuging removed 2-3 milliliters of brine from each centrifuge tube full of oil. Each oil sample was then weighted by the milliliter, in an electronic scale to know the sample's mass in grams. After this separation process was completed, the evaporation process began for the oil samples.

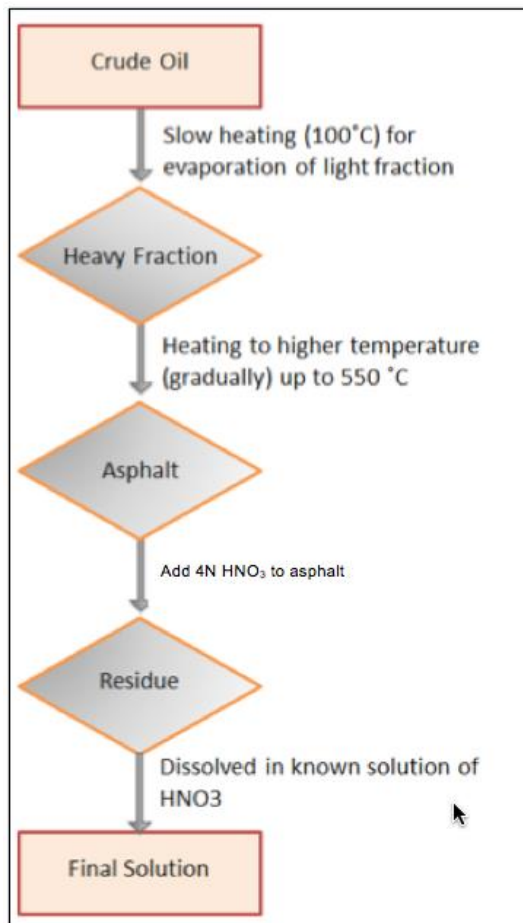


**Figure 24 Oil sample preparation flow chart (Modified from Ramirez, 2013).**

The evaporation process took place at Dr. Matthew Totten’s lab in Manhattan, KS. The room preparation in the Chemistry/Biochemistry Building was not adequate to do heavy oil evaporation. The black fumes emitted during heavy oil evaporation were too volatile to conduct the evaporation indoors. I used a process (Figure 21) implemented by Ramirez (2013). This consisted of preparing a homemade slow evaporation furnace with complete isolation to the outside and a ventilation conduct to dispose of the fumes.

The initial evaporation started at 200 degrees Celsius on a covered hot plate. At this temperature the samples will emit smoke, but not boil. The samples were monitored during the evaporation process to ensure continuous fuming with no boiling. Each oil sample took an average of 100 hours for slow evaporation. Small increases in temperature were applied to each sample during the 100 hours. As the temperature increased, the light fractions of the oil were volatilized. As explained in the crude oil composition section, the heavy fraction of the oil is the residue with a high percentage of Oxygen and Nitrogen. The purpose of evaporation of the oil

samples was to separate the heavy fraction. It was very apparent when the samples reached the heavy fraction of the oil because they ceased to emit fumes and the originally liquid oil had become a viscous, pasty material. In some cases the oil was completely hardened. When the sample wouldn't fume anymore at temperatures close to 550°C, the sample was removed and taken to the Chemistry lab for continued preparation. At this point the oil has evaporated off the light fraction materials, leaving a thick tar substance in the bottom of the evaporation beaker. To continue the evaporation processes, 4N HNO<sub>3</sub> solution was added to the crude oil. This process caused the sample to turn into a hard ash substance. The samples were left on the hot plates overnight and evaporated to dryness. After each sample was cooled, a mixture of 30ml of concentrated HNO<sub>3</sub> and 30ml of deionized H<sub>2</sub>O was used to rinse the dried ash and the solution was collected in a 100ml crucible. This process was repeated, and approximately 120ml of rinse solution was collected. The rinse solution was then placed on a hot plate at 150 degrees Celsius and evaporated to dryness. Each sample was allowed to cool to room temperature. Finally, 15ml of 1N HNO<sub>3</sub> was added to each crucible. The acid was swirled around ensuring that the evaporated solution dissolves into the 1N HNO<sub>3</sub>. The 15ml of 1N HNO<sub>3</sub> final solution was then filtered with 42mm hardened ashless filter paper, collected in 30ml samples bottles, and shipped to the lab for processing.

### ***2.3.1 Potential Sources for Analytical Error***

The ICP-MS and ICP-AES machines at the University of Strasburg show an analytical instrument error of 5%. There are also two sources of potential error that should be addressed in this study: REEs in the nitric acid and contamination by variable silicate dust. The acid used in this study is vacuum sealed double distilled purified concentrated nitric acid. Before each step of sample preparation all instruments are thoroughly cleaned by nitric acid bath and rinsed with deionized water. A blank sample of the nitric acid used in this study was run on the ICP-MS and the total REE concentrations were approximately 2.5 ppb. This small amount of REEs would have little to no effect on the samples. The second concern is variable silicate dust contaminating samples during preparation. Great care is taken to avoid dust contaminating the oil samples. Small amounts of dust will have little to no effect on the REE distribution patterns.

## Chapter 3 - Results

The Lansing-Kansas City oil and brine samples were prepared for analysis in the Kansas State University Chemistry/Biochemistry department. The oil and brine samples were sent to the Laboratory of Hydrology and Geochemistry at the University of Strasbourg, France, for analytical examination by ICP-MS and ICP-AES. Oil and brine sample results are shown in the following tables.

### 3.1 Crude Oil REE Concentrations

Table 6 shows the REE and trace element analysis of the ten oil samples taken from ten wells in Rooks County, Kansas. After receiving the raw ICP-MS and ICP-AES data, the samples were corrected to the sample amounts and final solution amounts. Each sample started with approximately 1000ml oil. This oil was burned down and dissolved in 15ml of 1N HNO<sub>3</sub>. Raw data was multiplied by 15 and divided by 1000 in a Microsoft Excel spreadsheet. From Si to P, all numbers are in parts per million (ppm). The remaining elements from Sc to U are in parts per billion (ppb). Elements that were below detection limit have been filled in with orange. REEs have been highlighted in blue. At the bottom of the table Ce and Eu anomalies, U/Th ratios, V/Ni ratios, K/Rb ratios, and Total REEs have been calculated.

**Table 6 REE and trace element analytical results for Lansing-Kansas City oil samples**

Element	MM-MC-01	MM-MC-1A	MM-MC-3A	MM-MC-04	MM-JS-02	MM-JS-03	MM-JS-04	MM-JK-01	MM-WM-11A
Si	0.22	0.27	0.27	0.18	0.045	0.060	1.05	0.048	0.395
Al	0.213	0.049	0.11	0.039	0.200	0.206	0.341	0.135	0.419
Mg	9.527	0.03	9.58	0.042	0.083	0.177	21.1	0.177	0.183
Ca	50.32	0.35	46.7	0.27	0.479	0.926	258	1.34	1.01
Fe	0.44	0.23	2.47	0.44	0.048	0.685	5.85	1.05	0.354
Mn	0.0127	0.00271	0.02344	0.00969	-	0.010	0.058	0.007	0.007
Ti	-	-	-	-	0.006	0.004	0.015	-	0.003
Na	-	0.58	-	2.18	2.15	6.54	0.02	13.3	14.5
K	2.34	-	1.97	-	0.220	0.224	10.7	0.288	0.312
P	0.15	0.1	0.19	0.1	0.038	0.036	0.242	0.066	0.092
Sr	2310	13	2706	9	4.9	38.4	26500	67.8	32.5
Ba	13.1	2	55.7	2.1	4.3	4.4	261	3.9	8.0
V	65300	36100	100000	42300	986	1480	40200	1720	9070
Ni	20300	10700	28300	11900	367	481	4481	465	1454
Co	98	43	147	59	3	4	49	5	9

<b>Zn</b>	226	85	197	79	25.5	64.9	123	24.5	86.3
<b>Cr</b>	16.2	7.3	14.5	7.0	2.8	1.7	13.2	2.7	9.0
<b>Cu</b>	31	8.3	224	12.0	11.0	8.3	12.4	5.5	26.3
<b>Rb</b>	1.69	0.054	1.93	0.040	0.11	0.12	12.2	0.16	0.30
<b>Y</b>	1.30	0.45	0.20	0.44	0.10	0.12	0.70	-	-
<b>Zr</b>	4.9	0.26	0.56	0.29	4.51	0.71	3.47	1.00	10.2
<b>Cs</b>	0.08	-	0.12	-	-	-	1.31	0.10	-
<b>La</b>	8.10E-02	3.90E-02	1.60E-02	1.59E-02	9.52E-04	1.29E-03	1.56E-02	8.10E-04	3.59E-03
<b>Ce</b>	1.64E-02	7.91E-03	1.28E-02	5.09E-03	1.70E-03	1.50E-03	1.56E-02	1.22E-03	6.02E-03
<b>Pr</b>	1.63E-02	8.48E-04	1.32E-03	4.58E-04	1.11E-04	1.88E-04	1.46E-03	1.11E-04	6.35E-04
<b>Nd</b>	7.50E-03	3.29E-03	4.68E-03	1.73E-03	4.13E-04	6.19E-04	4.78E-03	4.29E-04	2.38E-03
<b>Sm</b>	2.25E-03	7.43E-04	9.60E-04	3.15E-04	7.94E-05	9.38E-05	4.71E-04	9.52E-05	4.13E-04
<b>Eu</b>	8.25E-04	1.43E-04	-	6.75E-05	3.17E-05	3.75E-05	-	3.17E-05	7.94E-05
<b>Gd</b>	-	6.00E-04	9.00E-04	3.00E-04	1.43E-04	1.31E-04	5.14E-04	2.38E-04	3.97E-04
<b>Tb</b>	-	6.75E-05	1.28E-04	-	1.59E-05	1.88E-05	6.21E-04	1.59E-05	4.76E-05
<b>Dy</b>	1.73E-03	3.60E-04	6.68E-04	2.18E-04	6.35E-05	9.38E-05	4.07E-04	7.94E-05	2.70E-04
<b>Ho</b>	1.05E-03	6.00E-05	3.38E-04	4.50E-05	-	1.88E-05	2.06E-03	1.59E-05	4.76E-05
<b>Er</b>	1.13E-03	1.88E-04	3.83E-04	1.43E-04	4.76E-05	5.63E-05	2.79E-04	4.76E-05	1.43E-04
<b>Tm</b>	8.25E-04	-	5.25E-05	-	-	-	2.14E-05	-	1.59E-05
<b>Yb</b>	1.20E-03	2.03E-04	3.08E-04	1.65E-04	4.76E-05	5.63E-05	1.71E-04	4.76E-05	1.11E-04
<b>Lu</b>	8.25E-04	-	3.75E-05	-	6.35E-05	3.75E-05	4.29E-05	1.59E-05	1.59E-05
<b>Pb</b>	1.2278	1.4025	13.2750	1.3950	0.0308	0.0371	0.4241	0.0235	0.0646
<b>Th</b>	0.0090	0.0009	0.0016	-	-	-	0.0021	-	-
<b>U</b>	0.0596	0.0189	0.0938	0.0292	0.0004	0.0006	0.0089	0.0004	0.0021
<b>U/Th</b>	6.61666667	21.05	59.52380952	-	-	-	4.13	-	-
<b>V/Ni</b>	3.216748768	3.373831776	3.533568905	3.554621849	2.686376022	3.076923077	8.971211783	3.698924731	6.237964237
<b>K/Rb</b>	1384.6	-	1022.3	-	2000.0	1866.7	877.8	1800.0	1040.0
<b>TREE</b>	0.1310	0.0534	0.0385	0.0244	0.0037	0.0041	0.0420	0.0032	0.0142

An important calculation is the total REEs in each oil sample. This was calculated by adding each element's concentration in the oil sample. Figure 16 was created using the calculated total REEs. According to Figure 16, MM-JK-01 contains the smallest amount of total REEs and MM-MC-01 contains the largest amount of total REEs. Knowing the samples with the smallest and largest total REEs enables you to use those samples to normalize the remaining samples. The total REE concentrations may be representing the light hydrocarbon bearing enriched oil fraction analyzed.

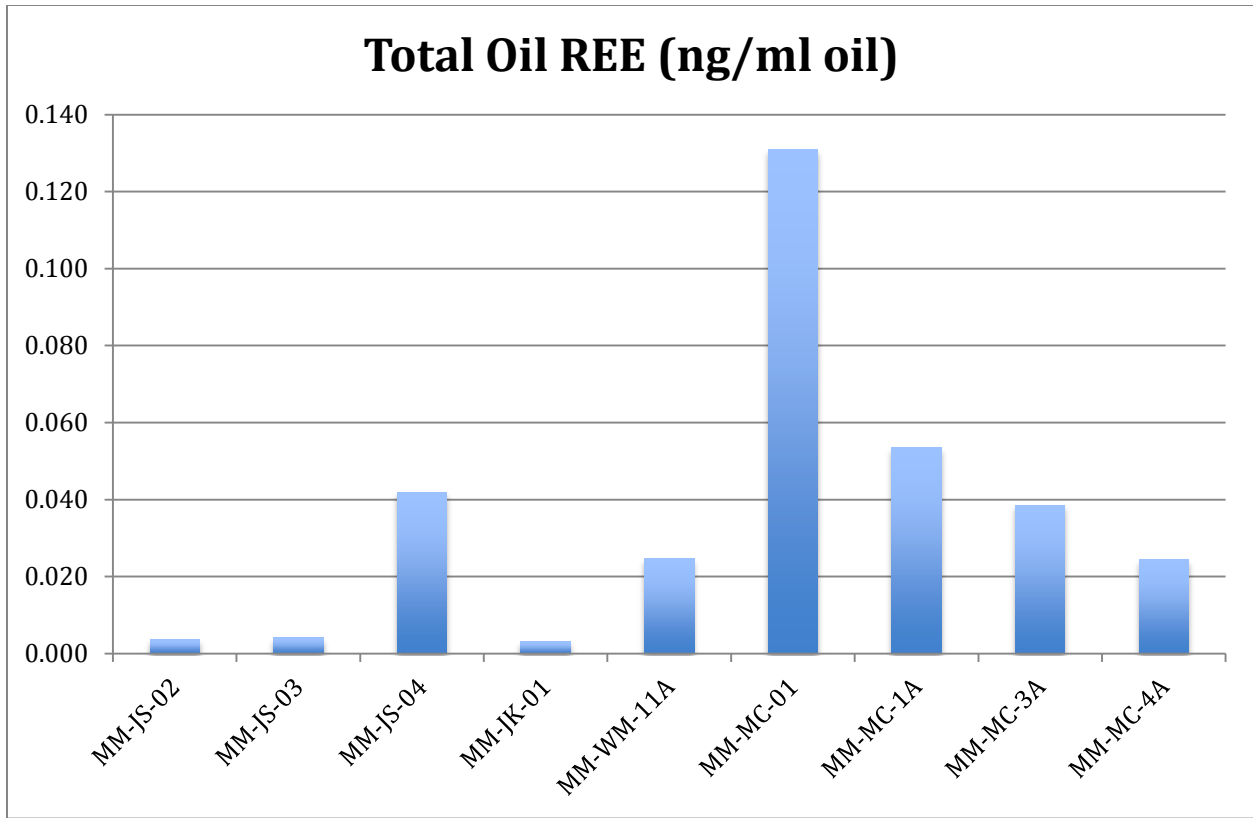


**Figure 25 Distribution of total REE concentration in Lansing-Kansas City oil samples.**

### 3.2 REE Distribution Patterns of Crude Oil

In order to analyze and compare the concentrations of REEs in crude oil samples, each sample must be normalized to set of constants. In this study REE distribution patterns were normalized to the Post Archean Australian Shale (PAAS) (Figure 17) and the smallest total REE, MM-JK-01 (Figure 18), as stated above. Values for REEs were plotted on a line graph with element name on the x-axis and normalized REE values on the y-axis.

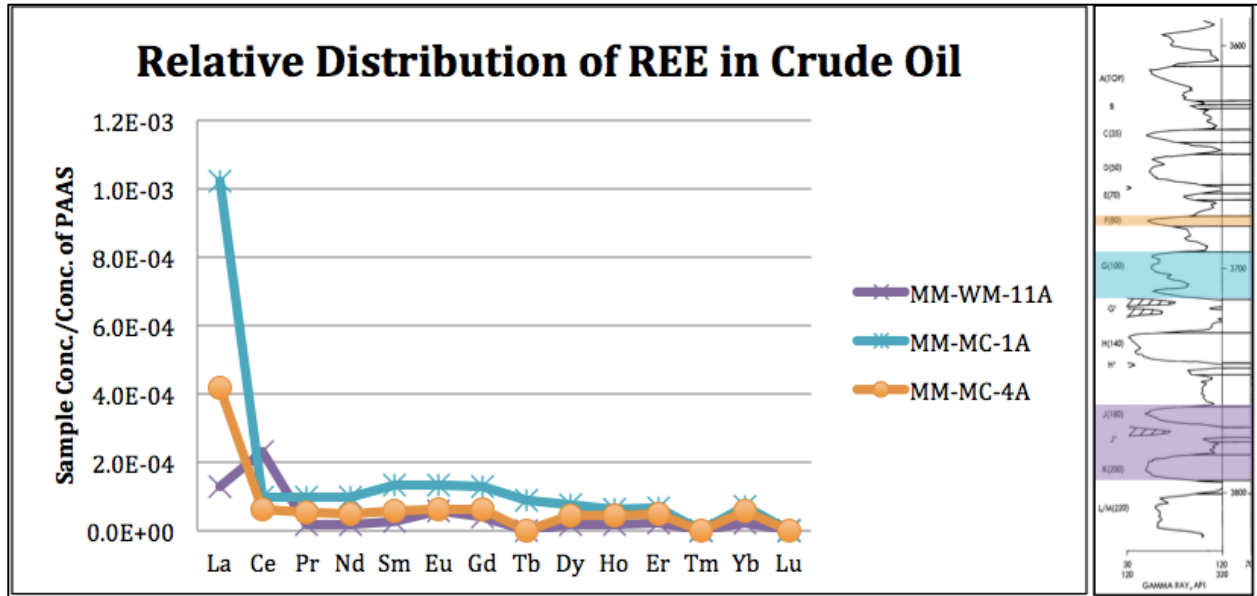


**Figure 26 Relative distribution patterns of REE concentrations in three Lansing-Kansas City oil samples (MM-WM-11A, MM-MC-1A, MM-MC-4A). Normalized to PAAS. Samples are grouped with similar distribution patterns. Zones of production are highlighted with correlating colors.**



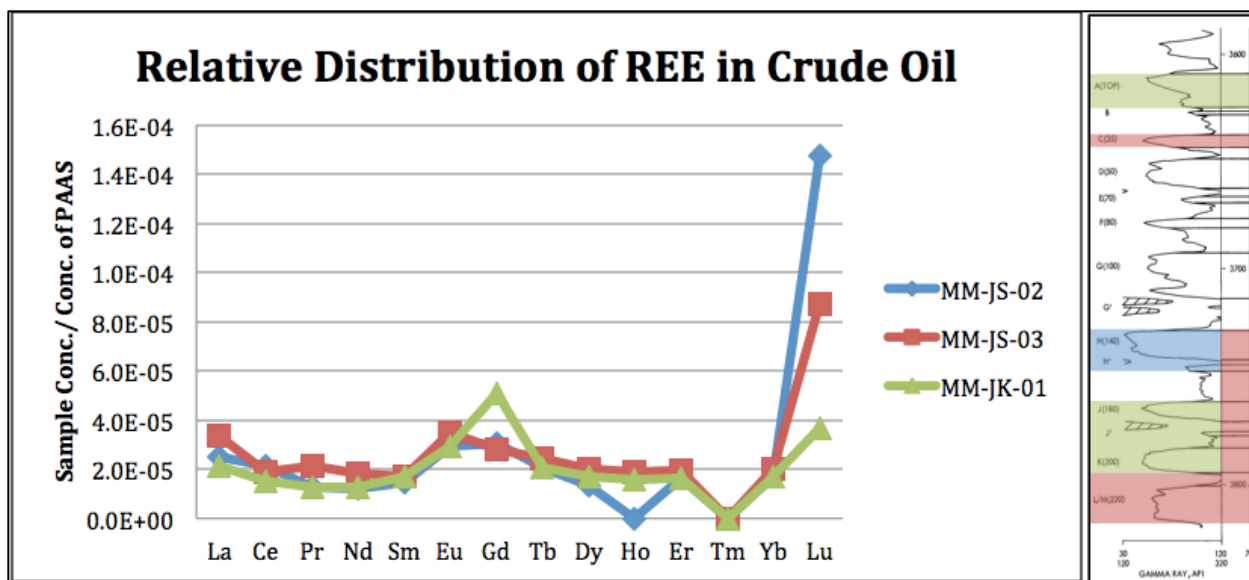


**Figure 27** Relative distribution patterns of REE concentrations in three Lansing-Kansas City oil samples (MM-JS-02, MM-JS-03, MM-JK-01). Normalized to PAAS. Samples are grouped with similar distribution patterns. Zones of production are highlighted with correlating colors.

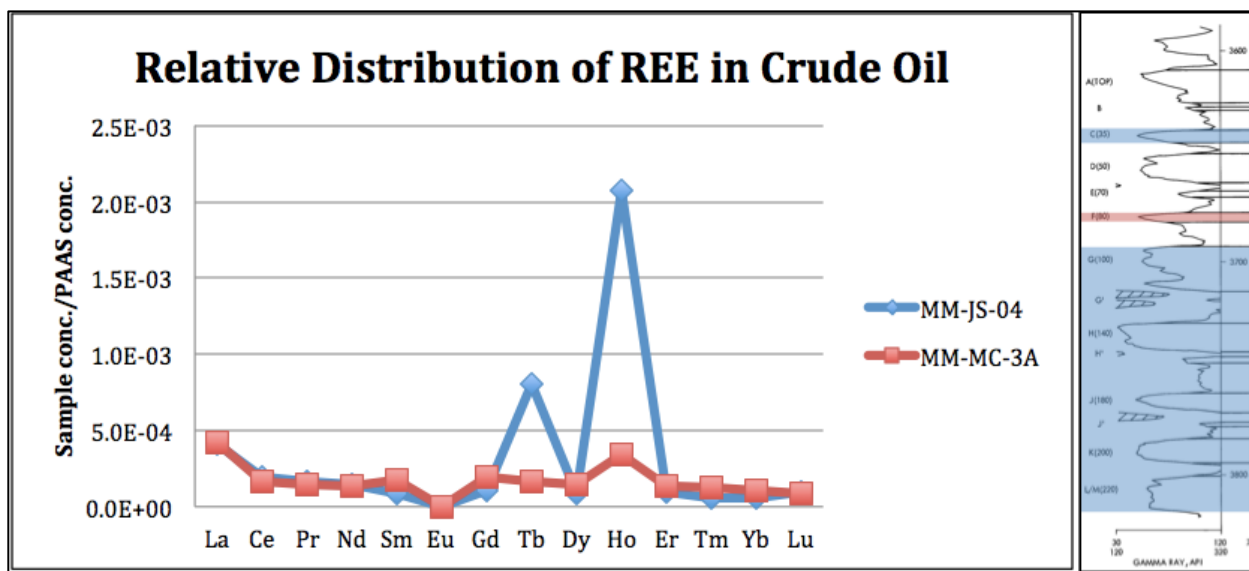


**Figure 28** Relative distribution patterns of REE concentrations in two Lansing-Kansas City oil samples (MM-JS-04 and MM-MC-3A). Normalized to PAAS. Samples are grouped with similar distribution patterns. Zones of production are highlighted with correlating colors.

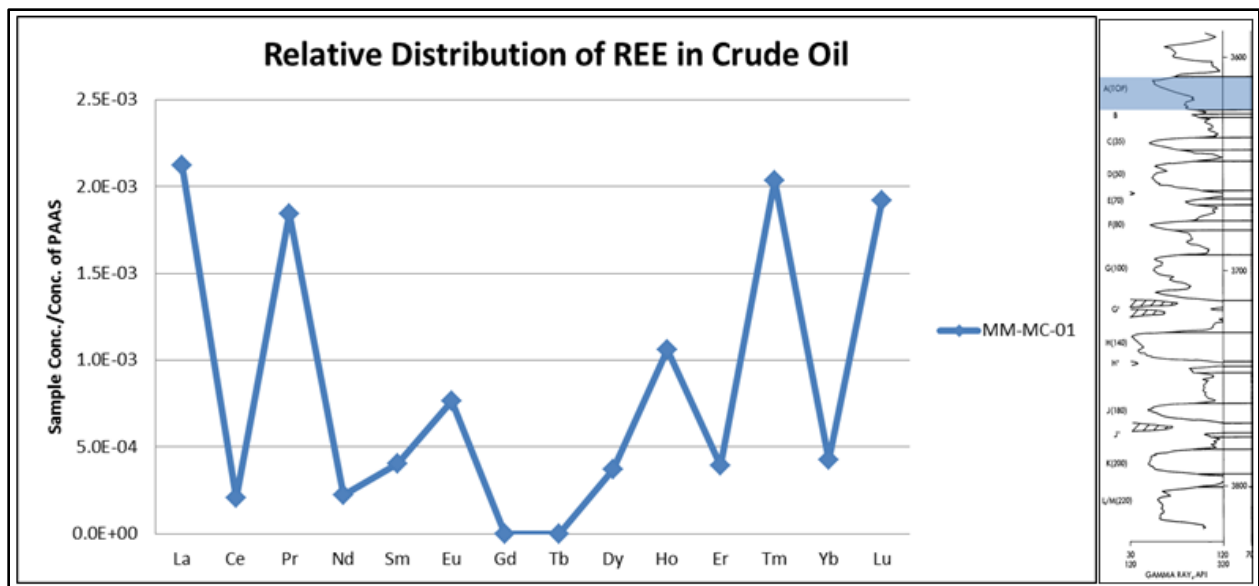


**Figure 29** Relative distribution patterns of REE concentrations in one Lansing-Kansas City oil samples (MM-MC-01). Normalized to PAAS. Zone of production is highlighted with a correlating color.

### 3.3 K/Rb Ratios

K/Rb ratios were calculated and plotted for Lansing-Kansas City oil samples and compared to a know average K/Rb ratio in silicate minerals (Figure 19). Rb values were taken from raw ICP-MS data and divided by K values taken from raw ICP-AES. Rb values were recorded in parts per billion (ppb) and K values were recorded in parts per million (ppm). After dividing Rb values by K values in an Excel spreadsheet, the samples needed to be multiplied by 1000.

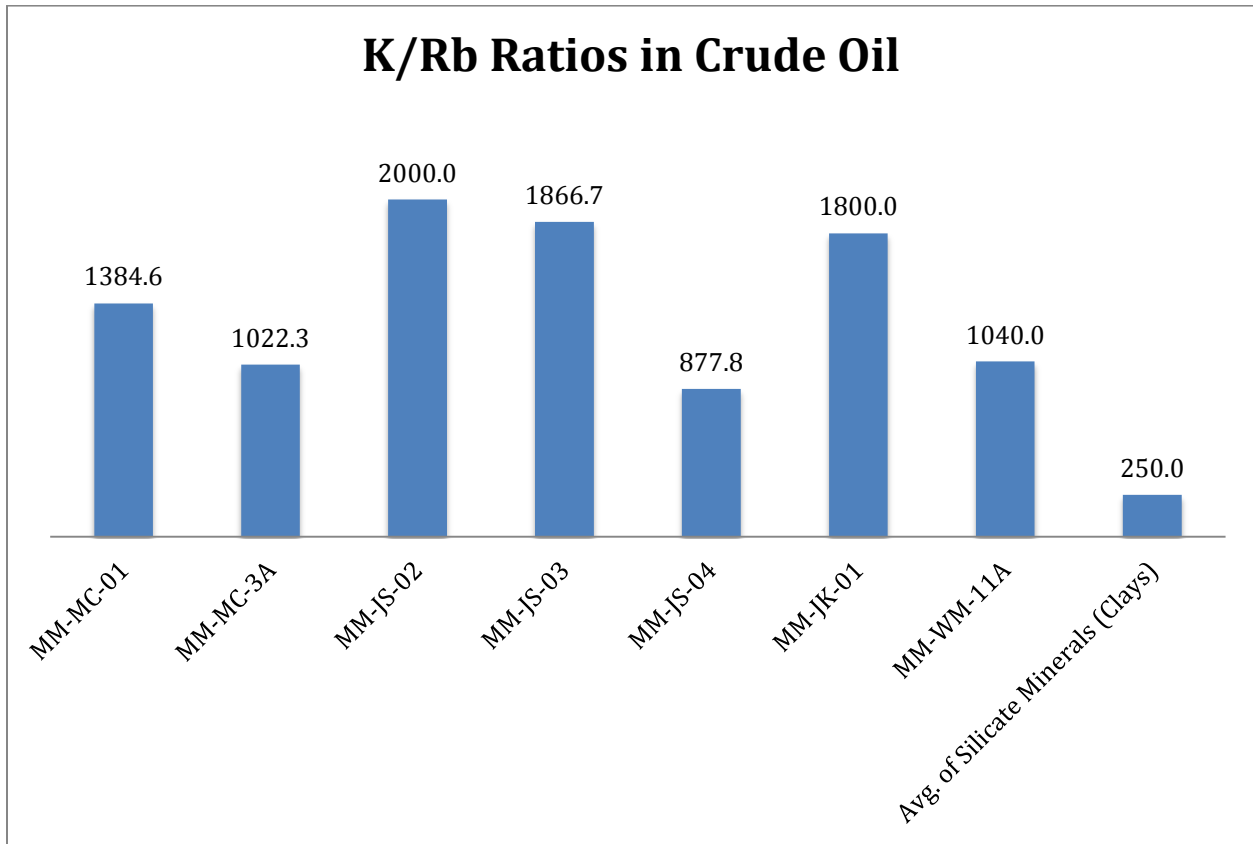


**Figure 30 K/Rb ratios of Lansing-Kansas City crude oil samples. Average of silicate minerals (clays) included for reference (Chaudhuri et al., 2007).**

### 3.4 Crude Oil Gas Chromatograph Analysis

Gas chromatographs were run on 11 crude oil samples in the Lansing-Kansas City group. Nine of the eleven samples also have been analyzed by ICP-MS and ICP-AES for trace element and REE concentrations. MM-DJ-02 and MM-PJ-01 were collected while sampling the other 9 wells, but were not producing enough crude oil for analysis of REEs. Dr. R.P. Philp and his colleagues at the University of Oklahoma provided gas chromatograph data. Approximately 10ml of crude oil was sent to Dr. Philp for whole oil analyses. He determined that the doublet at 40 minutes was the nC<sub>17</sub>/Pr. By identifying the nC<sub>17</sub> biomarker allowed for easy identification of the other biomarkers in the chromatograms. Figure 20 is a compilation of all 11 chromatographs with corresponding numbers to identify each graph. Full size chromatograms are located in Appendix B.

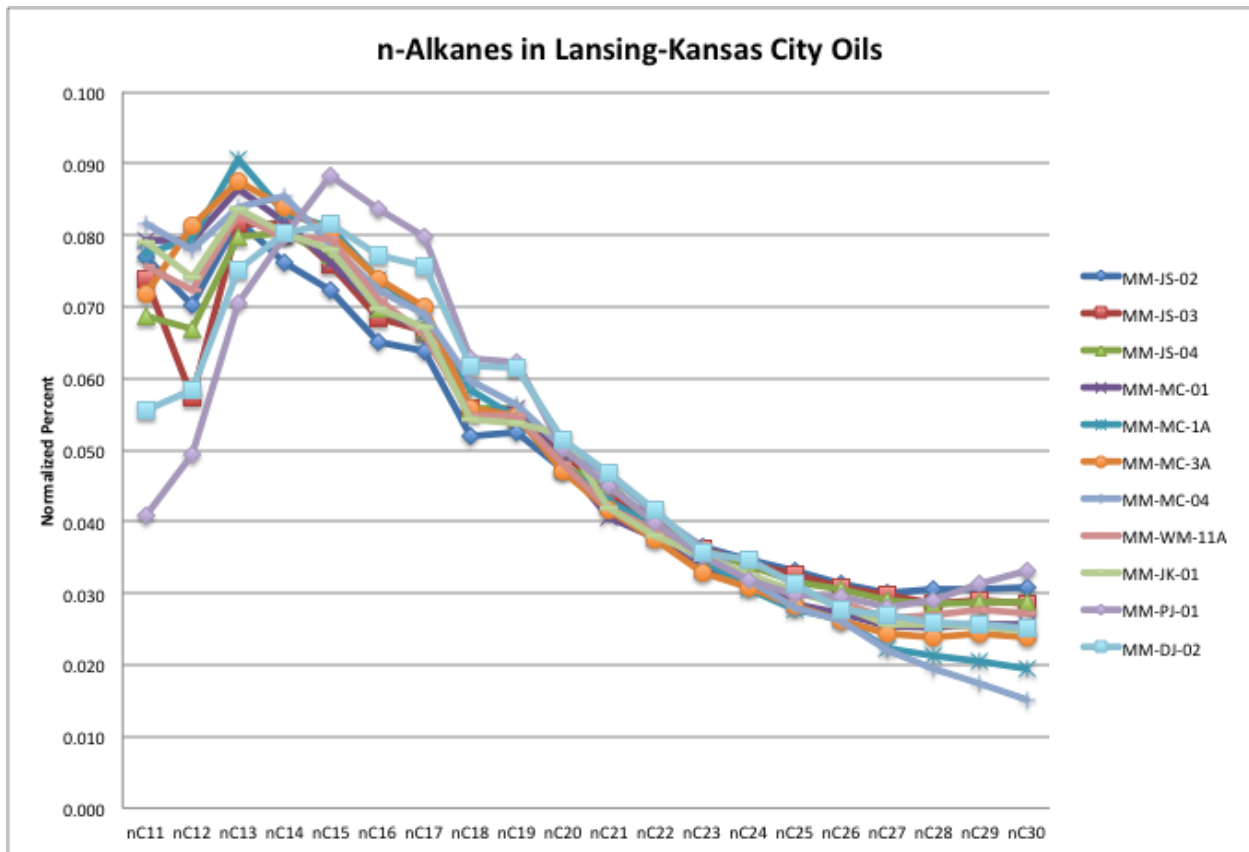
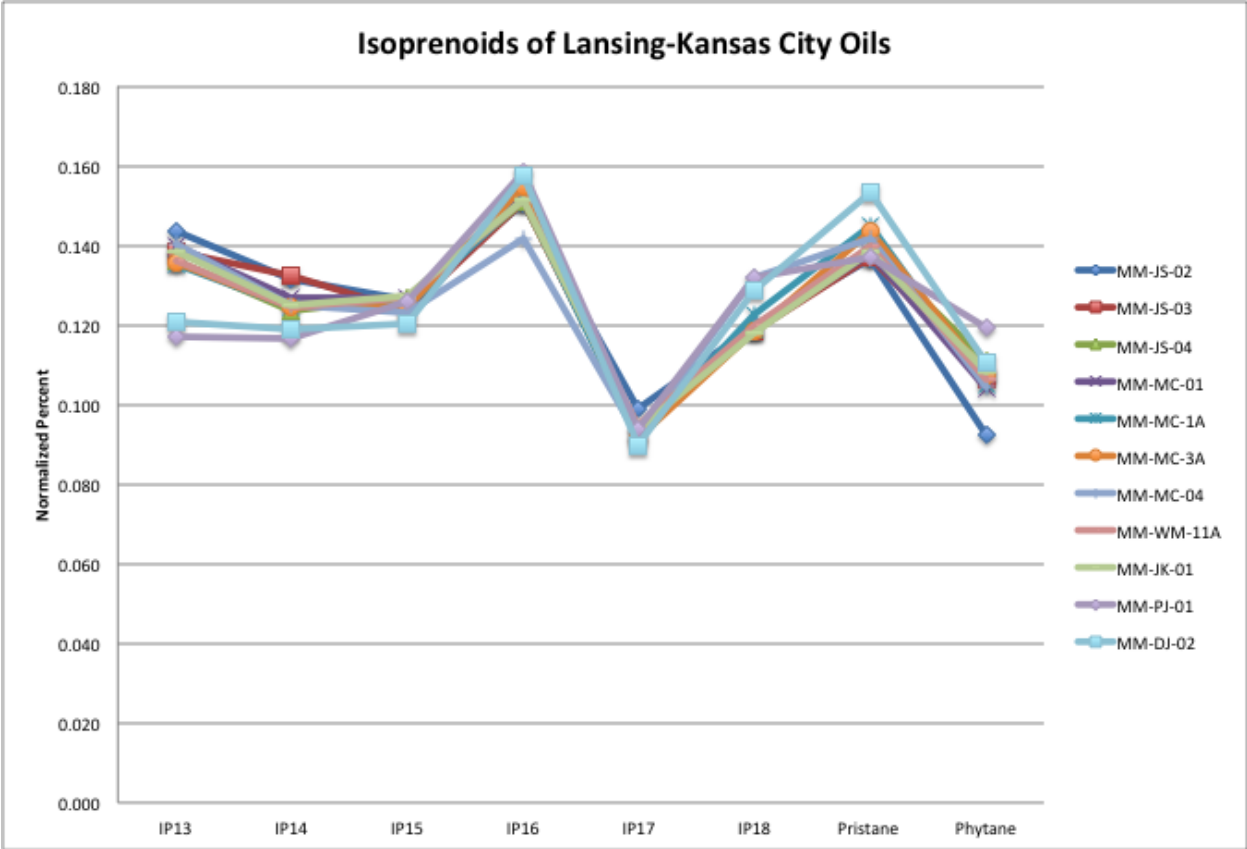
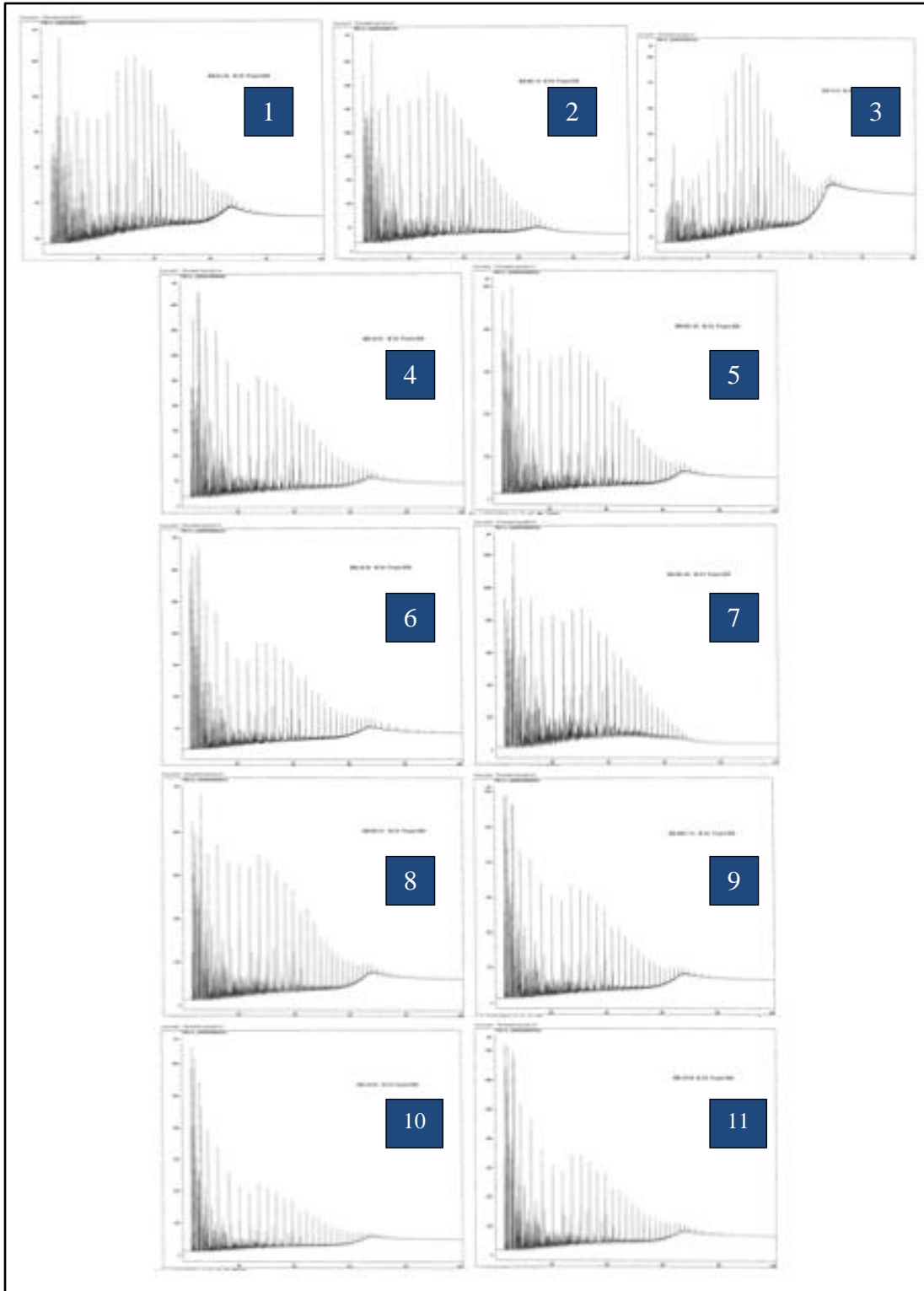


Figure 31 n-Alkanes in Lansing-Kansas City oils.



**Figure 32 Isoprenoids of Lansing-Kansas City oil samples.**



**Figure 33 Gas Chromatograms of Lansing-Kansas City crude oil. (1) MM-DJ-02 (2) MM-MC-3A (3) MM-MC-4A (4) MM-JK-01 (5) MM-WM-11A (6) MM-JS-04 (7) MM-JS-02 (8) MM-MC-01 (9) MM-JS-03 (10) MM-MC-1A (11) MM-JS-03.**

## Chapter 4 – Discussion

### 4.1 REE Relative Distribution Signatures in Crude Oil

Although samples for this study were taken from a relatively small area in central Kansas, the REE distribution patterns vary greatly. Nearly all oil samples investigated in this study have varied degrees of light REE-enrichment across the REE series from La to Sm, they differed in their relative Ce abundances. Some samples have positive Ce anomalies; some have negative Ce anomalies, and some others with the absence of any Ce anomaly. The oils also differed in their PAAS-normalized relative distribution of the middle rare earth elements (MREEs), ranging from Sm to Tb. All oil samples were relatively enriched in the MREEs, but with varied degrees of enrichment from a prominent one to almost a barely noticeable one. The oils differed in their relative distributions of Eu, as some were with a positive Eu anomaly, some with a negative Eu anomaly, and some with the absence of any Eu anomaly. The trends of the heavy rare earth elements (HREEs) from Tb to Lu among the oils ranged from nearly flat for the most oils to a progressive depletion across the series for few samples. Furthermore, the oils were varied in having prominently anomalous relative distributions, in some cases with a positive anomaly and in others with negative anomaly, for such elements as Tb, Ho, Tm, and Lu, which potentially implies biogenic enzyme influence.

**Table 7 Lanthanum to Lutetium ratio showing LREE enrichment.**

Sample	La/Lu
MM-JS-02	0.17
MM-JS-03	0.39
MM-JS-04	4.09
MM-JK-01	0.57
MM-WM-11A	-
MM-MC-01	1.11
MM-MC-1A	-
MM-MC-3A	4.80
MM-MC-4A	-

Cerium and Europium anomalies are measured by finding the value of cerium or europium that the distribution pattern should follow if there was no depletion or enrichment, by interpolating between the normalized values of Lanthanum and Praseodymium for cerium

anomaly, and Samarium and Terbium for the europium anomaly. The calculated value is designated as Ce\* or Eu\*. The analytical value of Ce and Eu is divided by the Ce\* and Eu\* calculated values. Due to analytical error margin of 10% from the laboratories used, when calculating the anomalies, a standard is set where my value is considered an anomaly when having a value of  $\pm 10\%$  for enrichment or depletion.

#### ***4.1.1 Light Rare Earth Elements (LREE)***

##### ***Cerium Anomalies***

**Table 8 Cerium anomalies in Lansing-Kansas City oil samples.**

<b>Sample</b>	<b>Ce/Ce*</b>
<b>MM-JS-02</b>	1.14
<b>MM-JS-03</b>	0.68
<b>MM-JS-04</b>	0.68
<b>MM-JK-01</b>	0.91
<b>MM-WM-11A</b>	3.13
<b>MM-MC-01</b>	0.10
<b>MM-MC-1A</b>	0.18
<b>MM-MC-3A</b>	0.57
<b>MM-MC-4A</b>	0.27

The most prominent feature shown throughout all LREE distribution patterns is a Cerium negative anomaly. Six of the nine samples show the presence of a negative Ce anomaly. Two samples show the presence of a positive Ce anomaly, and one sample shows no anomaly at all. An explanation for the variations in Ce concentrations from different wells may be linked to variations in organic source materials. Several studies have shown that Mn-oxyhydroxides partly controlled REE fractionation and mobility in natural water. This provides evidence that a negative cerium anomaly is developed through the oxidation of Ce (III) onto the surface of MnO<sub>2</sub> (Pourret et al., 2008; Davranche et al., 2005). Literature has also frequently reported Ce negative anomalies in terrestrial inorganic materials due to the manganese oxide precipitation effect. As manganese oxide precipitates as Mn-nodules found on ocean beds, the ocean beds have been reported to have positive cerium anomalies. Additionally, seawaters have also found to correlate with ocean beds, showing Ce negative anomalies. Adversely, focusing on the two samples with positive Ce anomalies, Pourret et al., 2008 explains that in multiple studies positive



Ce anomalies have only been reported in alkaline waters. Such positive Ce anomalies were interpreted as resulting from the stabilization of carbonato-Ce(IV)-complexes in solution leading to enhanced abundances of Ce (IV) in comparison with its trivalent REE neighbors (Moller and Bau, 1993). Pourret et al., 2008 introduces the idea that positive Ce anomalies may be more common features of alkaline, carbon-rich and aerobic waters than previously recognized.

#### ***4.1.2 Middle Rare Earth Elements (MREE)***

##### ***MREE Enrichment***

Seven out of the nine samples have been found to have MREE enrichments (MREE with convex upward trends). MREE enrichments can generally be attributed to increases in phosphates. It can be reasonably argued that organic matter associated with the source of the Lansing-Kansas City was a prime source of this phosphorous, which became available during organic matter transformation.

##### ***Europium Anomalies***

A commonality found in the most of the MREE portion of the distribution patterns is a Eu positive anomaly. Five of the nine samples exhibit a strong Eu positive anomaly. Two samples (MM-JS-04 and MM-MC-3A) recorded no Eu values because the element was below detection limit. The Eu anomaly couldn't be calculated for sample MM-MC-01 because Gd was below detection limit.

**Table 9 Europium anomalies in Lansing-Kansas City oil samples.**

<b>Sample</b>	<b>Eu/Eu*</b>
<b>MM-JS-02</b>	1.31
<b>MM-JS-03</b>	1.54
<b>MM-JS-04</b>	-
<b>MM-JK-01</b>	0.86
<b>MM-WM-11A</b>	1.69
<b>MM-MC-01</b>	-
<b>MM-MC-1A</b>	1.01
<b>MM-MC-3A</b>	-
<b>MM-MC-4A</b>	1.03

Most geochemists working on crustal inorganic materials have attributed positive Eu anomalies in such materials to crystallographic effects, especially feldspar minerals which favor

accommodation of  $\text{Eu}^{2+}$  over a trivalent species. But those who have worked on modern plants, like Chaudhuri and Clauer, have found Eu positive anomalies in plants relative to their growth substrates. The evidence from such studies does not support the idea of a crystallographic effect. Often finding differences in Eu anomalies among different organs of the same plant, Chaudhuri and Clauer (2007) believe that plant enzyme effect plays a significant role in Eu anomalies in the organic materials.

### 4.1.3 Heavy Rare Earth Elements (HREE)

#### *Terbium, Holmium, and Tm Enrichments*

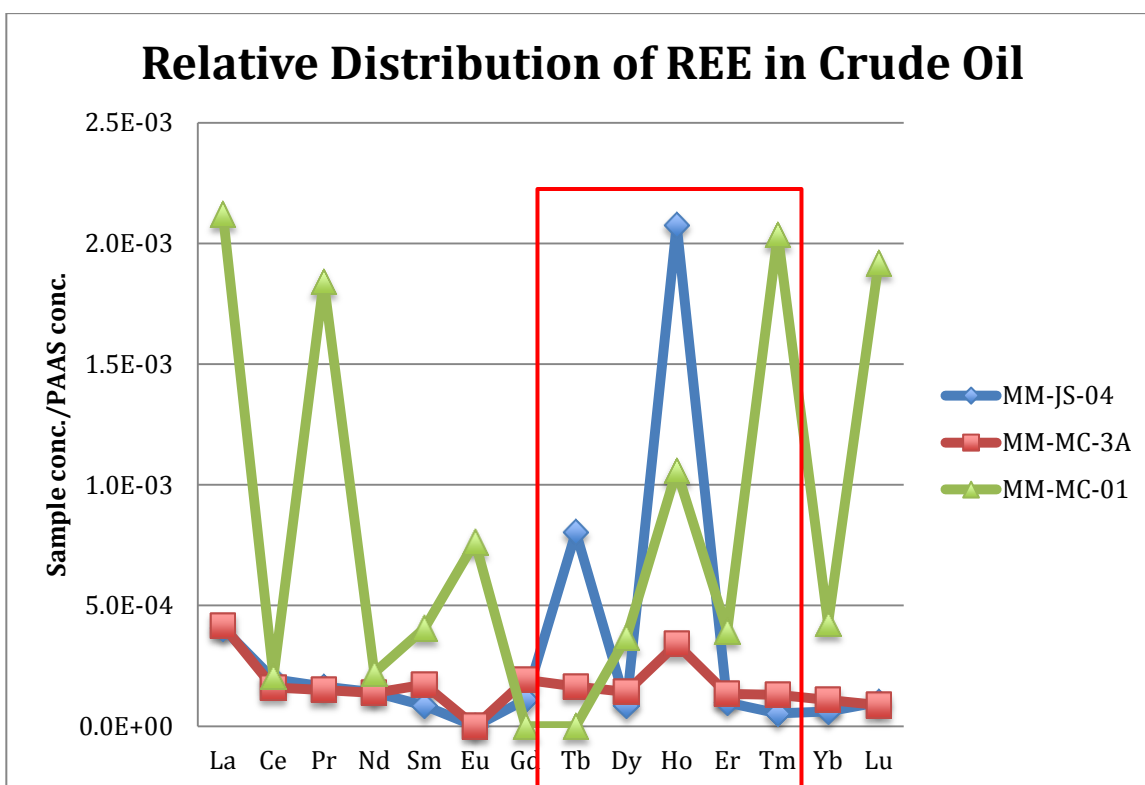


**Figure 34 Relative distribution patterns of Lansing-Kansas City oils. MM-JS-04 showing positive Tb and Ho anomalies. MM-MC-3A showing a positive Ho anomaly. MM-MC-01 showing positive Ho and Tm anomalies.**

There are several samples that show a Tb, Ho, or Tm positive anomaly, as shown in Figure 22. These anomalies were determined by looking at the overall trend of the REE distribution patterns. The anomalies have been common with Eu and Ce in natural materials because of the difference in the oxidation states from the natural (III) oxidation state for all the

REEs. Thus, Ho, Tb, and Lu anomalies, varied in different degrees among the samples, and these are reflections of the growth history of the organic source material, arising potentially from enzymatic influence during the growth of the organic materials.

#### **4.2- Lansing-Kansas City Zone Correlation**

There are four broadly distinct REE distribution patterns. These patterns correlate well to specific zones of production in the Lansing-Kansas City formations.

The first pattern (Figure 26) includes wells MM-WM-11A, MM-MC-1A, and MM-MC-4A. The REE distribution patterns in general were slight LREE enriched to nearly flat. All samples show a slight MREE enrichment. La enrichment is due to La-Ca replacement. Ca is an important component needed for plant growth. La has a similar size to Ca, often times replacing Ca in plant enzymes.

The second pattern (Figure 27) includes wells MM-JS-02, MM-JS-03, and MM-JK-01. All samples in this pattern show a slight MREE enrichment due to a phosphate influence. Each sample has mixed zone production. The mixed zones deferred sometimes to a positive Gd anomaly, in other situations Ho and Tm negative anomalies.

The third pattern (Figure 28) includes wells MM-JS-04 and MM-MC-3A. These distribution patterns are described as having nearly flat REE distribution patterns with a slight LREE enrichment. MM-JS-04 has very prominent Tb and Ho positive anomalies, unlike MM-MC-3A with a flat distribution pattern.

The fourth pattern (Figure 29) contains MM-MC-01. This pattern is showing production from solely the LKC “A” zone. It was characterized by a very rough concave upward distribution pattern, which may suggest an influence of phosphate depletion. Nevertheless, the most significant features of this distribution pattern are marked with positive anomalies of a number of REEs. The oil coming from this single zone must be derived from varied organic sources.

MREE enrichment (Figures 26 & 27) can be observed in samples with production from the middle Lansing-Kansas City zones (G-I). In samples with comingling LKC zones (Figures 27 & 28), amplification of anomalies from differing source materials can be observed.

### 4.3-K/Rb Ratios in Crude Oil

Potassium (K) is essential for all forms of life and is taken up by plants in its cationic form ( $K^+$ ). Rubidium (Rb), a trace element with similar properties as K, in contrast, has no biological function. The uptake of Rb is also much more sensitive to changes in soil properties such as K availability, acidity, and absorption properties of the soil. This results in typically higher K/Rb ratios in biological materials than in soils (Peltola et al., 2008). Based upon assumptions regarding average chemistry of smectites and illites, the average shale requires 13.4 % potassium feldspar to provide the necessary  $K^+$  (Totten and Blatt, 1996). As the average shale only contains 5% feldspar (Blatt, 1992), an additional source for potassium is required. A study by Chaudhuri et al., 2007 also showed that when K is studied in conjunction with Rb, the K/Rb ratio can be a strong geochemical tracer for the source of potassium into a system. Their study concluded that K/Rb ratios are much higher in organic materials than in common K bearing silicate minerals, like feldspar and mica. K/Rb ratios taken from eight Lansing-Kansas City crude oil samples range from 877 to 2000, which indicates a large influence from organic matter in the crude oils. According to Chaudhuri et al., 2007, silicate minerals have a K/Rb ratio range from 50-650, significantly lower than the crude oil samples in this study (Figure 19). According to the currently accepted petroleum system model for the midcontinent (Figure 1), oils in the Lansing-Kansas City group would have migrated from two potential sources in northern Oklahoma: Ordovician and Devonian aged rocks (Gerhard, 2004). The hypothesis presented by Gerhard argues that the intersection of fractures of the Nemaha and Central Kansas Uplift form a structural barrier to migration, so that oil moving from the south is shunted along the major fractures to fill reservoirs on and along the uplifts. If the oils in the Lansing-Kansas City reservoirs migrated along fracture pathways from the Anadarko basin, K/Rb ratios will be expected to have a narrow range of values. If the oils migrated such a long distance, the oils exchanged K/Rb values with the silicate values. This study is supportive of the idea based on significantly high K/Rb ratios in Lansing-Kansas City oil samples the local oil generation in the northwest Kansas is a strong possibility. The ratio range of 877-2000 is indicative of local source rock variations. The local source rocks may not appear to have attended the appropriate vitrinite reflectance in conformity with the accepted oil-window temperature. Hence the assertion of local source derivation for the oil will require an explanation. If either a metal aided catalytic effect on

the organic matter transformation or natural radioactive source radiation promoted a reaction or both might have played an important role in this local source transformation to generate oil.

### 4.3 Biomarkers

Biomarkers are a group of compounds found in hydrocarbons that are considered “molecular fossils.” Biomarkers are structurally similar to living organisms, but have been diagenetically altered. Biomarkers allow exploration geologists to evaluate the type of source rock, maturity of the oils, and alterations incurred upon the oils following accumulation (Evans 2011). The two groups of biomarkers looked at in this study are the n-alkanes and the isoprenoids. A discussion of these biomarkers can be found in chapter 1.3.1.

The original chromatograms show 3 different trends with normal alkanes or n-alkanes. The first trend shows a high peak around nC6 and nC7 with a rapid decrease until nC11/nC12, then a small hump between nC13-nC15 and a gradual decline until the end of the chromatograph. There are six samples showing trend one: MM-JS-02, MM-JS-03, MM-JS-04, MM-MC-01, MM-WM-11A, and MM-JK-01. The second trend is similar to the first, but without a prominent peak and decline around nC6/nC7. This trend shows one high peak at nC7 with nC8 significantly lower. Between nC8 and nC12 there is a gradual increase in size of the peaks, with the top of the hump occurring at nC13/nC14 and a gradual decrease until the end of the chromatogram. There are 4 samples showing trend two: MM-MC-1A, MM-MC-3A, MM-MC-4A, MM-DJ-02. The third trend only occurred in one sample, MM-PJ-01. This pattern shows the possibility of biodegradation of the oil. The values of the biomarkers between nC6 and nC12 are significantly lower than the ten other samples. There is a large hump that forms between nC13 and nC17 and a rapid decrease until the end of the chromatogram. Values for the n-alkanes between nC11 and nC30 were converted into a normalized percent and plotted on a graph for correlation of all 11 samples (Figure 20). The largest differences are observed between nC11 and nC17, as well as towards the end of the sequence.

After n-alkanes were determined, isoprenoids were studied and values were converted to normalized percent. Isoprenoid signatures show little differences between the eleven samples. In general, IP14 and IP15 share about the same value. IP16 has the highest peak with a depletion in IP17 and a high peak at pristane. The normalized percent of the isoprenoids were plotted on a graph for correlation of the eleven samples.

The pristane and phytane values were calculated and converted into a normalized percent, the same as the rest of the isoprenoids. A pristane/phytane ratio was calculated for each sample (Table 7). As stated in a previous chapter, pristane and phytane are commonly looked at together as a ratio (Pr/Ph). The Pr/Ph ratio of a crude oil is a reflection of the source of the original organic matter and the paleoenvironmental conditions during decomposition and early burial. Higher Pr/Ph values (3 to 15) indicate a source from mostly land derived organic matter that has passed through a highly oxygenated state in its decomposition. Low Pr/Ph values (1.1 to 2) indicate oil that has been generated from marine organic source materials. The Pr/Ph values for each of the eleven samples range from 1.15 to 1.48. These values indicate that the source of oils in the Lansing-Kansas City formations are a collection of marine organic source materials.

**Table 10 Pristane/Phytane ratios for Lansing-Kansas City oil samples.**

<b>Sample</b>	<b>Pr/Ph Ratio</b>
<b>MM-JS-02</b>	1.48
<b>MM-JS-03</b>	1.29
<b>MM-JS-04</b>	1.26
<b>MM-MC-01</b>	1.33
<b>MM-MC-1A</b>	1.38
<b>MM-MC-3A</b>	1.34
<b>MM-MC-04</b>	1.35
<b>MM-WM-11A</b>	1.32
<b>MM-JK-01</b>	1.28
<b>MM-PJ-01</b>	1.15
<b>MM-DJ-02</b>	1.39

Finally, the carbon preference index (CPI) was calculated for each oil sample (Table 11). The CPI is a measure of the odd and even n-alkane chain length preference in crude oil. Values for the Lansing-Kansas City oils ranged from 0.98 to 1.01, indicating the source was a marine carbonate (Evans, 2011).

**Table 11 Carbon Preference Index (CPI) of Lansing-Kansas City oil samples.**

<b>Sample</b>	<b>CPI</b>
<b>MM-JS-02</b>	0.989
<b>MM-JS-03</b>	1.008
<b>MM-JS-04</b>	0.987

<b>MM-MC-01</b>	0.981
<b>MM-MC-1A</b>	0.974
<b>MM-MC-3A</b>	1.001
<b>MM-MC-04</b>	0.988
<b>MM-WM-11A</b>	0.988
<b>MM-JK-01</b>	0.990
<b>MM-PJ-01</b>	0.980
<b>MM-DJ-02</b>	1.011

## **Chapter 5 – Conclusions**

Walters (1958) and Price (1980) both advanced the theory of long-distance migrations of oil from the Anadarko basin to central Kansas through Arbuckle rocks, during the mid-Permian. Their model calls for decreasing amounts of oil and gas to be emplaced northward as traps fill and correspondingly decrease the supply of petroleum for more northerly traps. The barriers to migration model suggested herein simply adds one more complication to the migration story and does not assume a restricted supply of petroleum from the Anadarko (Gerhard, 2004). It can be argued from this study that the belief that liquid hydrocarbons in northwest Kansas did not all migrate from the Anadarko basin, but instead have some component of local source generation.

When comparing results from tools such as REE distribution patterns and K/Rb ratios there are a significant amount of differences between each sample. Total REE concentrations range from 0.0032 to 0.131 ng/L of oil (Figure 16). REEs also vary in their distribution patterns, specifically in the HREE values. Depending on which elements are enriched or depleted could mean a different type of source material or difference in source rock. K/Rb values show the largest amount of differences, with values ranging from 877 to 2000. These values indicate a K/Rb source originating from organic materials. The difference in these results suggests a local oil source. We believe that if the oils in the Lansing-Kansas City originated from the Anadarko basin, the REE and K/Rb results would be similar due to hydrocarbon mixing over long distances. Looking at gas chromatograph data for each oil sample, there are three distinct oil classifications shown. Differences in biomarker patterns also supports the idea varying sources. The collective info from this study strongly suggests local source variation is a strong case for oil generation and accumulation in the Lansing-Kansas City formations in Rooks County, Kansas.

### **5.1 Future Work**

Much work still needs to be done to determine an exact source of the oils in the Lansing-Kansas City group. Shale units in the lower Kansas City and other formations around Kansas that show strong gamma ray signatures should be investigated for REE concentrations, TOC, and vitrinite reflectance.

Chaudhuri et al., 2011, has shown that oil field brine can be a useful tool for understanding organic processes during sediment deposition and hydrocarbon generation.



Lansing-Kansas City brines collected during this study should be analyzed and compared to the hydrocarbon data.

The idea of hydrocarbon generation, while probable in deep basin environments, only focused on the temperature increase on organic matter but does not take into account all five regimes present in petroleum source beds. Those regimes are the atmospheric gases, lithosphere or mineral matrices, hydrosphere or H<sub>2</sub>O, biosphere or organic materials, and the ergosphere or energy produced from temperature increase and radioactive decay of isotopes present in source beds (Kelly, 2014).

## Bibliography

- Abanda P.A., Hannigan R.E., 2006. Effect of diagenesis on trace element partitioning in shales: *Chemical Geology*, v. 230, p. 42-59.
- Andrews, R.D., 2009. Production decline curves and payout thresholds of horizontal Woodford wells in the Arkoma Basin, Oklahoma: *The Shale Shaker*, v. 60, p. 103–112.
- Arouri, K.R., Van Laer, P.J., Prudder, M.H., Jenden, P.D., Carrigan, W.J., and Al-Hajji, A.A.. 2010, Controls on hydrocarbon properties in a Paleozoic petroleum system in Saudi Arabia: Exploration and development implications: *AAPG Bulletin*, v. 94, p. 163-188.
- Barrat, J.A., Keller, F., Amosse, J., Taylor, R.N., Nesbitt, R.W., 1996. Determination of Rare Earth Elements in Sixteen Silicate Reference Samples by ICP-MS after Tm Addition and Ion Exchange Separation: *Geostandards Newsletter*, v. 20, issue 1, p. 133-139.
- Birdwell, J.E., 2012, Review of Rare Earth Element Concentrations in Oil Shales of the Eocene Green River Formations: U.S. Geological Survey Open-File Report 2012-1016, 20 p.
- Blakley, R., Colorado Plateau Geosystems, [cpgeosystems.com paleogeography map](http://www2.nau.edu/rcb7/globaltext2.html).  
<http://www2.nau.edu/rcb7/globaltext2.html>
- Blatt, H., 1992, *Sedimentary Petrology*, 2nd edition: New York, W.H., Freeman & Co., 514 p.
- Brenneman, M. C., Smith, P. V., 1958. The chemical relationships between crude oils and their source rocks, in Weeks, L. G., ed., *Habitat of Oil*, American Association of Petroleum Geologists, Tulsa, Okla., 1958, p. 818-849.
- Brewer, J.A., Good, R., Oliver, J.E., Brown, L.D., and Kaufman, S., 1983. COCORP profiling across the Southern Oklahoma aulacogen, overthrusting of the Wichita Mountains and compression with the Anadarko Basin: *Geology*, v. 11, p. 109–114.

- Brown, H. A., 1984, Lansing-Kansas City carbonate reservoirs of Haskell County, Kansas; in, *Limestones of the Midcontinent*, N. J. Hyne, ed.: Tulsa Geological Society, Special Publication No. 2, p. 75-85.
- Byrne, R.H., Liu X., Schijf, J., 1996. The influences of phosphate coprecipitation of rare earth distributions in natural waters: *Geochimica et Cosmochimica Acta*, v. 60, p. 3341–3346.
- Caldwell, C.D., Johnson, P.G., 2013. Anadarko Woodford Shale, Improving Production by Understanding Lithologies/Mechanical Stratigraphy and Optimizing Completion Design: AAPG Woodford Shale Forum, April 2013, Oklahoma City, OK, USA.
- Cardott, B.J., Lambert, M., 1982. Thermal Maturation by Vitrinite Reflectance of Woodford Shale, Anadarko Basin, Oklahoma: *AAPG Bulletin*, v. 69, p 1982-1998.
- Cardott, B.J., 2008. Overview of Woodford gas-shale play of Oklahoma, US: Oklahoma Geological Survey, Power Point Presentation, Oklahoma Gas Shale Conference. October 22<sup>nd</sup>, 2008. <http://www.ogs.ou.edu/pdf/AAPG08woodford.pdf>
- Cardott, B.J., 2012. Introduction to Vitrinite Reflectance as a Thermal Maturity Indicator: Search and Discovery Article # 40928, May 2012.
- Cardott, B.J., 2013. Woodford Shale, From Hydrocarbon Source Rock to Reservoir: AAPG Woodford Shale Forum, April 2013, Oklahoma City, OK, USA.
- Chaudhuri S., Clauer N., Semhi K., 2007. Plant decay as a major control of river dissolved potassium, A first estimate: *Chemical geology*, v. 243, p.178-190.
- Chaudhuri, S., Totten, M., Clauer, N., Miesse J., Riepl, G., Massie, S., Semhi, K., 2011. Rare-Earth Elements as a Useful Geochemical Tracer in Hydraulic Fracturing Schemes: Shale Shaker, *The Journal of the Oklahoma City Geological Society*, v. 62, p. 214-223.

- Comer, J.B., Hinch, H.H., 1987. Recognizing and quantifying expulsion of oil from the Woodford Formation and age-equivalent rocks in Oklahoma and Arkansas: AAPG Bulletin, v. 71, No. 7, p 844-858.
- Comer, J.B., 2008. Reservoir Characteristics and Production Potential of the Woodford Shale: World Oil Magazine. Special Focus: North American Outlook-Unconventional Resources, August 2008.
- Condie, K.C., 1993. Chemical Composition and Evolution of the Continental Crust, Contrasting Results From Surface Samples and Shales: Chemical Geology v. 104 p. 1-37.
- Corbett L.W., 1967, Distribution of heavy metals in asphalt residua: Preprints, v. 12, p. 83-87.
- Cotton F.A., Wilkinson, G., 1962. Advanced Inorganic Chemistry: Interscience Publishers, John Wiley and Sons, New York-London
- Dao-Hui P., Cong-Qiang L., Shields-Zhou, Graham A., Shao-Youn J., 2013, Trace and rare earth element geochemistry of black shale and kerogen in the early Cambrian Niutitang Formation in Guizhou province, South China: Constraints for redox environments and origin of metals: Precambrian Research, v. 225, p. 218-229.
- Davis, H.G., Northcutt, R.A., 1989. The Greater Anadarko basin, an overview of petroleum exploration and development: Proceedings of Anadarko Basin Symposium (1988), Oklahoma Geological Survey Circular 90. p. 13-24.
- Davranche, M. O., Pourret, G., Grauaud, A., Dia, M., Le Coz-Bouhnik, 2005. Adsorption of REE (III)-humate complexes onto MnO<sub>2</sub>, Experimental evidence for cerium anomaly and lanthanide tetrad effect suppression: Geochimica et Cosmochimica Acta v. 69, p. 4825-4835.

- Erdman, J.G., Saraceno, A.J., 1962. Investigation of the nature of free radicals in petroleum asphaltenes and related substances by electron spin resonance: *Anal Chem.*, v. 34 (6), p. 694-700
- Evans, C.H., 1990. *Biochemistry of the Lanthanides*. New York: Plenum Press.
- Evans, D.W., 2011, *The Compartmentalization and Biomarker Analysis of the Spivey-Grabs-Basil Field, South-Central Kansas*, Kansas State University, 101 p.
- Feinstein, S., 1981. Subsidence and thermal history of Southern Oklahoma aulacogen, Implications for petroleum exploration: *American Association of Petroleum Geologists Bulletin*, v. 65, p. 2521–2533.
- Filby, R.H., 1975, *The Nature of Metals in Petroleum: The Role of Trace Metals in Petroleum*, p. 31-58.
- Garner, D.L., Turcotte, D.L., 1984. The thermal and mechanical evolution of the Anadarko basin: *Tectonophysics*, v. 107, p. 1–24.
- Gerhard, L.C., 2004. A new Look at an Old Petroleum Province: *Kansas Geological Survey: Current Research in Earth Sciences, Bulletin 250*, pt 1, 27p.
- Gussow W.C., 1954, Differential entrapment of oil and gas: a fundamental principle: *AAPG Bulletin*, v. 38, p. 816-853.
- Hunt, J.M., 1995. *Petroleum Geochemistry and Geology*. 2nd edition, New York: W.H. Freeman and Company.

- Johnson, K.S., Amsden, T.W., Denison, R.E., Dutton, S.P., Goldstein, A.G., Rascoe, B., Jr., Sutherland, P.K., and Thompson, D.M., 1989. Geology of the Southern Midcontinent: Oklahoma Geological Survey, Special Publication 89-2.
- Jones, P. J., Philp, R. P., 1990. Oils and source rocks from Pauls Valley, Anadarko Basin, Oklahoma, US: Applied Geochemistry, Vol. 5, No.4, p. 429-448.
- Kennedy, C. L., Miller, J.A., Kelso J.B., and Lago, O. K., 1982. The deep Anadarko basin: Tulsa Petroleum Information Corporation, 359 p.
- Kidder, D.L., Eddy-Dilek, C.A., 1994. Rare-Earth Element Variation in Phosphate Nodules from Midcontinent Pennsylvanian Cyclothems: Journal of Sedimentary Research, Sedimentary Petrology and Processes, v. A64, p. 584-592.
- Lewan M.D., Maynard, J.B., 1982. Factors controlling enrichment of vanadium and nickel in the bitumen of organic sedimentary rocks: Geochimica et Cosmochimica Acta, v. 46, p. 2547-2560.
- McCarthy, K., Rojas, K., Niemman M., Peters, K., Stankiewicz, A., 2011. Basic Petroleum Geochemistry for Source Rock Evaluation: Schlumberger Oilfield Review 23, no. 2, p. 32-43.
- Merriam, D. F., 1963, The geologic history of Kansas: Kansas Geological Survey, Bulletin 162, 307 p.
- Moller, P. and Bau, M., 1993, Rare-earth patterns with positive cerium anomaly in alkaline waters from Lake Van, Turkey: Earth Planet. Sci Lett, v. 117, p. 671-676.
- Moldowan, J.M., Peters, K.E., Walters, C.C., 2005, The Biomarker Guide: Second Edition: Biomarkers and Isotopes in Petroleum Exploration and Earth History: 2nd edition, v. 2, United Kingdom, Cambridge University Press, 2005

- Nagarajan, R., Madhavaraju, J., Armstrong-Altrin, J., Nagendra R., 2011. Geochemistry of Neoproterozoic limestones of the Shahabad Formation, Bhima Basin, Karnataka, southern India: *Geosciences Journal*, v. 15, No. 1, p. 9-25.
- Newell, K. D., Watney, W. L., Chang, S. W. L., and Brownrigg, R. L., 1987, Stratigraphic and spatial distribution of oil and gas production in Kansas: Kansas Geological Survey, *Subsurface Geology Series 9*, 86 p.
- Pearson, R.G., 1963. Hard and soft acids and bases: *Journal of American Chemical Society*, v. 85, p. 3533–3539.
- Peltola, P., Brun, C., Astrom, M., Tomilina, O., 2008. High K/Rb ratios in stream waters— Exploring plant litter decay, ground water and lithology as potential controlling mechanisms: *Chemical Geology*, v. 257, p. 92-100.
- Peters, K.E., Kontorovich, A.E., Moldowan, J.M., Andrusevich, V.E., Haizinga, B.J., Demaison, G.J., Stasova, O.F., 1993, Geochemistry of selected oils and rocks from the central portion of the West Siberian Basin, Russia: *AAPG Bulletin*, v. 77, p. 863-887.
- Pourmand A., Dauphas, N., Ireland, T.J., 2012. A novel extraction chromatography and MC-ICP-MS technique for rapid analysis of REE, Sc and Y, Revising CI-chondrite and Post-Archean Australian Shale (PAAS) abundances: *Chemical Geology* v. 291, p. 38-54.
- Price, L., 1980, Shelf and shallow basin oil as related to hot-deep origin of petroleum: *Journal of Petroleum Geology*, v. 3, p. 91-116.
- Puckette J., 2013. Characteristics of Devonian-Mississippian strata in the Southern midcontinent: AAPG Woodford Shale Forum, April, 2013, Oklahoma City, OK.

- Ramirez D., 2013. Rare Earth Elements (REE) as Geochemical Clues to Reconstruct Hydrocarbon Generation History: Master's Thesis, Kansas State University, 92 p.
- Rascoe, B., Hyne, N.J., 1988. Petroleum geology of the mid-continent: Tulsa Geological Society Special Publication 3, 162 p.
- Rollinson, H.R., 1993. Using Geochemical Data, Evaluation, Presentation, Interpretation. 1<sup>st</sup> edition, England: Pearson Education Limited.
- Sandvik, E.I., Young W.A., Curry, D.J., 1992. Expulsion from hydrocarbon sources, the role of organic absorption: Organic Geochemistry, v. 19, Issues 1-3, p. 77-87.
- Schumacher J., 1988, Chemical and isotopic investigations of crude oils in some Paleozoic reservoirs; West-Central Kansas: M.S. Thesis, Kansas State University, 133p.
- Shirey W.B., 1931, Metallic Constituents of Crude Petroleum: Industrial and Engineering Chemistry, v. 23, no. 10, p.1150-1154.
- Smith F.G., 1963. Physical Geochemistry: Addison-Wesley Publishing Company, Reading, Massachusetts, 624 p.
- Sorenson R.P., 2005. A dynamic model for the Permian Panhandle and Hugoton fields, Western Anadarko Basin: AAPG bulletin, v. 89, p. 921-938
- Sullivan, K.L., 1983. Organic facies variation of the Woodford Shale in western Oklahoma: Master's thesis, University of Oklahoma, Norman, Oklahoma, 101 p.
- Taylor, S.R., McLennan, S.M., 1985. The Continental Crust, Its Composition and Evolution: Blackwell Scientific Publications, Carlton, 312 p.

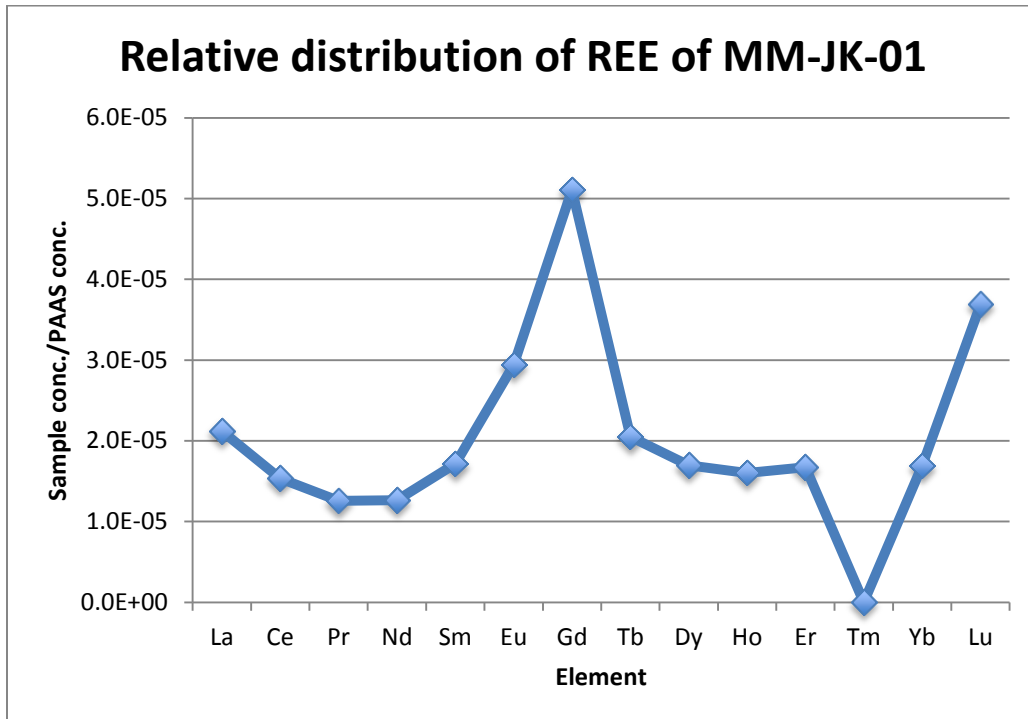
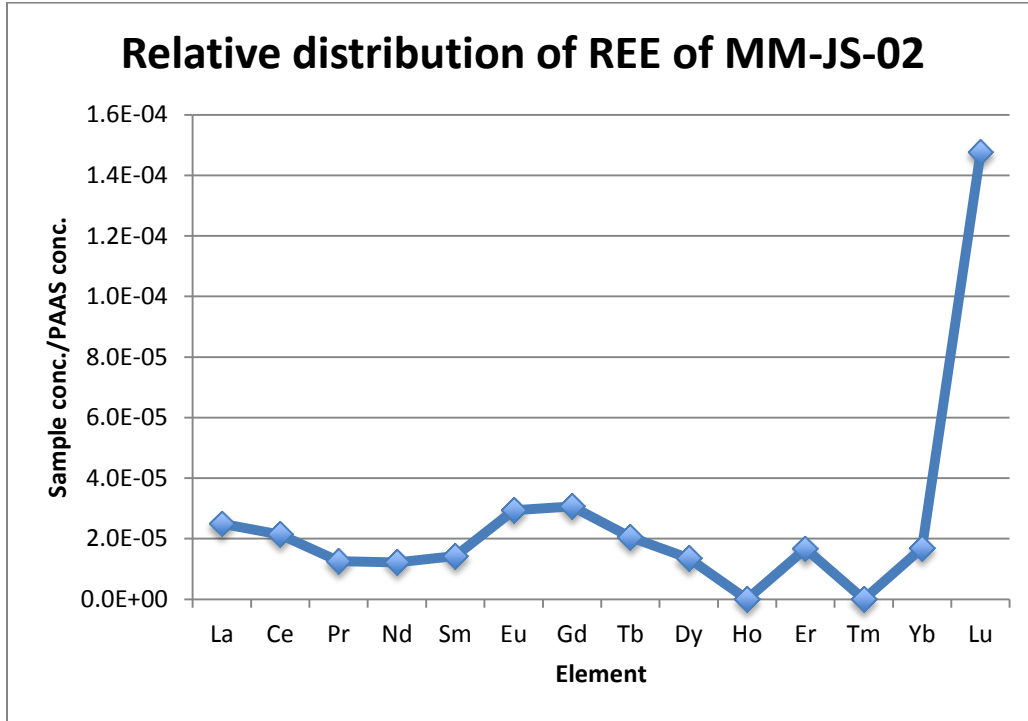


- Thompson, L. C., 1979. Complexes, *in* Gschneider, K.A., Jr., and L. Eyring (eds.), Handbook on the Physics and Chemistry of Rare Earths: Amsterdam, North-Holland Publishing Company, p. 209–298.
- Topp, N. E., 1965. The Chemistry of Rare Earth Elements: Amsterdam, Elsevier Publishing Company, 345 p.
- Totten, M. W., Blatt H., 1996. Sources of silica from the illite to muscovite transformation during late-stage diagenesis of shales, Siliciclastic diagenesis and fluid flow, Concepts and Applications: Society of Economic Paleontologists and Mineralogists, Special Publication No. 55, p. 85-92.
- Walters R.F., 1958, Differential entrapment of oil and gas in Arbuckle Dolomite of Central Kansas: AAPG Bulletin, v.42, p.2213-2174.
- Walper, J. I., 1977. Paleozoic tectonics of the southern margin of North America: Gulf Coast Association of Geological Societies Transactions, v. 27, p. 230–241.
- Wang, D.H., Philp R.P., 1997. Geochemical Study of Potential Source Rocks and Crude Oils in the Anadarko Basin, Oklahoma: AAPG bulletin, v. 81, No. 2, p. 249-275.
- Watney, W.L., 1980, Cyclic Sedimentation of the Lansing-Kansas City Groups in Northwestern Kansas and Southwestern Nebraska, Kansas Geological Survey Bulletin 220.
- Witherspoon P.A., Nagashima K., 1957, Use of Trace Metals to Identify Illinois Crude Oils: Illinois State Geological Survey, 16 p.
- Wood, S. A., 1990. The aqueous geochemistry of the rare-earth elements and yttrium: Chemical Geology, v. 82, p. 159–186.

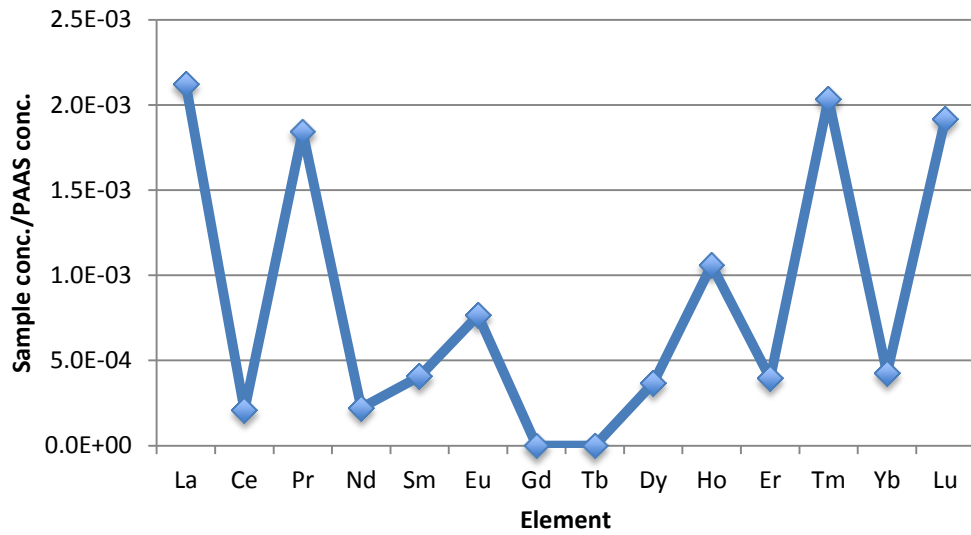
Wytttenbach A., Furrer, V., Schleppei, P., Tobler, L., 1997. Rare earth elements in soil and in soil-grown plants: *Plant and Soil*, v. 199, p. 267-273.

Yen T.F., 1975, *Chemical Aspects of Metals in Native Petroleum: The Role of Trace Metals in Petroleum*, p. 31-58.

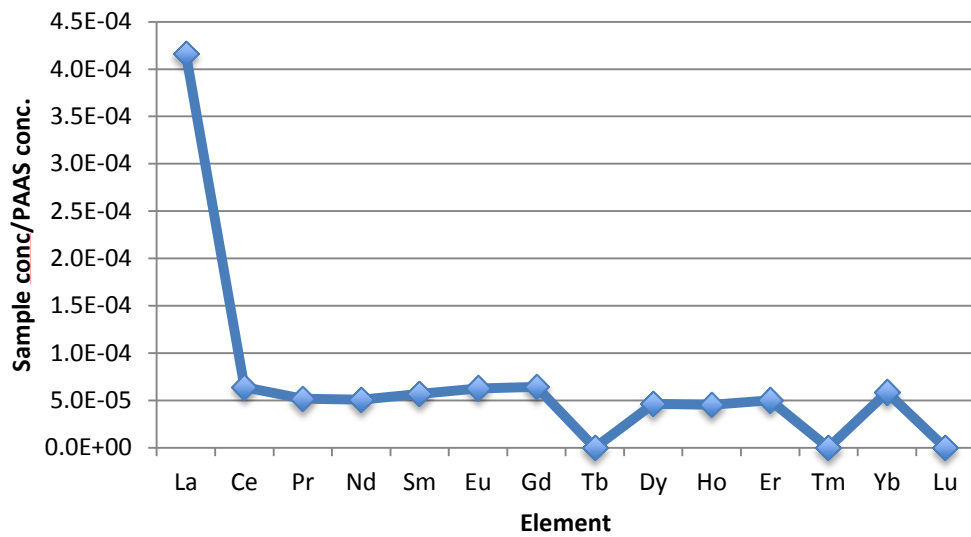
## Appendix A - REE Distribution Patterns in Crude Oil



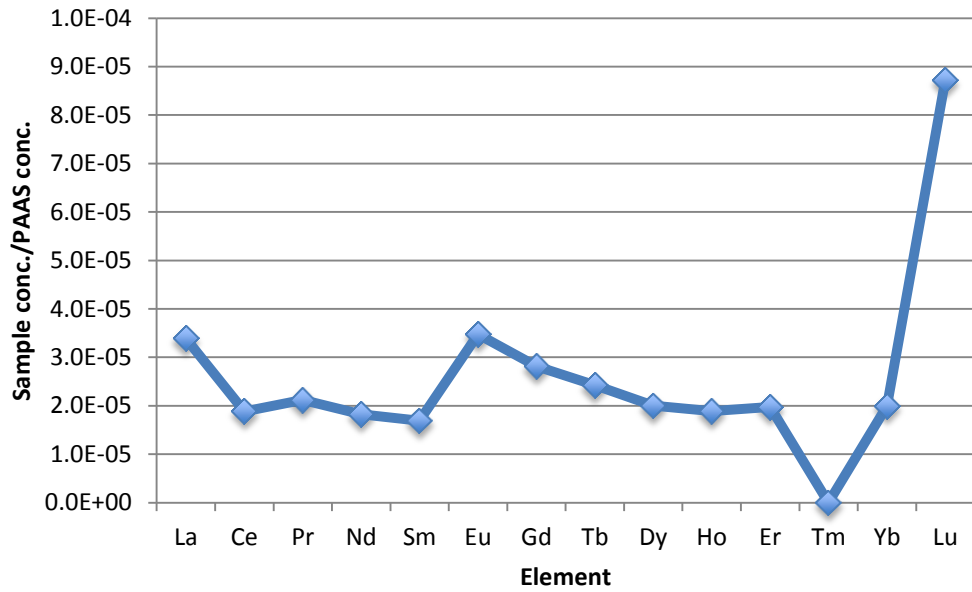
### Relative distribution of REE of MM-MC-01



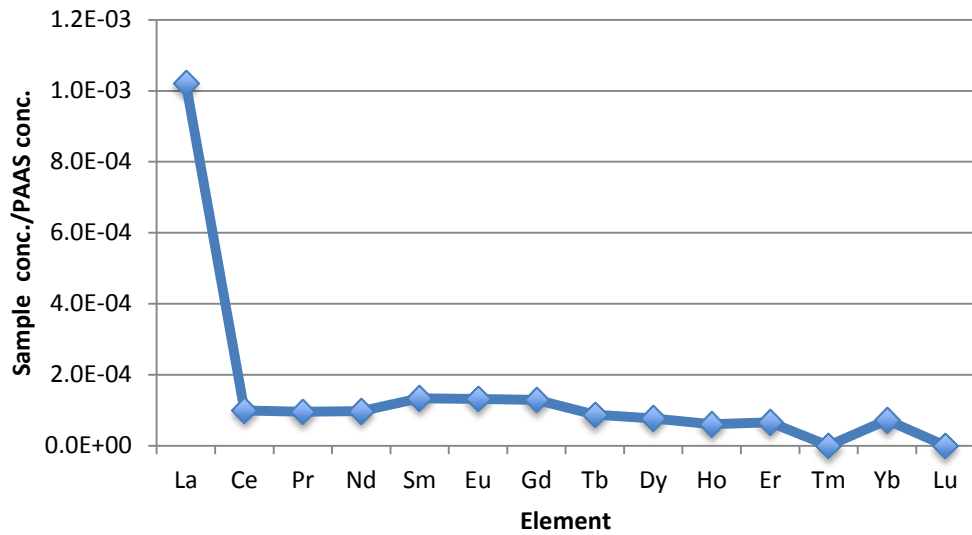
### Relative distribution of REE of MM-MC-4A



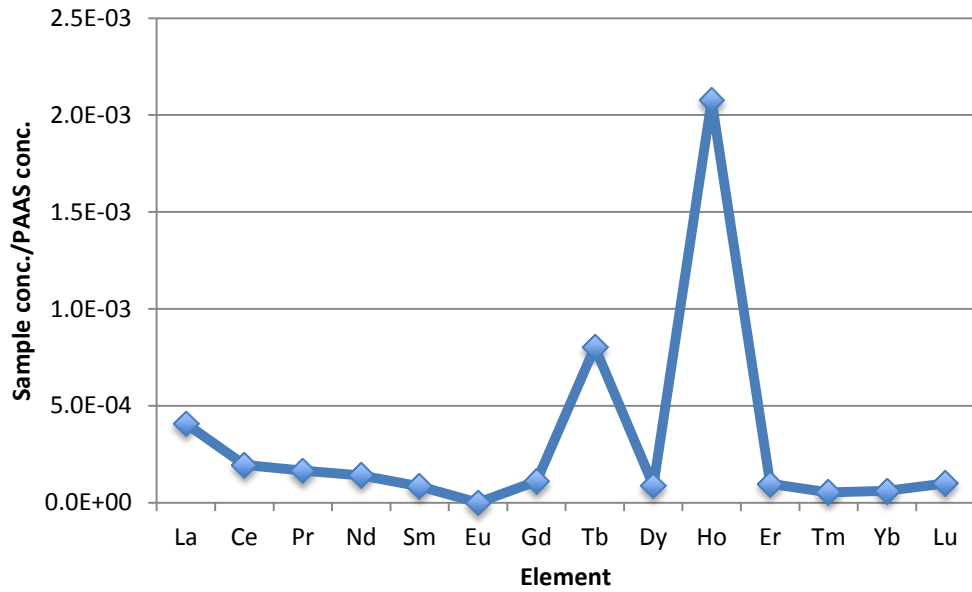
### Relative distribution of REE of MM-JS-03



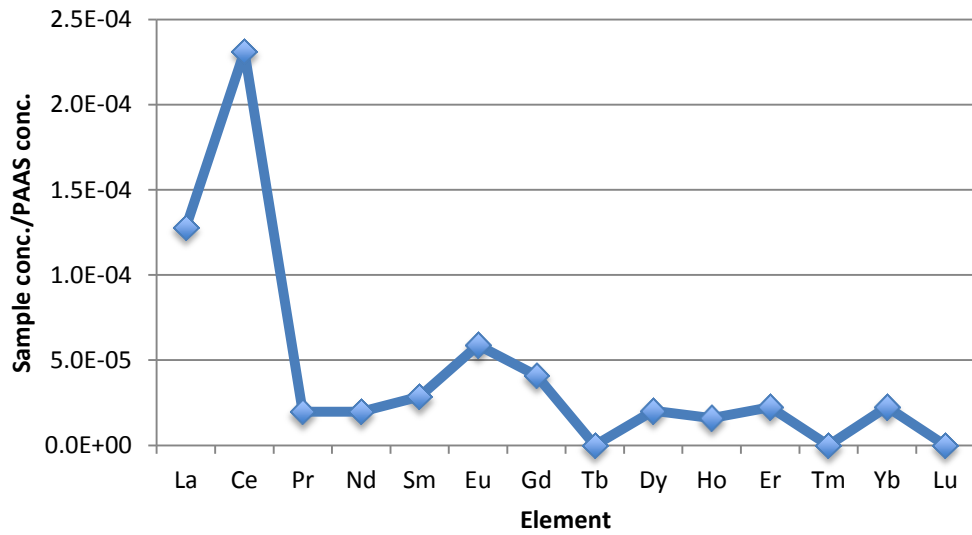
### Relative distribution of REE of MM-MC-1A



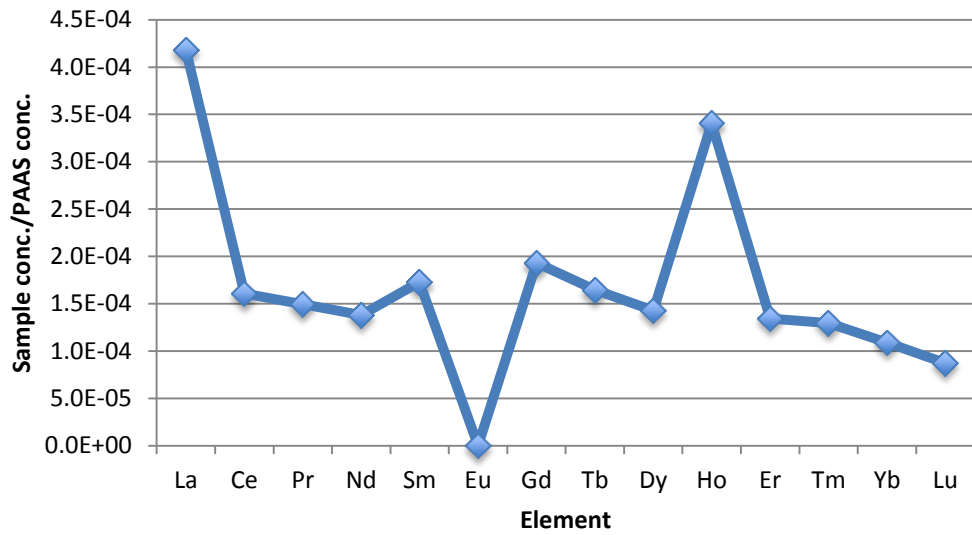
**Relative distribution of REE of MM-JS-04**



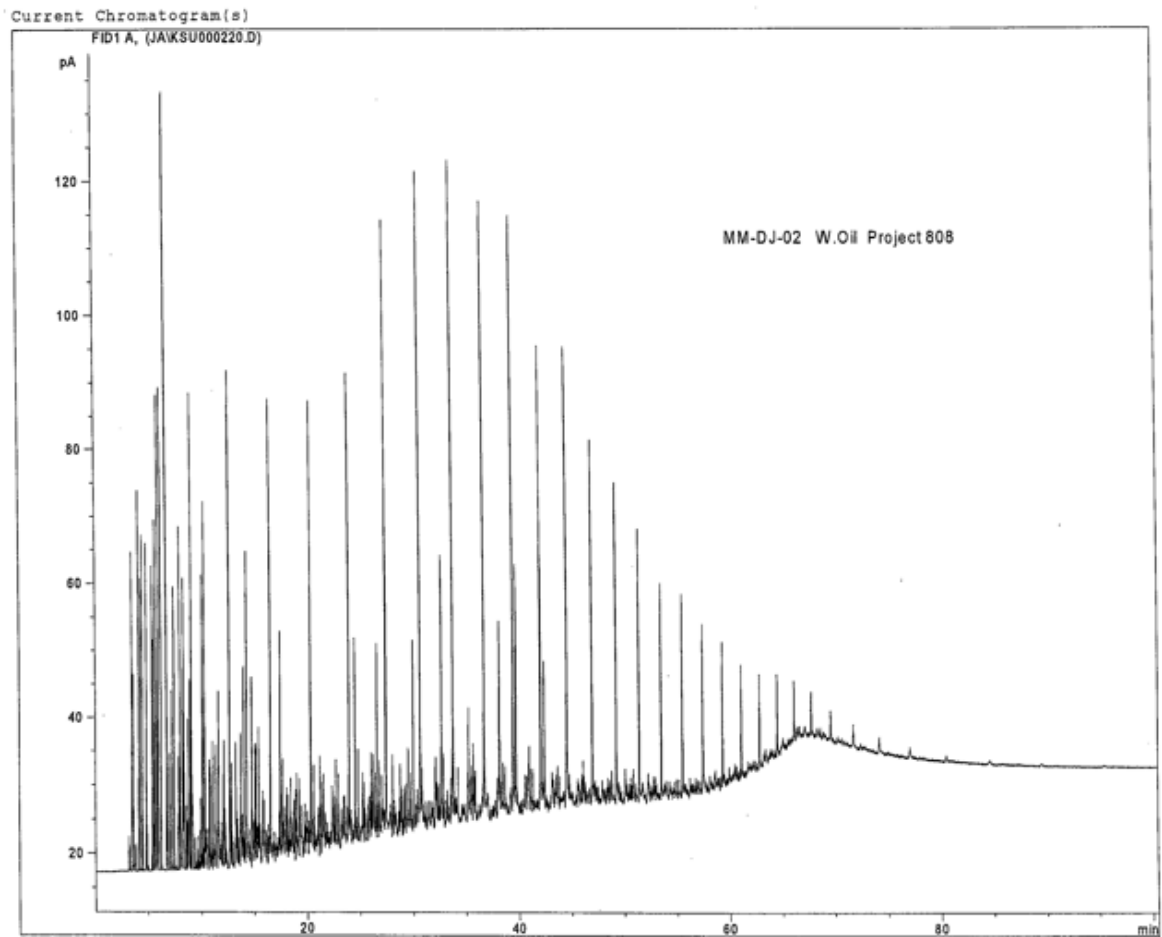
**Relative distribution of REE of MM-WM-11A**



### Relative distribution of REE of MM-MC-3A



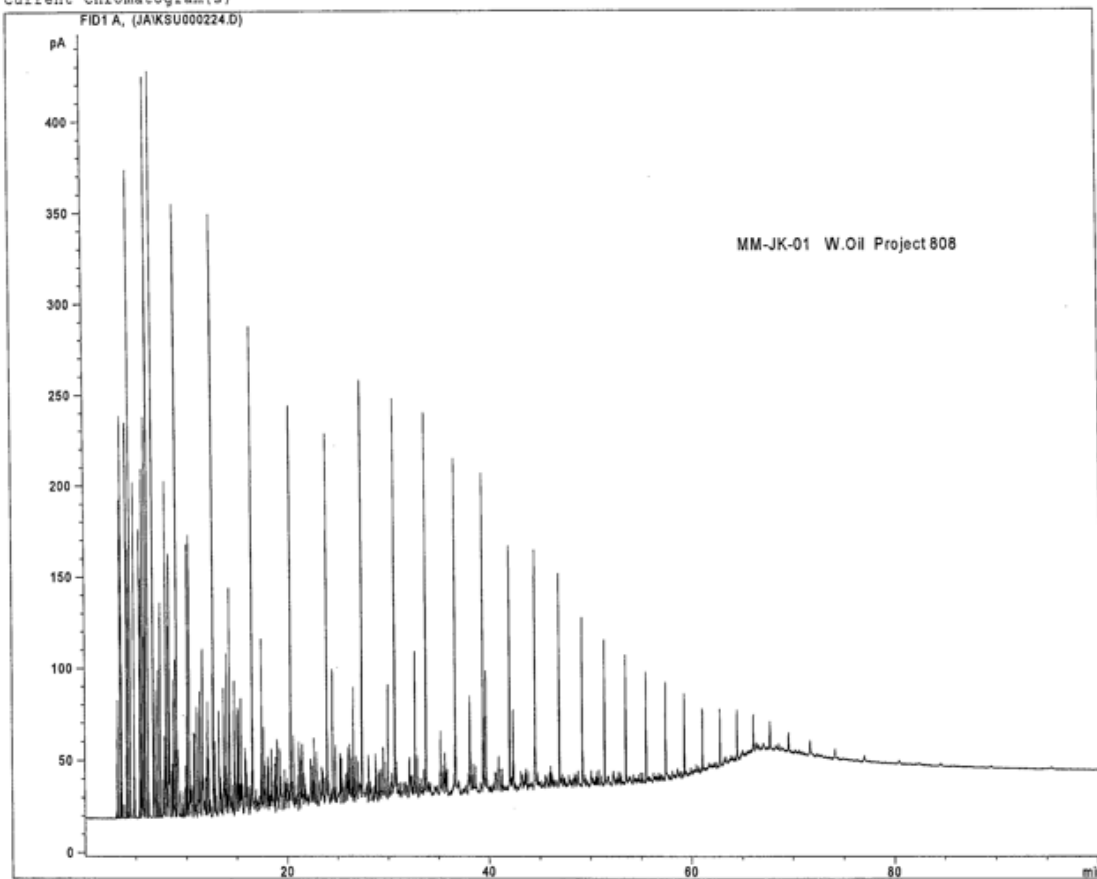
## Appendix B - Gas Chromatograph Analysis of Crude Oil





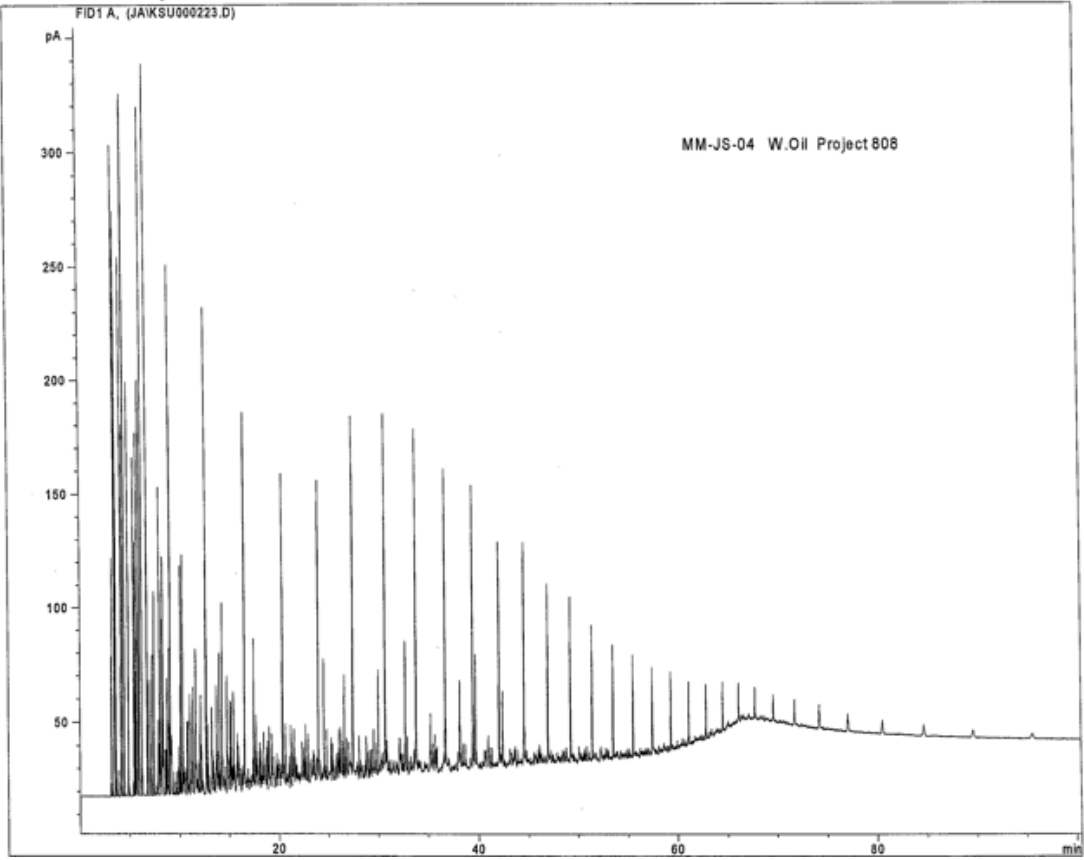
Current Chromatogram(s)

FID1 A, (JAKSU000224.D)

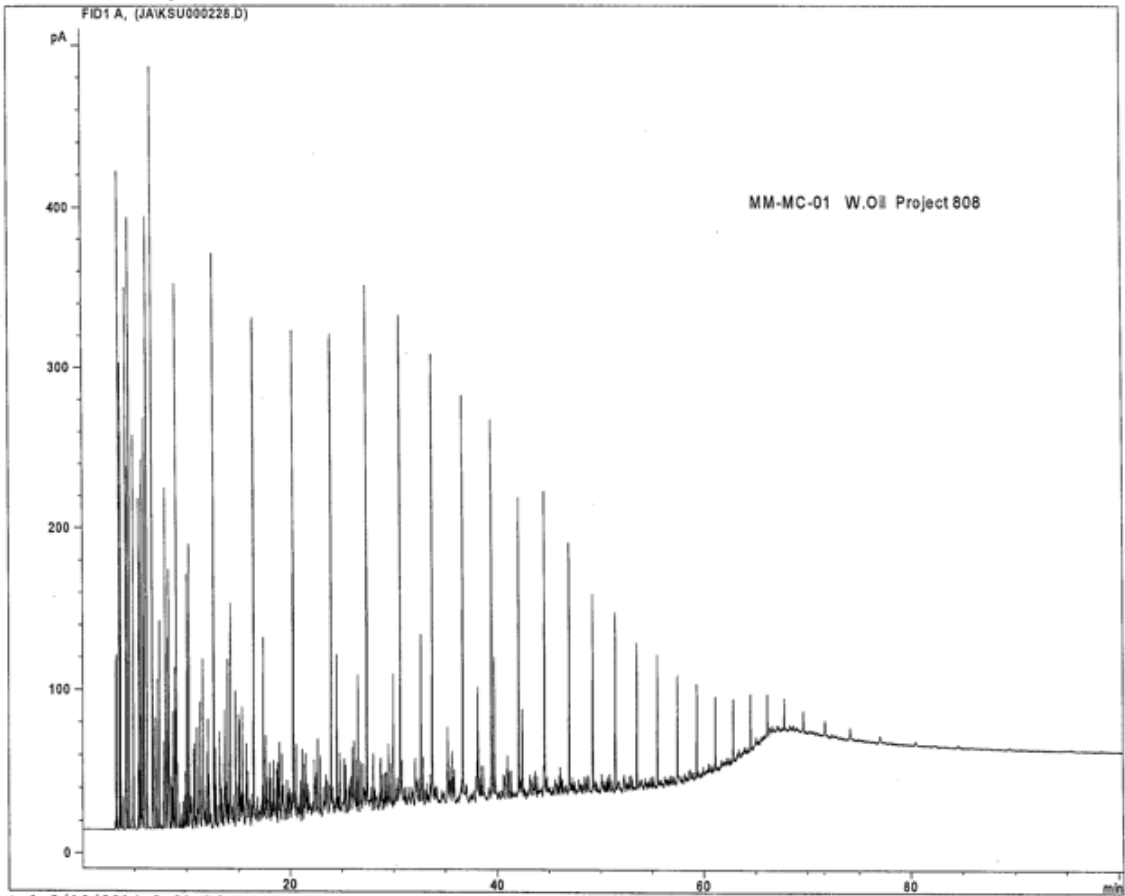


Current Chromatogram(s)

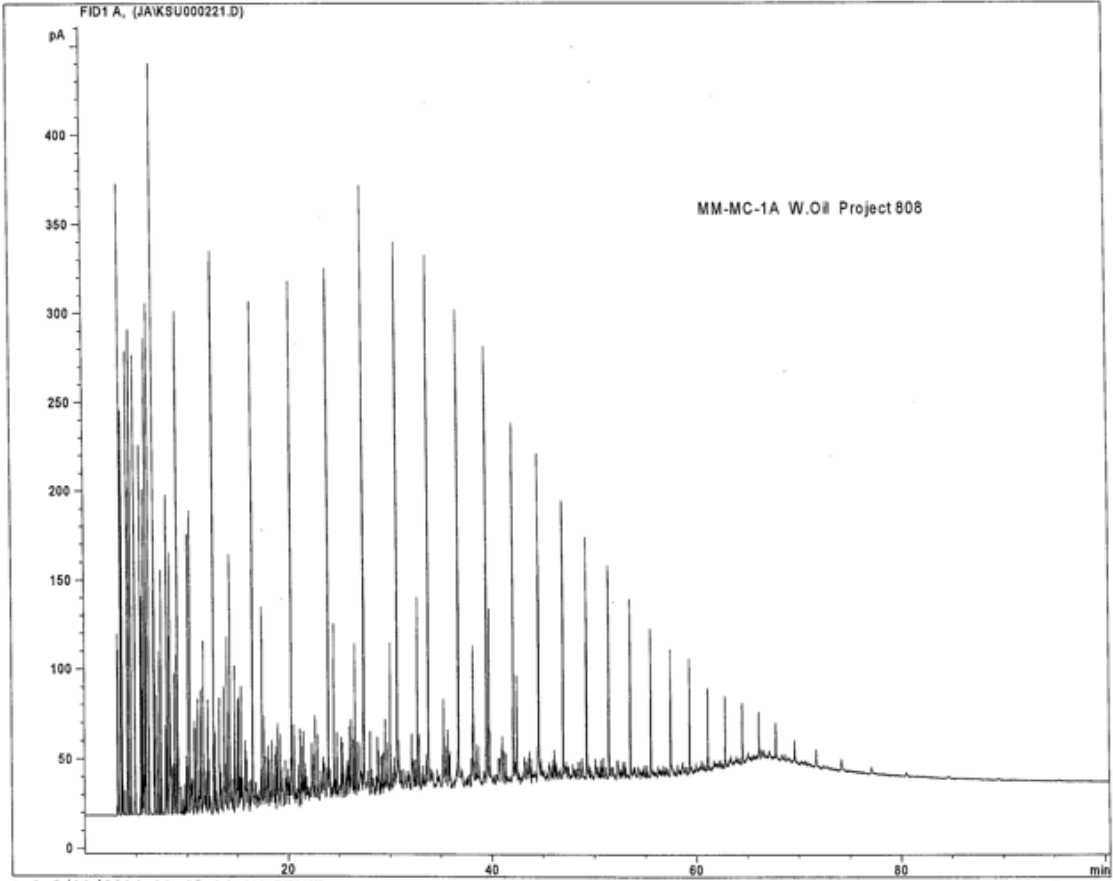
FID1 A, (JAKSU000223.D)

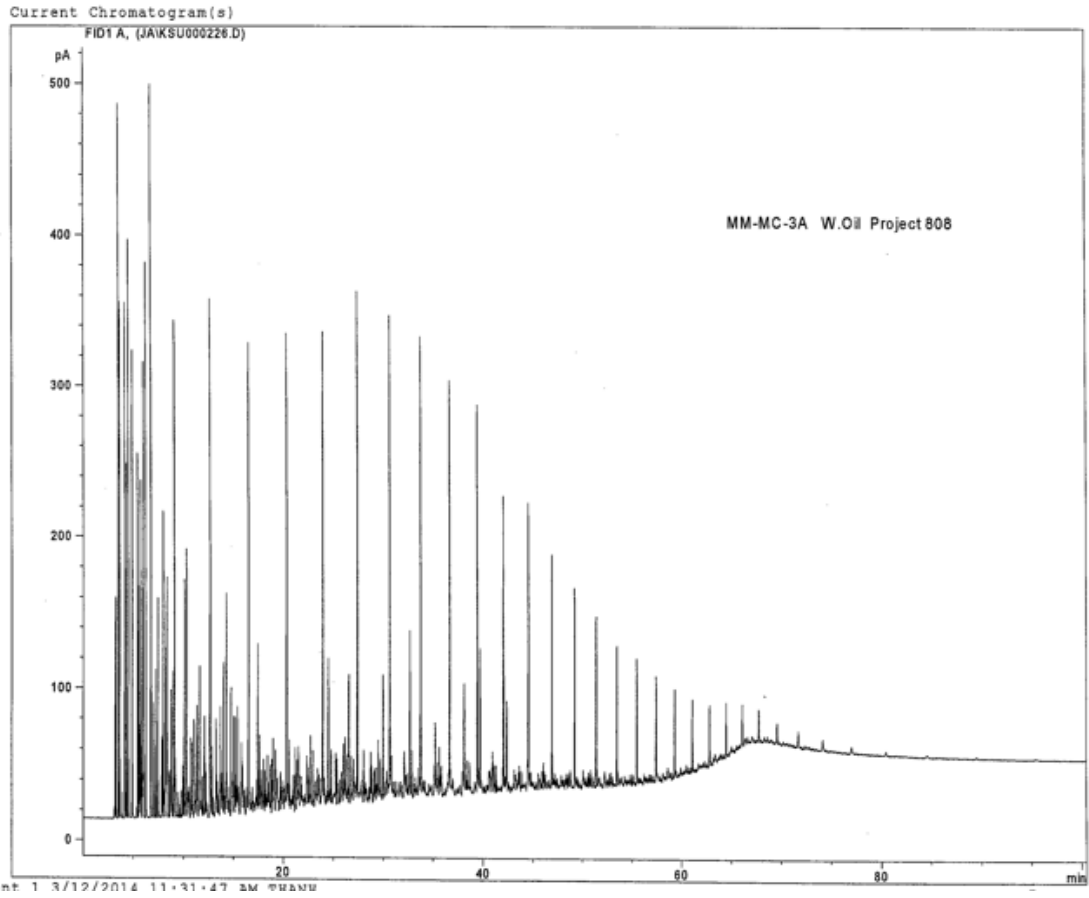


Current Chromatogram(s)  
FID1 A, (JAKSU000228.D)

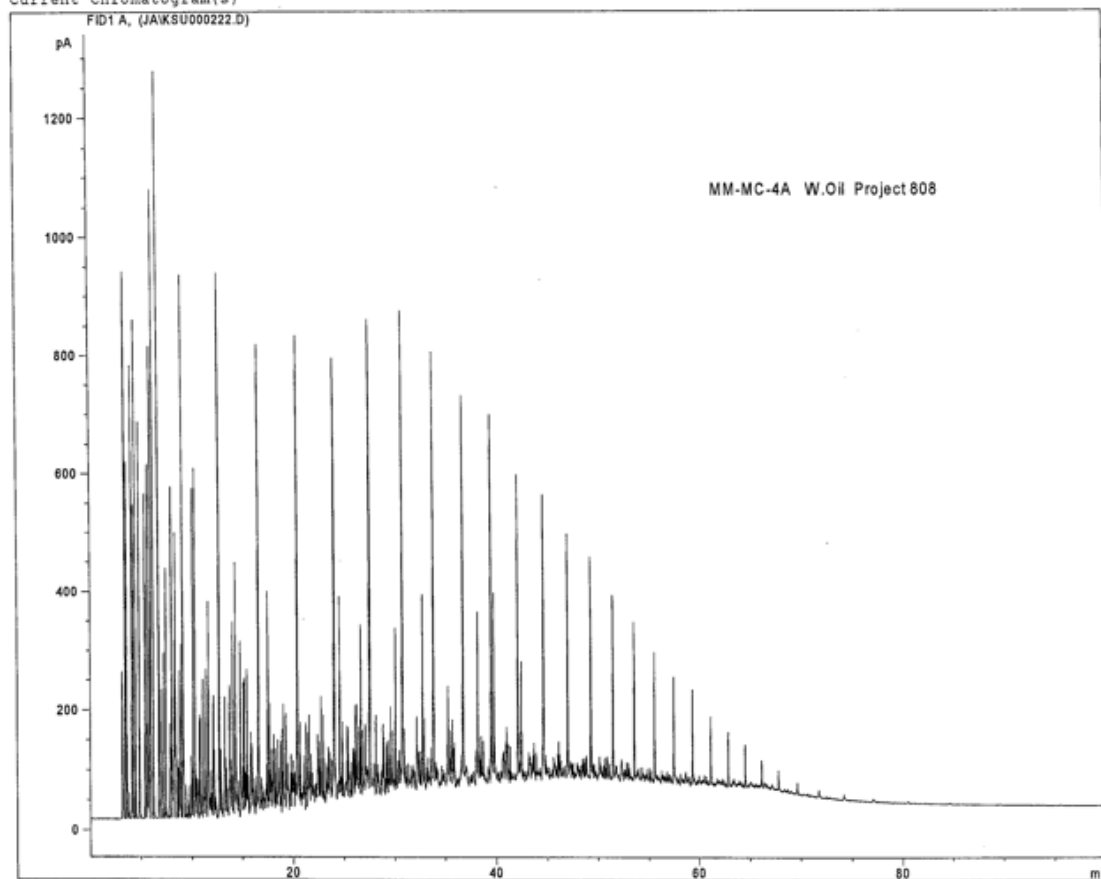


Current Chromatogram(s)

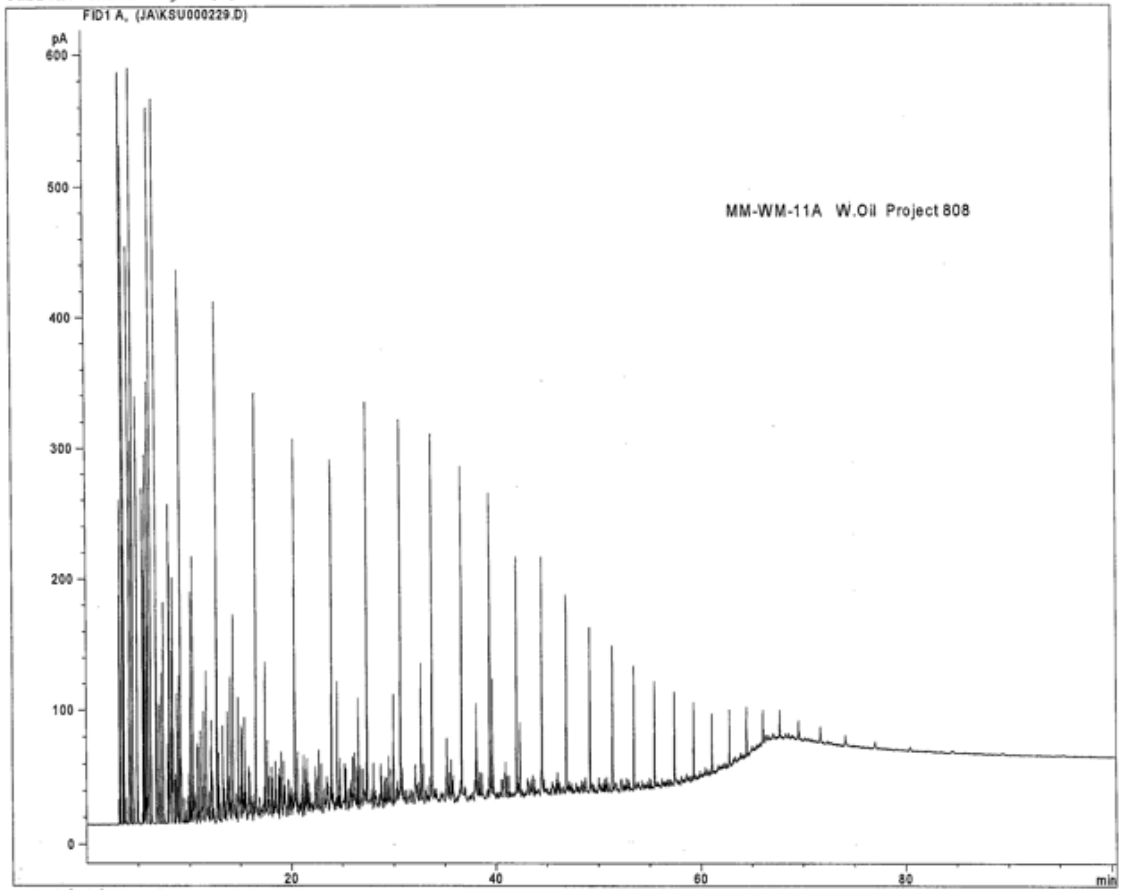




Current Chromatogram(s)

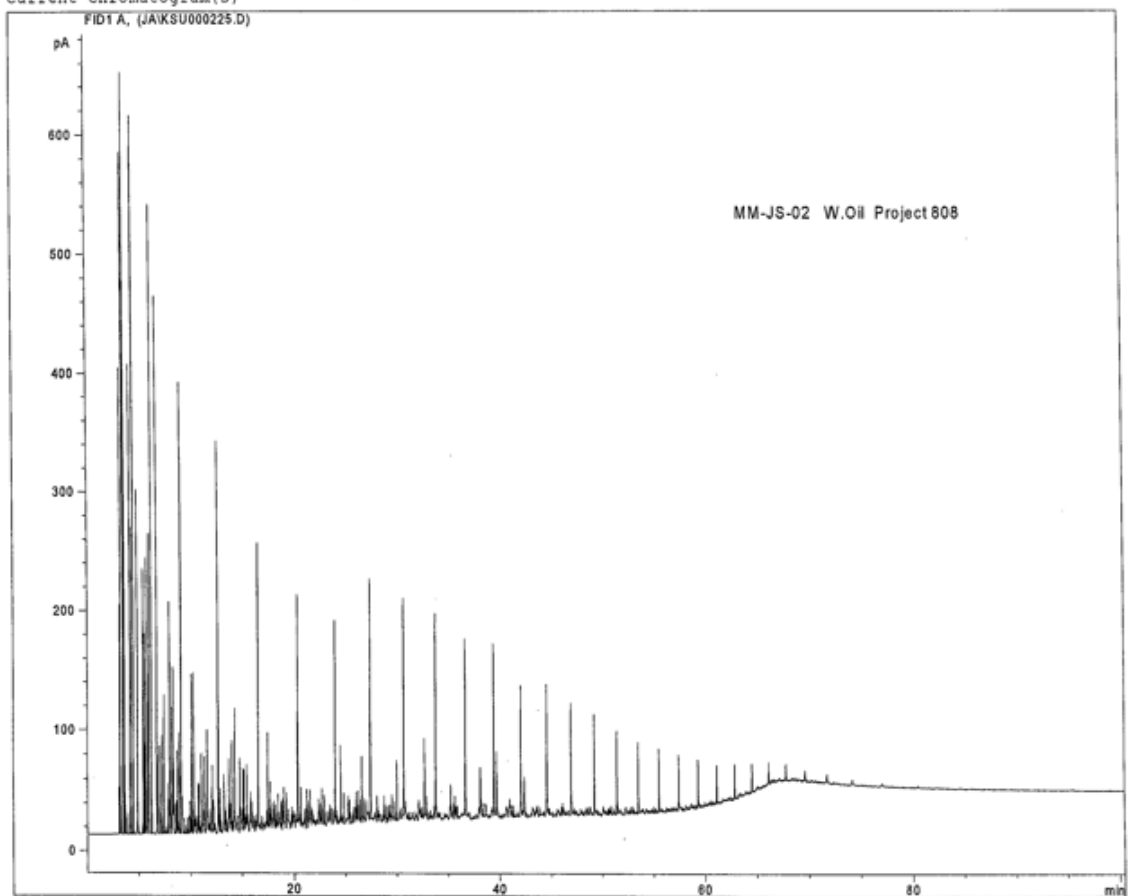


Current Chromatogram(s)  
FID1A, (JAISU000229.D)



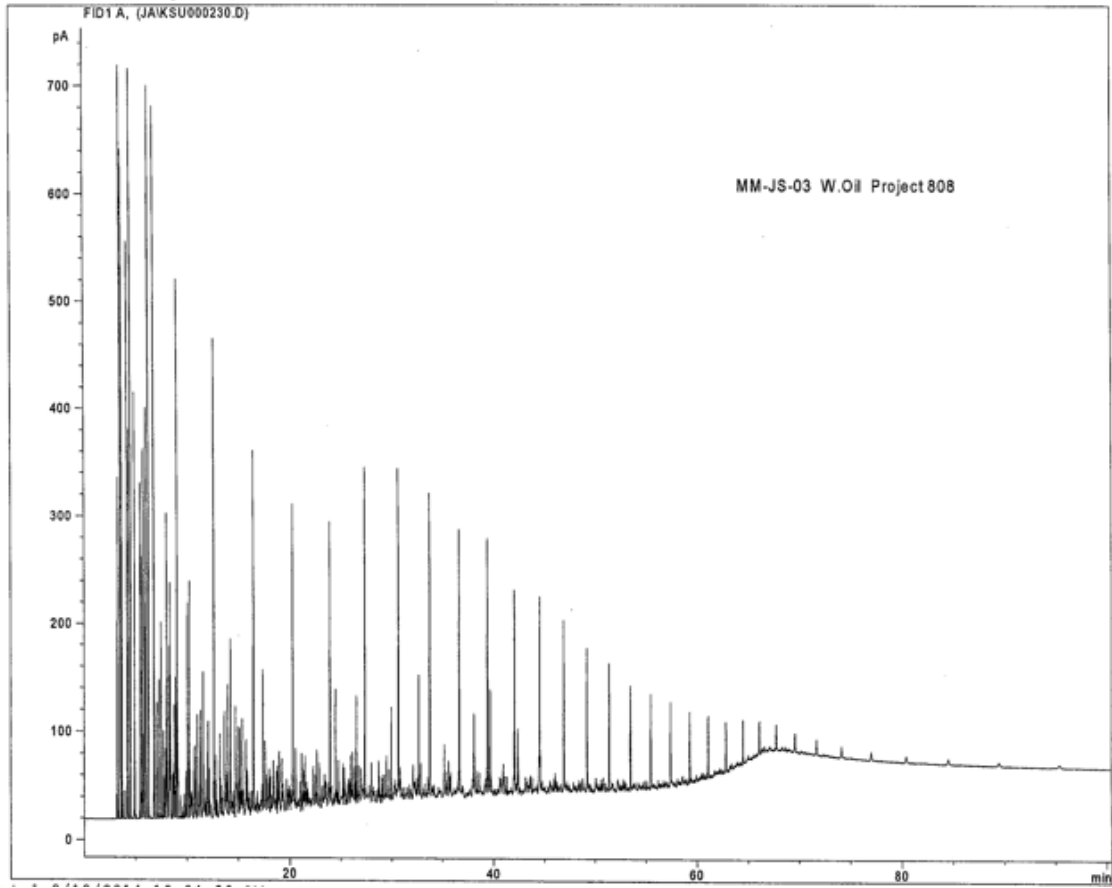
Current Chromatogram(s)

FID1A, (JAISU000225.D)



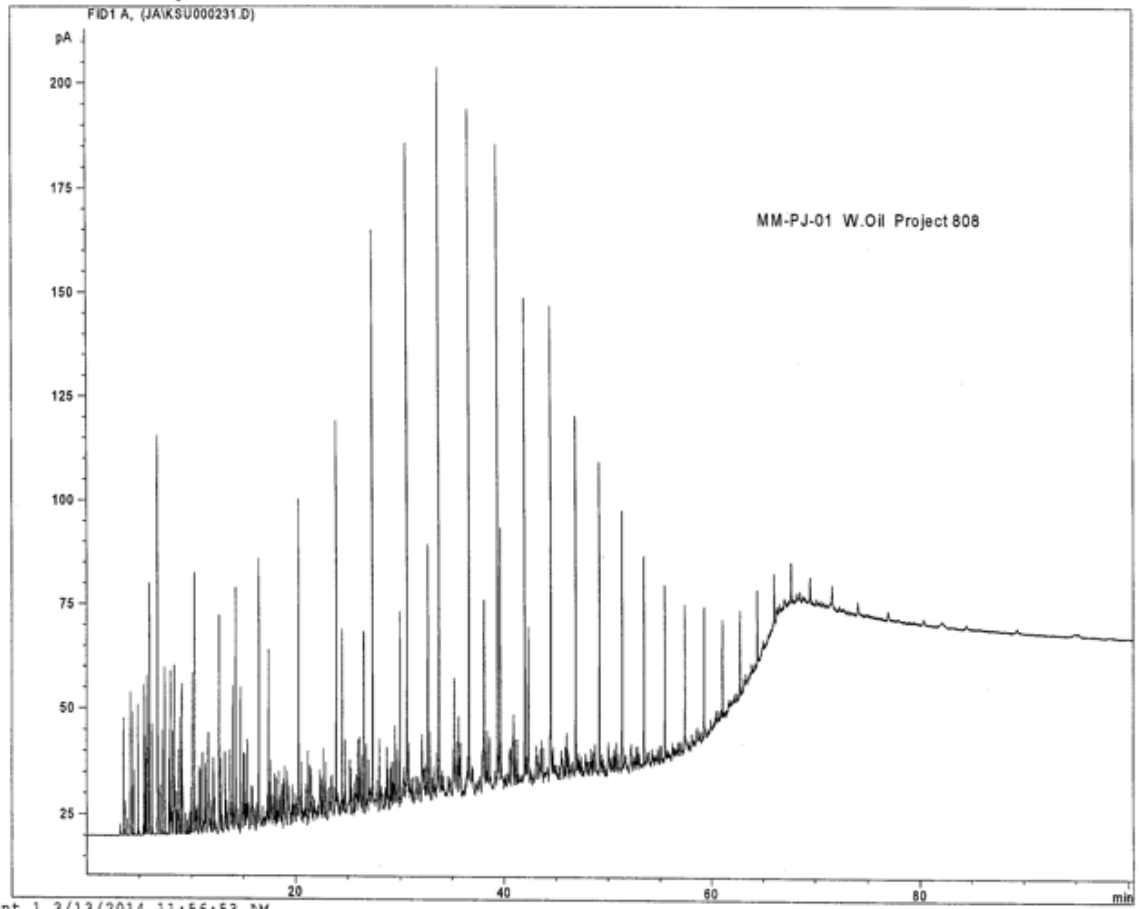


Current Chromatogram(s)



Current Chromatogram(s)

FID1 A, (JAISU000231.D)



APR 1 9 12 / 2014 11:52:53 AM